

DESIGN AND DEVELOPMENT OF MINIATURIZED TACTILE SENSORS FOR TACTILE IMAGING

Thotegodage Don Isuru Udayanga

148042F



University of Moratuwa, Sri Lanka.
Electronic Theses & Dissertations
Degree of Master of Science
www.lib.mrt.ac.lk

Department of Mechanical Engineering

University of Moratuwa
Sri Lanka

August 2016

DECLARATION

I declare that this is my own work and this thesis does not incorporate without acknowledgement any material previously submitted for a Degree or Diploma in any other University or institute of higher learning and to the best of my knowledge and belief it does not contain any material previously published or written by another person except where the acknowledgement is made in the text.

Also, I hereby grant to University of Moratuwa the non-exclusive right to reproduce and distribute my dissertation, in whole or in part in print, electronic or other medium. I retain the right to use this content in whole or part in future works (such as articles or books).

Signature

Date



University of Moratuwa, Sri Lanka.
Electronic Theses & Dissertations

The above candidates have carried out research for the Masters thesis under my supervision.

Name of the supervisor: Dr. Y.W.R. Amarasinghe

Signature of the supervisor:

Date

ABSTRACT

Tactile sensors are devices which acquire data from the physical world through sense of touch. These acquired data may be related to either, surface roughness, texture, force, or any other tactile parameter. Even though, tactile sensor systems are identified as a feasible method to acquire force feedback in robotics and automation systems, due to the requirement of physical interaction between the sensor and application, development of tactile sensors does not come to the spotlight during the past decades. Rather, researchers were more focused on developing non-contact sensors for various sensing modalities when comparing with the tactile sensors. Currently, importance of tactile sensors has come to the spotlight, as development of robotics, automation and biomedical applications are limited due to lack of tactile feedback. Also, many application areas are identified, where tactile sensors can be incorporated such as robotics, industrial automation, biomedical imaging, biomedical robotics, etc.

Tactile imaging is one of the medical imaging technique, which mimic manual palpitation to diagnose diseases such as breast cancer, prostate cancer, etc. Tactile sensor is the foremost element in a tactile imager. Comparing with the other medical imaging techniques, it was found that tactile imaging is the most cost effective method to screen breast cancers. Also it has other advantages such as minimum exposure to radiation, simple and easy operation, etc. Hence, main aim of this research is to develop miniaturized tactile sensors for tactile imaging applications.

Working with that aim, miniaturized tactile sensors were developed during this research. In these developed sensors, Quantum Tunnelling Composite (QTCTM), which is a conductive polymer composite, has been used as the sensing element. A novel structure was proposed to be incorporated with the sensing elements and analysis of the structure discussed. Proposed sensor was developed and calibrated. In the next stage of this research, a novel enclosed tactile sensor was designed and developed utilizing the same sensing and working principle as the developed 1-DOF tactile sensor. Main motive of developing this sensor is to include the proposed improvements for the 1-DOF tactile sensor based on the experimental results. An enclosed novel structure was proposed so that the sensing element and spring will be omitted from the environmental effects. Sensor was developed and calibrated so that it could be integrate with tactile imaging applications. Sensitivity of this developed tactile sensor, calculated to be 0.02 V/N and sensor displayed repeatability of ± 3 N.

An experiment was carried out to evaluate the usability of developed sensors in tactile imaging applications. Using the developed sensor pressure variation of a human left hand was mapped and visual images were constructed. Applicability of sensor arrays instead of a single sensor in tactile imaging applications and miniaturization techniques to be used to construct tactile sensor arrays with high Taxel density is discussed.

A MEMS based tactile sensor design was proposed to be developed to construct tactile sensor arrays with good performance for tactile imaging applications. Proposed sensor design analysed and simulated to validate the proposed working and sensing principles. Fabrication steps for the designed MEMS sensor was proposed.

Key Words: Tactile Imaging, Tactile Sensors, Force Sensors, MEMS

DEDICATION

I dedicate my dissertation work to my family and my teachers. A special feeling of gratitude to my loving parents, Jayasena and Padmini Perera whose words of encouragement and push for tenacity ring in my ears.



University of Moratuwa, Sri Lanka.
Electronic Theses & Dissertations
www.lib.mrt.ac.lk

ACKNOWLEDGMENT

I am deeply grateful to Head of Department of Mechanical Engineering Dr. W.K. Wimalasiri and all the academic and non-academic staff of the department for their constant encouragement in the period of research. Especially my research supervisor, Dr. Y.W.R Amarasighe gave me the best support and attention towards my work. Without his keen supervision none of this would have been possible for myself alone. I consider myself very fortunate for being able to work with such a resourceful individuals.

I also like to extend my sincere gratitude to Mr. V.S.C.Weragoda of the department of materials engineering for helping me in the process of testing of the developed tactile sensors. I had to invoke the help of him several times and he agreed to assist me without a reluctance each time.

I am particularly grateful for the assistance given by Mr. Janaka Mangala and Mr Janath Priyankara with all the non-academic staff at Die and Mould Centre of University of Moratuwa, when fabricating the designed sensor structures.

Furthermore, I would like to express my gratitude to Mr. Janaka Basnayake, Mr. Dumith Jayatilaka and Mr. Kanishka Madushanka for their assistance given me throughout my research. I would like to mentions the help given by Mr. Janaka Basnayake when fabricating electrodes for the developed tactile sensors.

Moreover, I'm particularly grateful to Dr. R.A.R.C. Gopura, who is the research coordinator of Mechanical Engineering Department and Dr. R.U. Weerasuriya, who is the chair of the progress review panel appointed for this research, for their valuable comments and advices given to me throughout this research.

Last but not the least, I owe my thankfulness to Mr. Salith Ranasinghe and Mr. Chathura Jeewantha of the Mechatronics and MEMS/NEMS laboratory for providing me the tools and facility required for conduction my research works whenever required.

Thotegodage Don Isuru Udayanga

MSc Postgraduate,

Department of Mechanical Engineering,

University of Moratuwa.

TABLE OF CONTENTS

Declaration	i
Abstract	ii
Dedication	iii
Acknowledgment	iv
List of Figures	ix
List of Tables.....	xv
List of Abbreviations.....	xvi
List of Appendices	xvii
1 Introduction.....	1
2 Literature Review.....	4
2.1 Tactile Sensors.....	4
2.1.1 What is Tactile Sensing.....	4
2.1.2 History of Tactile Sensing.....	4
2.1.3 Sensing Principles and Existing Tactile Sensors.....	5
2.1.4 Current Trends of Tactile Sensing.....	12
2.2 Tactile Imaging.....	13
2.2.1 Applications of Tactile Imaging.....	15
2.2.2 Existing Tactile Imagers.....	16
2.3 Conclusion – Literature Review.....	19
3 Development of 1-DOF Tactile Sensor.....	21
3.1 Introduction	21



University of Moratuwa, Sri Lanka.
Electronic Theses & Dissertations

www.lib.mrt.ac.lk

3.2	Sensing principle of the proposed 1-DOF Tactile Sensor	22
3.2.1	Challenges of QTC™	24
3.3	Mechanical Structure of the Proposed 1-DOF Tactile Sensor	27
3.3.1	Working Principle of the Proposed Sensor Structure.....	27
3.3.2	Proposed Structural Design 1 for 1-DOF Tactile Sensor	29
3.3.3	Proposed Structural Design 2 for 1-DOF Tactile Sensor	31
3.4	Analysis and Simulation of Proposed 1-DOF Tactile Sensor	34
3.5	Fabrication of Designed 1-DOF Tactile Sensor	40
3.5.1	Fabrication of Sensing Element Configuration	40
3.5.2	Structural Fabrication and Assembling	41
3.6	Testing of Developed 1-DOF Tactile Sensor and Results.....	43
4	Development of enclosed 1-DOF Tactile Sensor.....	46
4.1	Introduction	46
4.2	Proposed Structural Design for 1-DOF Enclosed Tactile Sensor	46
4.3	Analysis and Simulation of Proposed 1-DOF Enclosed Tactile Sensor	49
4.4	Fabrication of Designed 1-DOF Enclosed Tactile Sensor	56
4.4.1	Fabrication of Sensing Element Configuration	56
4.4.2	Structural Fabrication and Assembling	57
4.5	Testing of Developed 1-DOF Enclosed Tactile Sensor and Results..	59
5	Application of Tactile Sensors for tactile Imaging	63
5.1	Introduction	63



5.2	Development of Graphical User interface	63
5.3	Tactile Imaging using Developed 1-DOF Tactile Sensors.....	67
5.3.1	Experiment Conducted to Construct Tactile Images Using Developed 1-DOF Tactile Sensors	67
5.3.2	Results of the Experiment to Construct Tactile Images	69
6	Design and Simulation of MEMS based Tactile Sensor	71
6.1	Introduction	71
6.1.1	Why MEMS?.....	71
6.1.2	Literature Review	72
6.2	Structural Design of 5-DOF MEMS Tactile Sensor.....	74
6.3	Working Principle of 5-DOF MEMS Tactile Sensor.....	76
6.4	Sensing Principle of 5-DOF MEMS Tactile Sensor.....	78
6.5	Structural Analysis of the Proposed 5-DOF MEMS Sensor Structure	80
6.6	Sensing Element Placement in Proposed 5-DOF MEMS Sensor Structure	85
6.7	Multiphysics Analysis of 5-DOF MEMS Tactile Sensor.....	86
6.8	Results of the Simulation of proposed 5-DOF MEMS Tactile Sensor	93
6.9	Fabrication of Proposed 5-DOF MEMS Tactile Sensor.....	96
6.9.1	Proposed Wiring Design for 5-DOF MEMS Tactile Sensor..	96
6.9.2	Proposed Fabrication Steps for 5-DOF MEMS Tactile Sensor	96



University of Moratuwa, Sri Lanka
Electronic Theses & Dissertations
www.lib.mrt.ac.lk

7 Conclusion	99
References	101
Appendices	xviii
Appendix A: Sensor Enclosure (Design 1)	xviii
Appendix B: Production Drawings of Sensor Structure (Design 2)	xx
Appendix C: Material Properties Chart	xxiv
Appendix D: Production Drawings of Sensor structure (Enclosed sensor) .	xxv
Appendix E: Arduino Code of Graphical User Interface.....	xxix
Appendix F: Production Drawings of 5-DOF MEMS Sensor Structure ...	xxxii



University of Moratuwa, Sri Lanka.
Electronic Theses & Dissertations
www.lib.mrt.ac.lk

LIST OF FIGURES

Figure 1.1: Miniaturized tactile sensor development process	2
Figure 2.1: Application areas of tactile sensing	13
Figure 2.2: General view of breast tactile imager	16
Figure 2.3: Representation of the breast examination results by breast tactile imager.....	17
Figure 2.4: General view of prostate tactile imager.....	17
Figure 2.5: Representation of prostate examination results by prostate tactile imager.....	18
Figure 2.6: General view of vaginal tactile imager.....	18
Figure 2.7: Representation of stage III prolapse by vaginal tactile imager.	19
Figure 3.1: Categories to be considered when developing a 1-DOF tactile sensor ...	21
Figure 3.2: SEM image of the cut surface of QTC™, (a) 50 μm scale. (b) 2 μm scale.....	23
Figure 3.3: Variation in resistance as a function of compression for a soft silicone-Ni type 123 QTC™ composite.	24
Figure 3.4: Experiment setup to find Young's modulus of QTC™	25
Figure 3.5: Experiment results of QTC™ pill	26
Figure 3.6: Free body diagram of the proposed working principle of the mechanical structure.....	28
Figure 3.7: Isometric view conceptual design of structural design 1 and component assembly.....	29
Figure 3.8: Sectional Front elevation conceptual design of structural design 1 and component assembly	30

Figure 3.9: Basic dimensions of the proposed sensor structure 1	30
Figure 3.10: Isometric view conceptual design of structural design 2 and component assembly.....	32
Figure 3.11: Sectional Front elevation conceptual design of structural design 2 and component assembly	32
Figure 3.12: Basic dimensions of the proposed structural design 2.....	33
Figure 3.13: Components arrangement in the assembly of proposed structural design 2.....	33
Figure 3.14: Geometry Considered for the FEA.....	35
Figure 3.15: Total deformation of the sensor structure under loading for spring gauge 1.0 mm	36
Figure 3.16: Total deformation of the sensor structure under loading for spring gauge 1.5 mm	37
Figure 3.17: Equivalent Stress of sensor structure under loading for spring gauge 1.0 mm.	37
Figure 3.18: Equivalent Stress of sensor structure under loading for spring gauge 1.5 mm.	38
Figure 3.19: Total deformation plot of QTCTM pill.	38
Figure 3.20: Equivalent stress plot of QTCTM pill.	39
Figure 3.21: Electrode Fabrication; (a) Electrode arrangement with sensing element. (b) Electrode Design	41
Figure 3.22: Fabricated structural components and assembled sensor structure	42
Figure 3.23: Fabricated 1-DOF Tactile Sensor	43
Figure 3.24: System layout of the experimental setup.....	44



Figure 3.25: Experiment Results; voltage vs. force plot.....	44
Figure 4.1: Isometric view of proposed design of novel enclosed sensor structure ..	47
Figure 4.2: Sectional front elevation of proposed design of novel enclosed sensor structure.....	47
Figure 4.3: Exploded view of the proposed novel enclosed sensor structure	48
Figure 4.4: Geometry Considered for the FEA.....	50
Figure 4.5: Boundaries selected to apply boundary conditions for FEA.....	52
Figure 4.6: Total deformation variation of the sensor structure.....	53
Figure 4.7: Force vs. Deformation plot.....	53
Figure 4.8: Equivalent stress variation of the sensor structure	54
Figure 4.9: Force vs. Equivalent stress plot.....	54
Figure 4.10: Total deformation plot result of QTCTM pill.....	55
Figure 4.11: Equivalent Stress plot result of QTCTM pill.....	55
Figure 4.12: Proposed revised electrode design.....	56
Figure 4.13: Steps of electrode fabrication and fabricated electrode.....	57
Figure 4.14: Fabricated structural components and Assembled and finalized novel enclosed 1-DOF tactile sensor	58
Figure 4.15: System layout of experimental setup.....	59
Figure 4.16: Developed experimental setup.....	60
Figure 4.17: Calibration Results for Continuous Loading & Unloading.....	60
Figure 4.18: Repeatability analysis for Continuous Loading & Unloading.....	61
Figure 4.19: Calibration Results for Dead Weight Loading & Unloading	62



Figure 5.1: Proposed system layout for the graphical user interface	64
Figure 5.2: Developed Hardware Interface	65
Figure 5.3: LabVIEW program developed for the proposed graphical user interface	66
Figure 5.4: Developed GUI based on LabVIEW software	66
Figure 5.5: Chosen posture for the experiment	68
Figure 5.6: Data points considered on the left hand	68
Figure 5.7: System layout of the proposed experimental setup	69
Figure 5.8: Graphical representation of pressure values on data points considered on the left hand.....	69
Figure 5.9: Constructed pressure mapping image of the left hand for given posture	70
Figure 5.10: Constructed Contour color mapping image of the pressure variation of left hand for given posture.....	70
Figure 6.1: Comparison between tactile sensor arrays; (a) Sensor array constructed with novel enclosed tactile sensors. (b) Sensor array constructed with MEMS tactile sensors	72
Figure 6.2: Isometric view of the conceptual design of proposed MEMS tactile sensor	74
Figure 6.3: Plan view of the conceptual design of proposed MEMS tactile sensor...	75
Figure 6.4: Degrees of freedoms of the structure.....	77
Figure 6.5: Possible structural deformations for loading condition A.	77
Figure 6.6: Possible structural deformations for loading condition B	78
Figure 6.7: Piezoresistive sensing element arrangement in full Whetstone Bridge...	80
Figure 6.8: Piezoresistive sensing element arrangement in half Whetstone Bridge..	80



Figure 6.9: Selected boundary to apply boundary load.....	82
Figure 6.10: Selected Boundaries to apply fixed constraint boundary condition	82
Figure 6.11: Displacement plot of the sensor structure for load condition A.....	83
Figure 6.12: Displacement plot of sensor structure for load condition B.	83
Figure 6.13: Equivalent stress plot of sensor structure for load condition A.....	84
Figure 6.14: Equivalent stress plot of sensor structure for load condition B.	84
Figure 6.15: Stress variation along a beam under loading and suitable position to place sensing elements.....	85
Figure 6.16: integrated sensing elements on the structure and their positions with electrical connections	85
Figure 6.17: Geometry considered for the Multiphysics analysis.....	86
Figure 6.18: Considered Piezoresistive layer for material assignment in the Multiphysics analysis.....	87
Figure 6.19: Specified thin Piezoresistive sensing elements	88
Figure 6.20: Specified thin conductive layer	88
Figure 6.21: Specified electrical terminals for the Multiphysics analysis	89
Figure 6.22: Change in resistance of elements in beam 1 for Loading Condition A.	90
Figure 6.23: Change in Resistance of elements in beam 3 for Loading Condition A	90
Figure 6.24: Change in Resistance of elements in beam 1 for Loading Condition B	91
Figure 6.25: Change in resistance of elements in beam 3 for Loading Condition B.	91
Figure 6.26: Voltage variation of a Whetstone Bridge in a beam.....	92
Figure 6.27: Current direction of a Whetstone Bridge.....	92

Figure 6.28: Plot result for loading condition A showing the relationship between output voltage of Whetstone Bridge and force applied to the sensor 95

Figure 6.29: Plot result for loading condition B showing the relationship between output voltage of Whetstone Bridge and force applied to the sensor 95

Figure 6.30: Proposed wiring design with wire bonding pads for 5-DOF MEMS tactile sensor 96

Figure 6.31: Proposed fabrication steps for the designed 5-DOF MEMS tactile sensor. 98



University of Moratuwa, Sri Lanka.
Electronic Theses & Dissertations
www.lib.mrt.ac.lk

LIST OF TABLES

Table 2.1: Piezoresistive Tactile Sensors.....	5
Table 2.2: Capacitive Tactile Sensors.....	7
Table 2.3: Optoelectric Tactile Sensors	8
Table 2.4: Piezoelectric Tactile Sensors	9
Table 2.5: Conductive Polymer Tactile Sensors	10
Table 2.6: Advantages and disadvantages of sensing principles	11
Table 3.1: Input Parameters for the ANSYS finite element analysis.....	34
Table 3.2: Results of FEA Analysis for different spring gauges	40
Table 4.1: Input parameters of FEA.....	51
Table 4.2: Sensor characteristics values calculated for the developed sensor	61
Table 5.1: Specifications of Arduino Mega 2560	64
Table 6.1: Literature regarding MEMS tactile sensors	73
Table 6.2: Basic dimensions of the sensor structure	75
Table 6.3: Piezoresistive element specification	79
Table 6.4: Parameters specified for the structural analysis.....	81
Table 6.5: Parameters specified for the Multiphysics analysis	87
Table 6.6: Voltage output for each whetstone bridge for Loading condition A	93
Table 6.7: Voltage output for each whetstone bridge for Loading condition B	94



LIST OF ABBREVIATIONS

Abbreviation	Description
ADC	Analogue to Digital Converter
BSF	Breast Self-Examination
CAD	Computer Aided Drawing
CBE	Clinical Breast Examination
CNC	Computer Numerical Controller
CT	Computed Tomography
DOF	Degrees of Freedom
DRE	Digital Rectal Examination
FEA	Finite Element Analysis
GUI	Graphical User Interface
MEMS	Micro Electro Mechanical Systems
MIS	Minimally Invasive Surgery
MRI	Magnetic Resonance Imaging
PSA	Prostate Specific Antigen
PVDF	Polyvinylidene Fluoride
PZT	Lead Zirconate Titanate
QTC	Quantum Tunneling Composite
SOI	Silicon on Insulator
TRUS	Transrectal Ultrasound
USB	Universal Serial Bus



University of Moratuwa, Sri Lanka.
Electronic Theses & Dissertations
www.lib.mrt.ac.lk

LIST OF APPENDICES

Appendix	Description	Page
Appendix A:	Sensor Enclosure (Design 1)	xviii
Appendix B:	Production Drawings of Sensor Structure (Design 2)	xx
Appendix C:	Material Properties Chart	xxiv
Appendix D:	Production Drawings of Sensor structure (Enclosed sensor) .	xxv
Appendix E:	Arduino Code of Graphical User Interface.....	xxix
Appendix F:	Production Drawings of 5-DOF MEMS Sensor Structure ...	xxxii



University of Moratuwa, Sri Lanka.
Electronic Theses & Dissertations
www.lib.mrt.ac.lk

1 INTRODUCTION

Tactile sensor is a device, which incorporates tactile sensing principles to sense the physical parameters by physically interacting with the environment. Such sensors need to physically touch the surface of the application to acquire data related to the measuring parameter. The tactile parameters that can be measured through such tactile sensor may vary from force, pressure, surface roughness, surface texture, temperature, etc. There are many transduction techniques available so far regarding the tactile sensors, such as capacitive, Piezoresistive, Piezoelectric, strain gauges, etc. They have their own advantages and disadvantages. Since the sensitivity and the range of these sensors mostly depend on the transduction technique, it is utmost important to have most suitable technique for a particular sensor. Tactile sensors are widely used in many developing areas such as robotics, industrial automation, Biomedical, Aerospace, etc. Unlike non-contact sensors (temperature, vision, motion), tactile sensors hasn't developed much over the past decades. Nevertheless, at the present many industrial and commercial applications now appear to be on the cusp of accepting tactile sensing technology.



University of Moratuwa, Sri Lanka.

Electronic Theses & Dissertations

www.lib.mrt.ac.lk

Tactile sensor is the foremost element in a tactile imaging equipment. Tactile imaging, also known as computerized palpation or mechanical imaging is an area of medical imaging, which mimic manual palpation by converting sense of touch to a digital image. This is done by mapping pressure variations of the surface to be imaged under applied deformation. Tactile imaging is one of the medical imaging technique. Medical imaging consists of non-invasive methods of constructing visual images of inner body parts, tissues and organs for clinical diagnosis. Other than this method, there are several other techniques available for medical imaging such as radiography, magnetic resonance imaging, ultrasound, elastography, and thermography. Tactile imaging has several advantages comparing to other medical imaging techniques. Cancer nodules present under the skin can be identified easily and patient's exposure to radiation is minimum in this method.

To develop better tactile imaging equipment, it is vital to develop tactile sensors with good performance and optimum spatial resolution. Therefore, main aim of this

research is to develop miniaturized tactile sensors with good performance for tactile imaging application. When developing a tactile sensor, there are several areas to be focused on. Working principle, sensing principle, fabrication, testing and calibration are some of those areas. Figure 1.1 shows the development process of developing a tactile sensor. According to this development process, development of tactile sensors were conducted in this research.

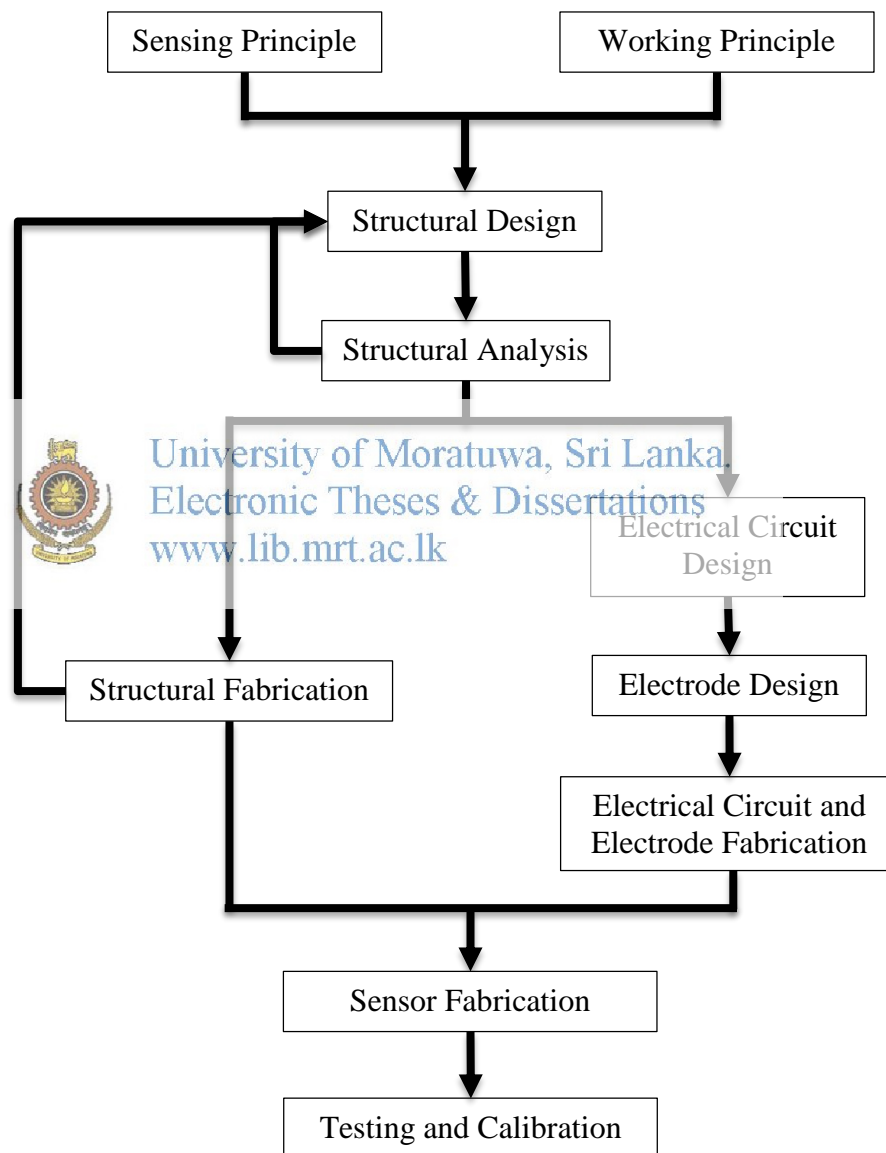


Figure 1.1: Miniaturized tactile sensor development process

When developing tactile sensors, it is vital to conduct a literature review, regarding tactile imaging and tactile sensors, to identify current stage of development regarding them. Hence, in this thesis, chapter two consist of the details about the conducted literature review.

Then tactile sensors were developed according to the identified areas as shown in Figure 1.1. Chapter three of this thesis consist of the details about the first stage of developing tactile sensors and chapter four consist of the details about second stage of developing tactile sensors.

After the development of tactile sensors, they were tested for feasibility to use them in tactile imaging applications. Details about this work is consist in the chapter five of this thesis. After these experiments, it was identified that it is more feasible to use further miniaturised tactile sensors to achieve better performance regarding tactile imaging. As, instead of using a single tactile sensor, it is feasible to use sensor arrays to get the tactile feedback from an application. In tactile sensor array, number of taxels defines the performance characteristics of it. Hence, miniaturization is a method to increase taxel density or number of taxels present in the sensor array, so as to increase the performance of the sensor array.



University of Moratuwa, Sri Lanka
Electronic Theses & Dissertations
www.lib.mrt.ac.lk

Hence, chapter six of this thesis consist of the details about designing a MEMS based tactile sensor. With the improved spatial resolution with this proposed MEMS tactile sensor, better performance can be achieved in tactile imaging applications.

2 LITERATURE REVIEW

2.1 Tactile Sensors

2.1.1 What is Tactile Sensing

Tactile Sensing is measuring tactile parameters with the aid of physical touch. Tactile parameters may often include, temperature, vibration, softness, texture, shape, composition shear and normal force. Even though, pressure and torque is not identified as tactile parameters in this list, they are important parameters that can be sense by physical touch. Using tactile sensors, one or more of these tactile parameters can be sensed and measured from the external environment [1], [2].

Human tactile sensing or more specifically, human skin have been a reference point for tactile sensing as researchers tries to mimic human tactile sensing through tactile sensors. Although human tactile sensing act as a reference point, current developed tactile sensors are not that much refined comparing with human skin. Because, unlike human skin, tactile sensors are capable of sensing limited number of tactile parameters simultaneously [3].

2.1.2 History of Tactile Sensing

In the 1970s, with the increase of robotics and automation activities, tactile sensing came to the attention of researchers, as a mean of acquiring force feedback. Based on that, there were wide variety of devices and transduction techniques invented and developed in that era. But almost all of these developed devices were either in a primitive stage or experimental prototypes. Despite the fact that, tactile sensing can provide feasible mean of acquiring force feedback of robotics and automation systems, researchers in that era were more focused on developing non-contact sensing methods such as machine vision. This can be proved by comparing the quantity of research articles published related to machine vision and tactile sensing. Even though, tactile sensing and related devices weren't developed up to the usage of industrial applications in that era, many researchers were hopeful that tactile sensing will soon adapt with industrial applications such as robotics, automation, and so on [4], [5].

2.1.3 Sensing Principles and Existing Tactile Sensors


Over the past decades there have been many sensing principles were identified and developed which can be incorporated with tactile sensing.


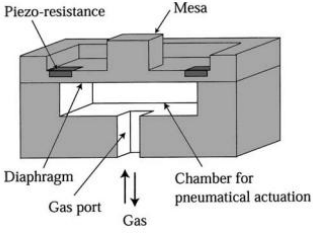
- Piezoresistive
- Capacitive
- Optoelectric
- Piezoelectric
- Conductive Polymer

Above mentioned sensing principles are some of the sensing principles that are widely used in tactile sensing devices [1].

Piezoresistive sensing principle associated with change of resistance with respect to the applied force, pressure or strain. Such change of resistance can be easily quantified as Piezoresistive sensing generally associate with the ohms law. Hence, they generally require less electronics, as change in resistance can easily be quantified and are therefore to manufacture and integrate. Piezoresistive tactile sensing is particularly popular among the MEMS based and silicon based tactile sensors [6], [7]. Table 2.1 shows some developed tactile sensors, which incorporates Piezoresistive sensing principle.

Table 2.1: Piezoresistive Tactile Sensors

Name	Figure	Discription
Flexiforce Sensor [8]		<ul style="list-style-type: none"> • Constructed of two layers. • On each layer, a conductive material (silver) is applied, followed by a layer of pressure-sensitive ink. • Resistance vary from $M\Omega$ to $10\text{ k}\Omega$ or lower • Hysteresis = 4.5%

<p>FSR 400 Series Sensor [9]</p>		<ul style="list-style-type: none"> • A thick-film device • Have much lower performances comparing to flexiforce sensor. But have good robustness comparing to it. • Force sensitivity range is lower than flexiforce sensors. • Hysterisis = 10%
<p>Active Tactile Sensor [10]</p>		<ul style="list-style-type: none"> • Can detect both the contact force and hardness of the object. • Contact force can be detected using the deformation of the diaphragm. • For hardness detection, pneumatic force is applied.

Tactile sensors with capacitive sensing principle, consists of two conductive plates with a dielectric material sandwiched between them. Capacitance of parallel plate capacitors can be expressed using equation 2.1,



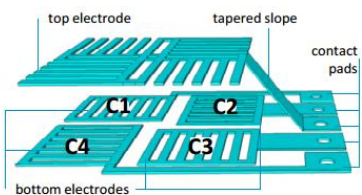


University of Moratuwa, Sri Lanka.
Electronic Theses & Dissertations
www.lib.ug.ac.lk

$$C = (A\epsilon_0\epsilon_r)/d \quad (2.1)$$

Where, A is the overlying area of the two plates, ϵ_0 is the permittivity of free space, ϵ_r is the relative permittivity of the dielectric material and d is distance between the plates. Capacitive sensing technology is also popular among the tactile sensors based on MEMS and silicon micromachining. Capacitive tactile sensors generally exhibit a good frequency response, high spatial resolution, and have a large dynamic range [11], [12]. Table 2.2 shows some of the developed tactile sensors which incorporates capacitive sensing principle.

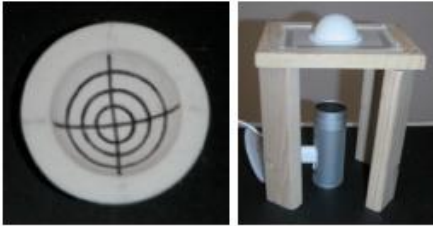
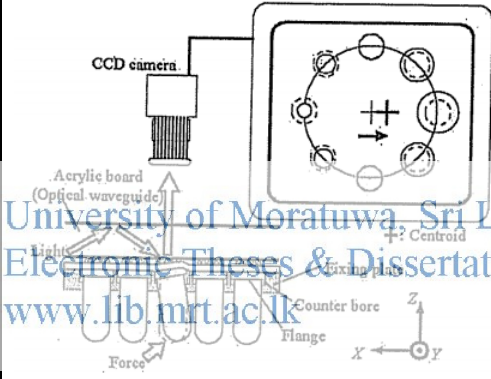
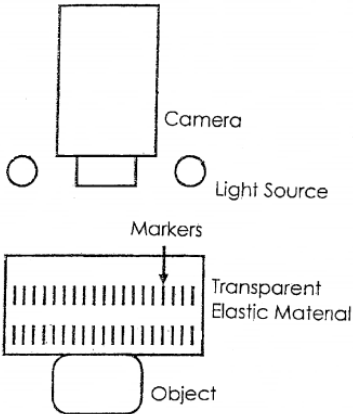
Table 2.2: Capacitive Tactile Sensors

Name	Image	Description
ROBOTOUCH & DigiTacts™ [13]		<ul style="list-style-type: none"> • Off the shelf product • Developed by Pressure Profile Systems. • This is the highest performance tactile sensing system in the market. • Provides outstanding sensitivity (0.7 kPa) and repeatability
Stretchable Capacitive Tactile Skin [14]		<ul style="list-style-type: none"> • Can be used to environmental exploration (obstacle detection, surface reconstruction) by tactile information. • Design fabrication done by using MEMS techniques. • This sensor can be subjected to tactile strains of 15% across a pressure range of 250 kPa.
Capacitive flexible force sensor [15]		<ul style="list-style-type: none"> • Composed of four redundant capacitors. • Have typical force sensitivity of 1-2 fF/N

Tactile sensors with optical mode of transduction use the properties of optical reflection between media of different refractive index. Usually such sensors consist of, light source, transduction medium and a photo-detector. Transduction occurs when changes in the tactile medium modulate the transmission or reflectance intensity, or the spectrum of the source light, as the applied force varies. They have high spatial resolution, and are immune to common lower frequency electromagnetic interference

generated by electrical systems. Some of the developed tactile sensors associated with Optoelectric sensing principle is shown in Table 2.3.


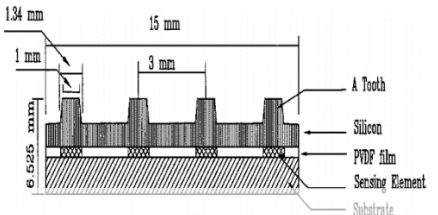
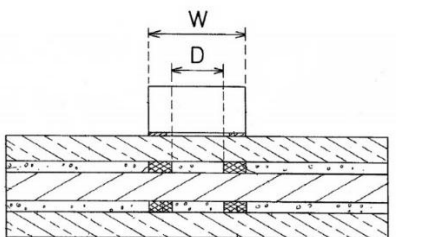
Table 2.3: Optoelectric Tactile Sensors

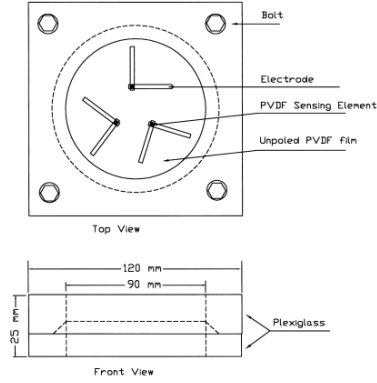
Name	Image	Description
Optical Tactile Sensor for Medical Palpation [16]		<ul style="list-style-type: none"> • Deformable semi-spherical silicon shells are used. • This system cannot provide depth information directly.
Optical 3-Axis Tactile Sensor [17]		<ul style="list-style-type: none"> • Based on the principles of an optical waveguide-type tactile sensor • Has sufficient dynamic sensing capability to detect normal and shearing forces.
Optical Tactile Sensor [18]		<ul style="list-style-type: none"> • Sensor comprised of a tactile section and imaging section. • Using imaging section information of external force applied at multiple directions is achieved.

The piezoelectric materials have the property of generating charge/voltage proportional to the applied force/pressure which distort the crystal lattice.

Alternatively, they are capable of generating force due to electrical input. The sensitivity of the crystal depends on its cut/structure, allowing it to distinguish between transverse, longitudinal and shear forces. These sensors exhibit a very good high-frequency response. While quartz and some ceramics (PZT) have good piezoelectric properties, the polymers such as PVDF normally have been used in touch sensors because of some excellent features, such as, flexibility, workability and chemical stability [19], [20]. Some of the tactile sensors developed using piezoelectric sensing principle is shown in Table 2.4.

Table 2.4: Piezoelectric Tactile Sensors

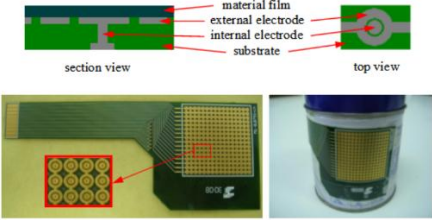
Name	Image	Description
Micromachined Piezoelectric Tactile Sensor for Endoscopic Grasper [21] 		<ul style="list-style-type: none"> • Sensor Structure is consist of 3 layers • Compared to other similar type of sensors, this is fairly simple to fabricate. • Sensor exhibits high sensitivity, large dynamic range, a wide bandwidth with good linearity and a high signal-to-noise ratio.
Flexible Piezoelectric Tactile Sensor [22]		<ul style="list-style-type: none"> • Consist of thin layer of PVDF sandwiched between two flexible substrates. • Electrodes are formed within the substrates so that they are in contact with the PVDF layer. • This design claims to reduce the cost of manufacturing.

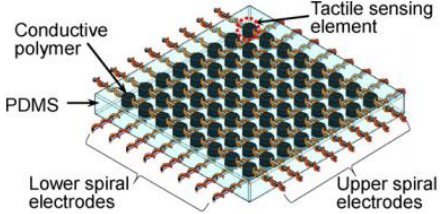
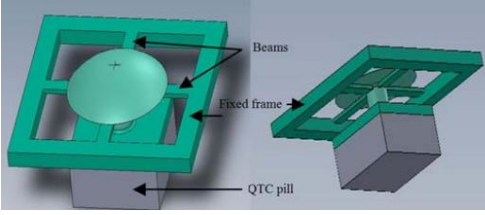
<p>Piezoelectric Tactile Sensor with three Sensing Elements [23]</p>		<ul style="list-style-type: none"> • Both magnitude and position of the applied force can be identified. • Use triangulation approach combined with membrane stress to do so. • Has high sensitivity as PVDF film used as a membrane.
--	---	--

The principle of Electrical conductive composites is one of the most important finding in the past century. Despite the useful material properties that the polymers provide, they have been neglected by many applications because of their electrical insulation property. But by combining polymers with filler materials, it was found that the polymers can show electrical conductive property to some extent [24].

Electrical conductivity of these composites vary with the type and the amount of filler material used in the process. A polymer material become conductive if its filler content exceeds beyond the percolation threshold. Main mechanism behind such composites is that the fillers inside tend to form paths between them, so that the electrical current could flow [25]. Most effective methods to determine the filler content for a composite are Statistical Percolation [25] and Effective Medium Model [26]. Table 2.5 shows some of the tactile sensors developed using conductive polymers/composites.

Table 2.5: Conductive Polymer Tactile Sensors

Name	Image	Description
<p>Conductive Polymer based Tactile sensor [27]</p>		<ul style="list-style-type: none"> • Consist of conductive polymer layer and electrodes. • Design allows fabrication of low cost flexible tactile sensors. • Sensitivity is less due to the smaller area of electrodes.

<p>Highly Twistable Tactile Sensing Array [28]</p>		<ul style="list-style-type: none"> • The design claims to be a highly flexible and durable artificial skin. • Employs extendable spiral electrodes. • sensor array can be twisted up to 700 without any damage.
<p>QTC based MEMS Tactile Sensor [29]</p>		<ul style="list-style-type: none"> • Use of novel material Quantum Tunneling Composite (QTC). • Due to improved performance of the sensing material, sensor exhibits good performance.

When compare and contrast each and every of these sensing principles, there can be found advantages and disadvantages associated with them [1], [30]. Table 2.6 shows the summerised advantages and disadvantages for each sensing principles.

Table 2.6: Advantages and disadvantages of sensing principles
Source: Tiwana, M.I., et.al. [1] and Cutkosky, M.R., et.al. [30]

Sensing Principle	Modulated Parameter	Advantages	Disadvantages
Piezoresistive	Changed in resistance	High spatial resolution High scanning rate in mesh Structured sensors	Lower repeatability Hysteresis High power consumption
Capacitive	Change in capacitance	Excellent sensitivity Good spatial resolution Large dynamic range	Noise susceptible Complexity of measurement electronics
Optoelectric	Light intensity/ spectrum change	Good sensing range Good reliability High repeatability High spatial resolution Immunity from EMI	Bulky in size Non-comfortable

Piezoelectric	Strain polarization	High frequency response High sensitivity High dynamic range	Poor spatial resolution Dynamic sensing only
Conductive Polymer/ Composites	Change in conductivity	High sensitivity Good spatial resolution Low cost	Low sensing range Hysteresis occur at certain range

When designing a tactile sensor, it is crucial to choose an optimum sensing principle according to their benefits and limitations so that the designed tactile sensor is suitable for the application.

2.1.4 Current Trends of Tactile Sensing

Figure 2.1 shows some of the current application areas of tactile sensing. Currently, specifically regarding the robotics and biomedical fields, research were limited by having lack of tactile feedback systems. Hence, tactile sensing has come to the spotlight of research and has developed so considerably when comparing with the past decades [31]. Henceforth, numerous research has been conducted regarding tactile sensing and various devices were developed regarding variety of applications. Also application areas of tactile sensing has been expanded as new fields of applications has emerged recently regarding tactile sensing. Figure 2.1 shows some of the application areas of tactile sensing.

Entertainment and communication applications are one of emerging application area considering tactile sensing. Currently, tactile sensing is used in mobile phone displays to input method in gaming consoles [32].

Robotics is one general application area of tactile sensing where many researches were conducted to improve the tactile feedback systems of robots. Considering robotics, tactile sensing is defined as “the continuous sensing of variable contact force”. In robotics, tactile information is useful in object manipulation, force feedback, stability of grasp, contact verification and so on. Hence, currently, researchers are trying to develop sensing fingers, smart skins, industrial grippers and multi-fingered hands for dexterous manipulation associated with tactile sensing [33].

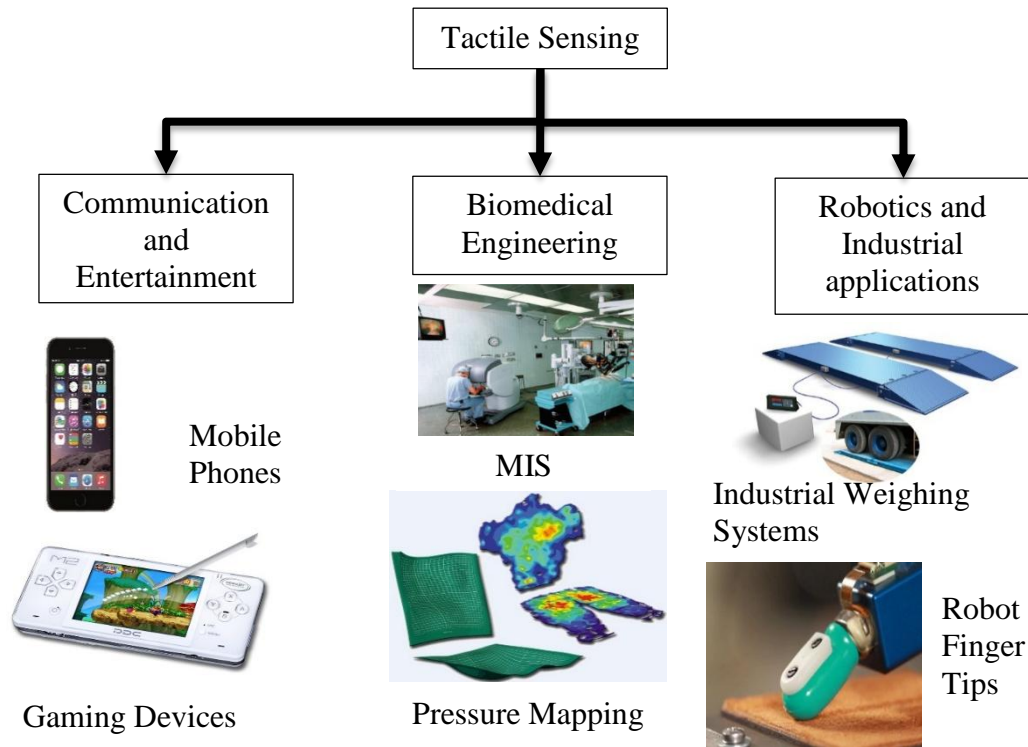


Figure 2.1: Application areas of tactile sensing

Medical field is one another application area of tactile sensing. With the advancements of biomedical engineering, many applications are emerged regarding tactile sensing. Tactile imaging is one such field, which uses tactile sensors to acquire tactile information to construct images. These images are later used to diagnose diseases such as breast cancer, prostate cancer, etc. [34]. Minimally invasive surgery (MIS) is one another biomedical related application of tactile sensing. MIS, which uses minimum incision on a patient's body while doing a surgery, has great advantages considering the patients point of view. Tactile feedback is one of the main feedback channel used in MIS which provide information regarding variety of tissue properties to the surgeon [35], [36].

Other than those applications, usefulness of tactile sensing in medical, prosthetic, agriculture/livestock and food industry are presented in published review articles [37].

2.2 Tactile Imaging

Tactile Imaging, also known as “Mechanical Imaging” or “Stress Imaging”, is one of the method used in medical diagnosing [34]. This technique involves with constructing

high definition stress variation pattern on tissue surfaces by using non-invasive methods [38]. Usually, a probe equip with pressure/force sensor or sensor array, is pressed against the tissue with a constant pressure and map the stress variation pattern, in this imaging method. Information about the elastic properties of internal tissues structures can be taken by these mapped stress variation patterns. Hence, calculations of the properties such as size, shape, nodularity, mobility and consistency, of internal lesions can be done using these acquired data. This process can be identified as mimicking the manual palpation, as traditionally, physicians use manual palpation to identify abnormalities present under soft tissues. But when comparing with manual palpation, tactile imaging has much more sensitivity and therefore it can be taken as a reliable medical diagnosing method [34], [39], [40].

Tactile imaging is a branch of medical imaging techniques available for medical diagnosing. Medical imaging consists of several imaging techniques which uses non-invasive methods to visualize the anatomical structure to monitor and diagnose medical conditions. Other than tactile imaging, there are several other medical imaging techniques available such as

- Ultrasound imaging, which uses high frequency sound waves to visualize anatomical structure.
- Radiography imaging, which uses X-rays to construct images of human body structure.
- Computed Tomography (CT), which uses multiple X-ray projection to construct detailed cross sectional images of human.
- Magnetic Resonance Imaging (MRI), which uses radio waves and a magnetic field to create images of anatomical structure.

When comparing with tactile imaging, these medical imaging techniques have several disadvantages such as,

- Exposure to harmful radiation
- Low specificity
- Complexity of machineries and process
- Excessive cost

Also, most of these imaging techniques only provide spatial information whereas tactile imaging is capable of providing both spatial information and mechanical properties of lesions [41], [42], [43].

2.2.1 Applications of Tactile Imaging

Tactile imaging is frequently used in applications involving diagnosing cancer such as breast cancer and prostate cancer, and screening pelvic organ prolapse [39]. Other than that tactile imaging is also used in applications such as Minimally Invasive Surgery (MIS) [44].

Breast cancer is one of the most common causes of death from cancer among women. According to cancer statistics 2014 by The American Cancer Society, probability of developing a breast cancer for women is stated as 12.3 (1 in 8). The American Cancer Society estimates that in 2014, approximately 235 030 new cases of invasive breast cancer will be diagnosed in the U.S. alone, and 40 430 deaths (40 000 women and 430 men) from this disease are predicted. Current methods of breast screening and diagnosis include Breast Self-Examination (BSE), Clinical Breast Examination (CBE), Mammography, Ultrasound, and Magnetic Resonance Imaging (MRI), biopsy and Tactile Imaging. It has proven that Tactile Imaging is the most cost effective technique to screen breast tumours [45], [46], [47].

Prostate cancer is one of the most common causes of death from cancer among men. According to cancer statistics 2014 by The American Cancer Society, probability of developing a prostate cancer among men is stated as 15.3 (1 in 7). The American Cancer Society estimates that in 2014, approximately 233 000 new cases of invasive prostate cancer will be diagnosed in the U.S. alone, and 29 840 deaths from this disease are predicted. Current methods of prostate assessment include digital rectal examination (DRE), prostate specific antigen (PSA) blood test, transrectal ultrasound (TRUS), computerized axial scanning tomography (CT), endorectal magnetic resonance imaging (MRI) and Tactile Imaging. Several studies demonstrated that Tactile Imaging is a quantitative method to assess several mechanical parameters such as elasticity index of prostate which can be used to differentiate normal tissues with diseased tissues [45], [48].

Pelvic organ prolapse, or genital prolapse, is the descent of one or more of the pelvic structures (bladder, uterus, and vagina) from the normal anatomic location toward or through the vaginal opening. 40% of women older than 50 years have some degree of prolapse on examination. A sense of bulging or protrusion in the vagina is the most specific symptom. Tactile Imaging allows quantitative evaluation of elastic properties of vaginal walls and has a potential for differentiation of normal tissue and diseased tissue under prolapse condition [49], [50].

Minimally invasive surgery (MIS) is a form of surgery intended to provide great benefits to the patient over conventional open surgery by minimizing unnecessary trauma caused in the process of performing a medical procedure. However, it is also well documented that this approach brings a number of corresponding difficulties such as highly limited workspace, specialized tools requiring further staff training and adaption for use, and greatly reduced visual and touch information to the clinical staff performing it. Tactile Imaging can be used to get the touch information in a graphical manner which allows the surgeon to improve surgical performance via autonomous, semiautonomous, or tele-operated control [35], [44].

2.2.2 Existing Tactile Imagers

There have been various tactile imagers developed regarding earlier mentioned tactile imaging applications. Figure 2.2 and Figure 2.3 shows a breast tactile imager developed to screen breast cancer.[51]



Figure 2.2: General view of breast tactile imager
Source: Mechanical Imaging of the Breast [51]

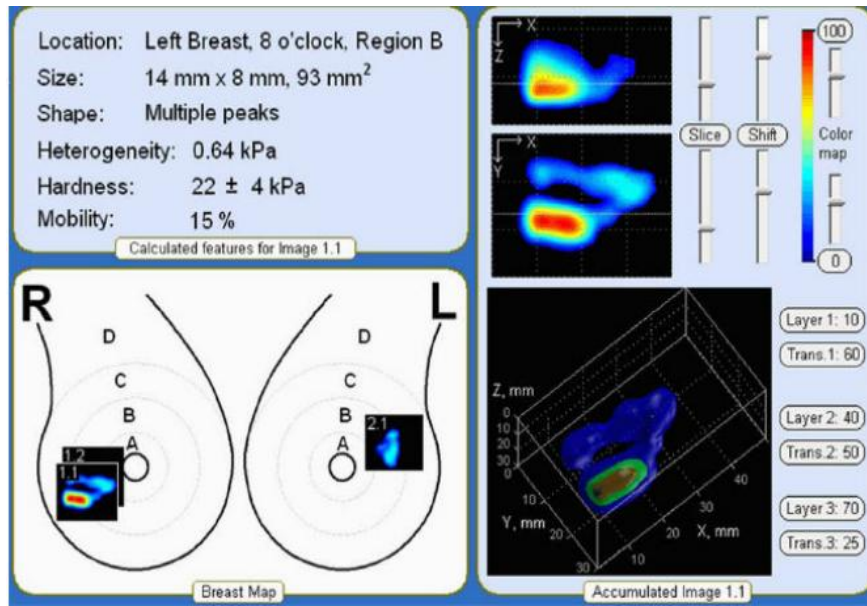


Figure 2.3: Representation of the breast examination results by breast tactile imager.
Source: Mechanical Imaging of the Breast [51]

This developed breast tactile imager consist of a tactile sensor array and a computer to process the acquired data. Currently this tactile imager is produced under the trademark “SureTouch”.[51]

Figure 2.4 and Figure 2.5 shows a prostate tactile imager developed to screen prostate cancer.



University of Moratuwa, Sri Lanka.
Electronic Theses & Dissertations
www.lib.mrt.ac.lk



Figure 2.4: General view of prostate tactile imager.
Source: Prostate Mechanical Imaging: A New Method for Prostate Assessment [52]

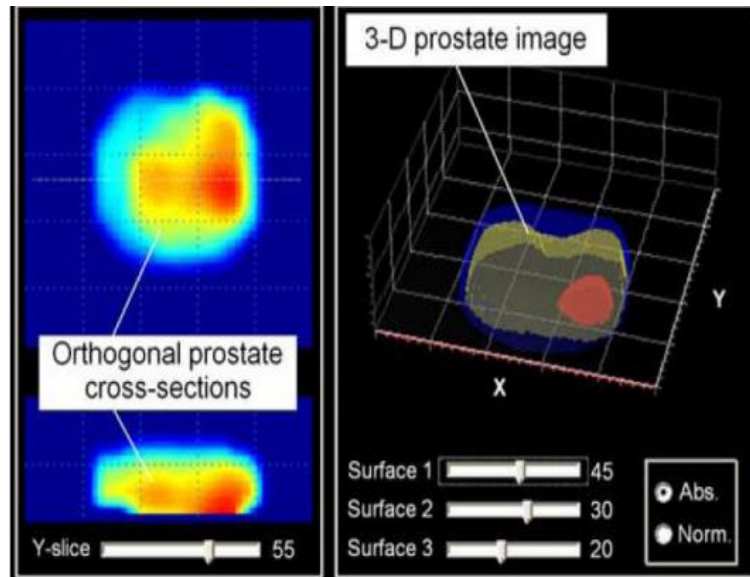


Figure 2.5: Representation of prostate examination results by prostate tactile imager.
 Source: Prostate Mechanical Imaging: A New Method for Prostate Assessment [52]

This developed tactile imager is consist of a trans-rectal probe, data acquisition system and a computer to process the acquired data. The trans-rectal probe is consist of two separate tactile sensor arrays and orientation sensors [52].

Figure 2.6:  Figure 2.7 shows a developed vaginal tactile imager to screen Pelvic Organ Prolapse

University of Moratuwa, Sri Lanka.
 Electronic Theses & Dissertations
www.lib.mrt.ac.lk



Figure 2.6: General view of vaginal tactile imager
 Source: Quantifying vaginal tissue elasticity under normal and prolapse conditions by tactile imaging [53]

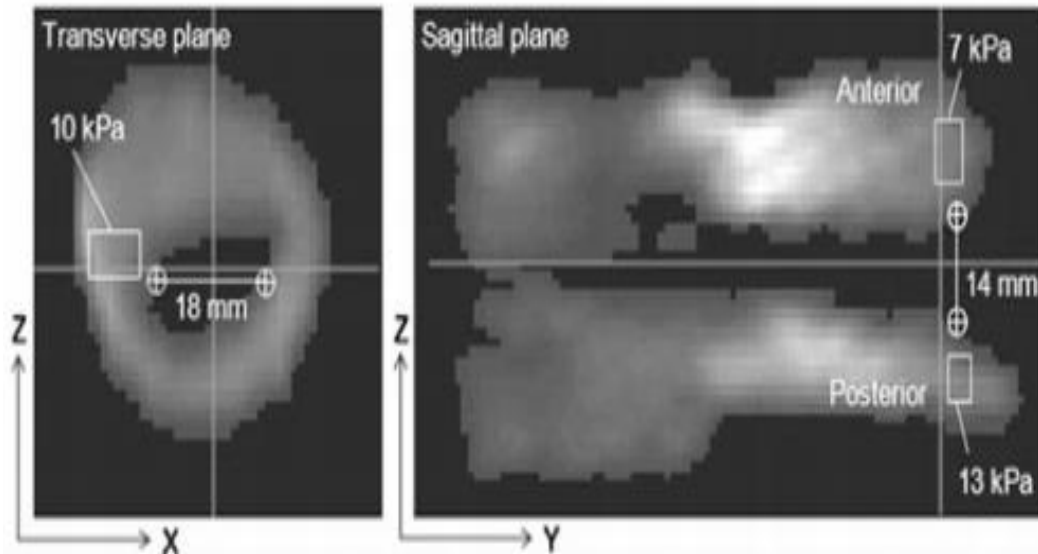


Figure 2.7: Representation of stage III prolapse by vaginal tactile imager.

Source: Quantifying vaginal tissue elasticity under normal and prolapse conditions by tactile imaging

[53]

This developed tactile imager is consist of a trans-vaginal probe, motion tracking system, data acquisition system and a computer to process the acquired data. The vaginal probe consist of a tactile sensor array and a motion tracking system [53].



University of Moratuwa, Sri Lanka
Electronic Theses & Dissertations

www.lib.mrt.ac.lk

2.3 Conclusion – Literature Review

Early cancer screening is a major factor to minimize the fatalities occurs due to cancer, as it allows the physicians to treat cancer patients with a goal of curing cancer. When comparing with 1991 to 2010, risk of death due to cancer has been decreased to 20%. This is mainly due to the advancements in cancer screening methods over the past decades. But when considering the cancer patients in under-developed or developing countries, there is still a high risk of dying from cancer due to the unbearable cost of cancer screening. Optimum solution for this problem is to reduce the cost of cancer screening. As it has been proven that tactile imaging is a cost effective method to screen breast cancers, one method of achieving the early stated goal is to develop low cost tactile imagers [45], [47].

Tactile sensors is the basic element in all the tactile imagers, as they use tactile sensors to acquire stress variation of a surface to construct visual images. So it is vital to

improve sensitivity, response time, long-time stability and cyclic reliability of a tactile sensor, so as to improve the performance to tactile imagers. In other words, it is necessary to develop novel tactile sensors with good performance to develop tactile imagers with best performance [54].



University of Moratuwa, Sri Lanka.
Electronic Theses & Dissertations
www.lib.mrt.ac.lk

3 DEVELOPMENT OF 1-DOF TACTILE SENSOR

3.1 Introduction

According to the conclusion of the literature review related to this research, it was identified that it is important to develop novel tactile sensors with good performance. Hence, one of the main objective of this research is to design and develop tactile sensors for tactile imaging purposes. As per this stated objective, considering the application requirement and resource limitation, a 1-DOF tactile sensor was developed. This chapter describes the procedure and the findings of that newly developed 1-DOF tactile sensor.

There are several aspects to be considered when developing a 1-DOF tactile sensor. These aspects can be categorised in to three categories as shown in Figure 3.1.

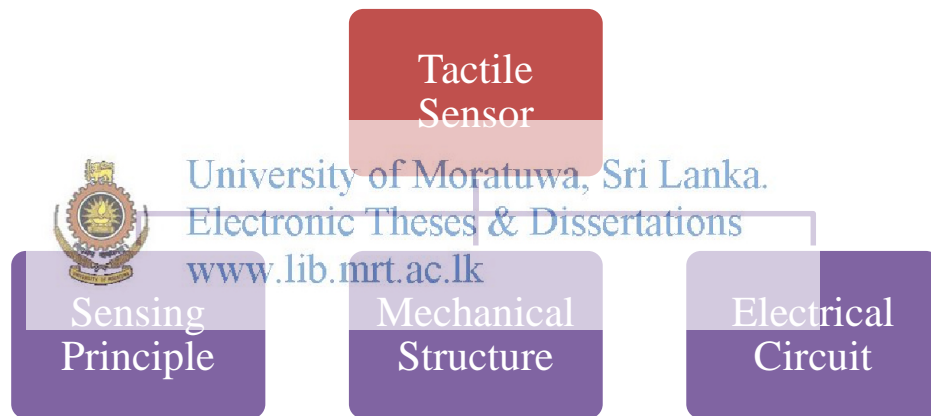


Figure 3.1: Categories to be considered when developing a 1-DOF tactile sensor

Sensing element in a tactile sensor is the element which convert the applied force to the sensor in to the measurable, useful electrical signal. Since there are various sensing principles that can be incorporated with tactile sensors, it is imperative to select an optimum sensing principle considering the application of the proposed tactile sensor.

Mechanical structure is also one important aspect considering the tactile sensor, as it transfer the applied tactile force to the sensor to the sensing element. Force scaling down, overload protection and protection of sensing element can be accomplished by carefully designing the mechanical structure of a tactile sensor.

The next important aspect in developing a tactile sensor is the electrical circuitry of it. This is used to get the electrical signal generated by the sensing element out of the tactile sensor, so that it can be used for further decision making purposes. Development of electrical circuit is critical as unwanted noises can be added to the sensor output signal through this.

All three of these categories directly affect the performance of the tactile sensor in its operation. Hence great care must be taken when developing the tactile sensor under these three categories.

3.2 Sensing principle of the proposed 1-DOF Tactile Sensor

From the literature review, by carefully reviewing the advantages and disadvantages of available sensing principles for tactile sensing, conductive polymer/composite has been chosen to integrate with the proposed sensor so as to sense the force applied to the sensor.

Quantum tunneling composite (QTC™) is such a commercially available conductive composite which is developed by the Peratech Ltd., United Kingdom [55]. QTC™ is a novel material which is developed to enhance the pressure switching and sensing capability, in which conductive filler particle bind with elastomeric binder (typically Silicon Rubber) [56]. This material shows extensive reversible increase in electrical conductivity when mechanically deformed. This is an improved property comparing to the other composite available. Also response to an applied voltage changes according to the amount of deformation from ohmic to nonlinear and hysteresis.

Usually most of the conductive polymers or polymer composites consist of high percentage of carbon black which act as the conductive particles which was enclosed by vulcanised rubber insulators. When such conducting polymer is compressed, the number of conducting elements touching each other increases so that the current conducting paths through the element increases. However, resistance range of such materials restricted between $10^2 \Omega$ and $10^3 \Omega$. However, QTC™ use Inco Nickel Powder as the conducting elements enclosed with elastomeric binder. These nickel nanoparticles contain sharp spikes like protrusions. Figure 3.2 shows the scanning

electron microscopy (SEM) images of the QTCTM. According to these images, spikes present in the nickel particles can be seen clearly. Also it can be identified that these nanoparticles are completely covered and insulated by the elastomeric binder. Hence, even at the extreme deformations, these nanoparticles will not touch with each other. Hence electrical conducting through this material is different from the traditional conductive polymers. In QTCTM, electrical charge is transferred through the tunnelling with the help of sharp protrusions in the nickel nanoparticles [57], [58].

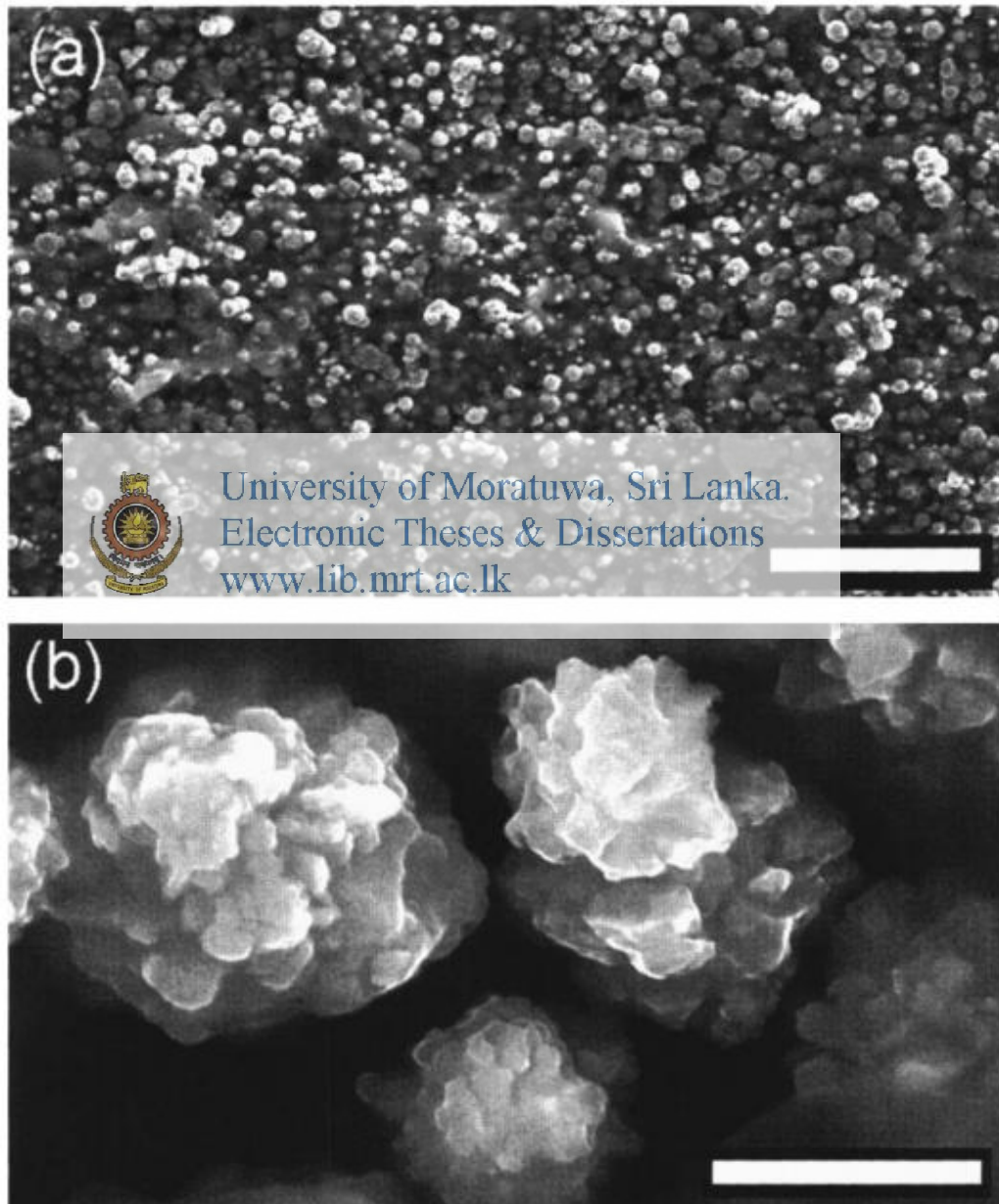


Figure 3.2: SEM image of the cut surface of QTCTM; (a) 50 μm scale. (b) 2 μm scale.
Source: Metal-polymer Composite with Nanostructured Filler Particles and Amplified Physical Properties [57]

Under compression resistance of the QTC™ can fall from $10^{12} - 10^{13}$ Ohm to less than 1 Ohm. Also when the QTC™ compressed into low resistance state, it can carry a large current without damaging the element [58]. Figure 3.3 shows the variation in resistance as a function of compression for a soft silicone-Ni type 123 QTC™.

QTC™ comes in the form of pills of size $3 \text{ mm} \times 3 \text{ mm} \times 1 \text{ mm}$. So the maximum deflection that could obtain for the force applied is limited to under 0.8 mm. this affects the sensor range severely. It is suitable to use a force scaling down structure along with this material to increase the sensor range

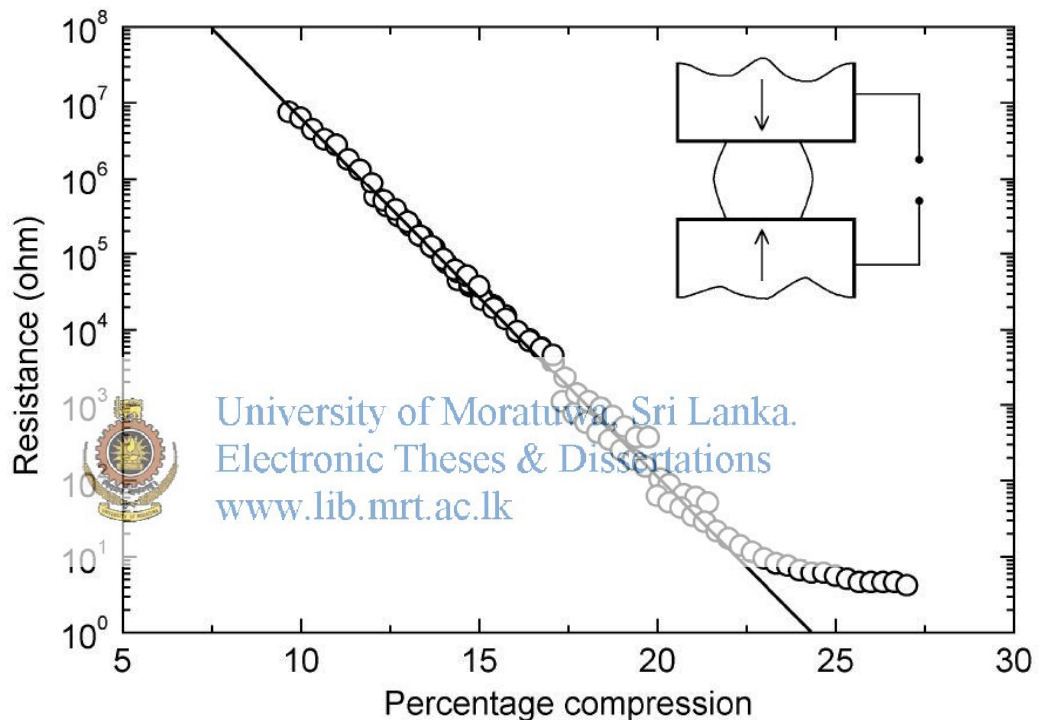


Figure 3.3: Variation in resistance as a function of compression for a soft silicone-Ni type 123 QTC™ composite.

Source: Metal-polymer Composite with Nanostructured Filler Particles and Amplified Physical Properties [57]

3.2.1 Challenges of QTC™

Since this is a novel material, its mechanical properties were not specified in the literature. Founding company, Peratech Ltd. is also focused their research on finding its electrical properties rather than finding mechanical properties of the material such as young's modulus, poissons ratio, etc.

So an experiment was carried out to find the young's modulus of the QTC™ material. Figure 3.4 shows the experimental setup and experiment procedure as follows,

- A gradually increasing force will be applied to the QTC™ material using Universal Tensile Testing Machine.
- Force required to deflect the material at each set displacement points is noted down.
- Relationship between the force applied and the material deflection will be found.
- Young's modulus of the material will be calculated using the relationship found.

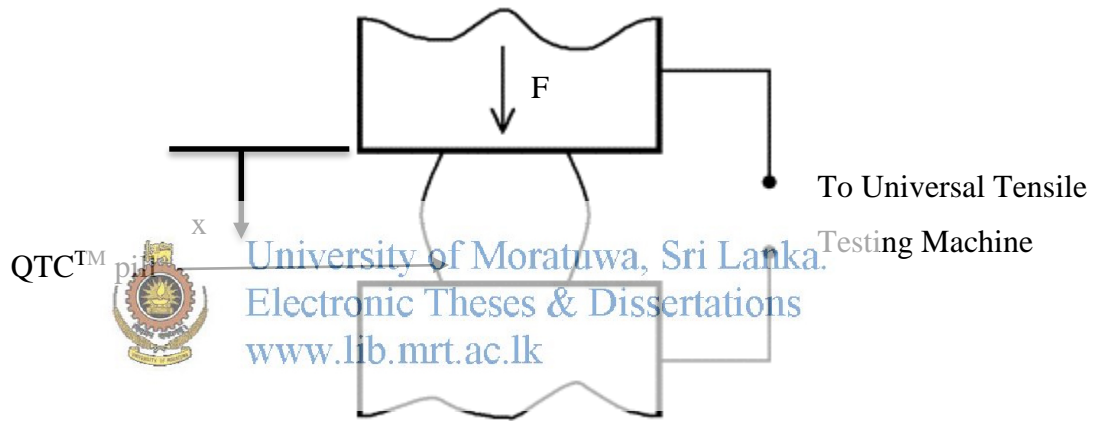


Figure 3.4: Experiment setup to find Young's modulus of QTC™

Considering the forces acting on the QTC™ pill by Hook's Law, Equation 3.1 can be stated,

$$\frac{F}{A} = E \times \frac{x}{t} \quad (3.1)$$

Where, E is the Young's modulus, A is the area of the QTC™ pill and t is the thickness of the QTC™ pill.

Hence, relationship between force applied and the deflection of QTC™ pill should be as follows as Equation 3.2,

$$F = \frac{E \times A}{t} x \quad (3.2)$$

Figure 3.5 shows the experiment results for the QTC™ pill.

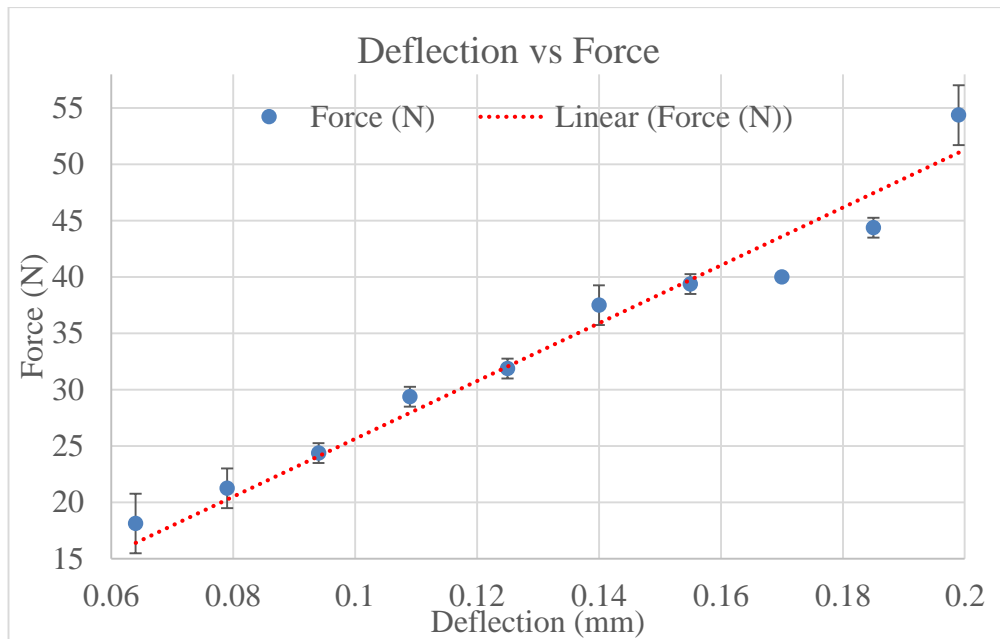


Figure 3.5: Experiment results of QTC™ pill

Two data sets were taken from the experiment and the above plot was plotted by taking the mean values among those two data sets. Standard deviation with respect to the mean at each data point is also plotted in the Figure. 3.5. A linear trend line was plotted corresponding to the experimental data, so that equation of the line will be taken by Equation 3.2.



University of Moratuwa, Sri Lanka
Electronic Theses & Dissertations
www.lib.mrt.ac.lk

From the results, slope of the trend line is taken as,

$$m = 256.43 \frac{N}{mm}$$

From Equation 3.2, m can be taken as,

$$m = \frac{E \times A}{t}$$

Hence we can expect that the Young's Modulus of the QTC™ material takes a values as following Equation 3.3,

$$E = \frac{m \times t}{A} \tag{3.3}$$

Hence, Equation 3.4 can be taken as

$$E = (256.43 \frac{N}{mm}) \frac{A}{t} \quad (3.4)$$

QTC™ pills that was used for this experiment had standard size of 3 mm × 3 mm × 1 mm. Hence, thickness of the QTC™ pill can be taken as 1 mm and the surface area of the QTC™ pills can be taken as 9 mm².

Following are the values measured for each unknown of Equation 3.4,

$$t = 1 \text{ mm}, \quad A = 9 \text{ mm}^2$$

Hence,

$$E = \left(\frac{256.43 \text{ N}}{\text{mm}} \right) \frac{1 \text{ mm}}{9 \times 10^{-6} \text{ m}^2}$$

$$E = 28.49 \times 10^6 \text{ Pa}$$

$$E = 28.49 \text{ MPa}$$

Hence Young's modulus for the QTC™ pill can be taken as 28.49 MPa. This value can be taken for further analysis corresponding to the mechanical properties of the QTC™.



University of Moratuwa, Sri Lanka.

3.3 Mechanical Structure of the Proposed 1-DOF Tactile Sensor

3.3.1 Working Principle of the Proposed Sensor Structure

After finalising the sensing element, the next step of developing a tactile sensor is to develop the mechanical structure. When developing a mechanical structure for a tactile sensor, it is important to have an idea about the working principle of the sensor, as it will act as a guide when developing a mechanical structure. Figure 3.6 shows the free body diagram of the proposed working principle regarding the 1-DOF tactile sensor. For this free body diagram effect of structure and sensing element is taken and behaviour of these elements under loading is evaluated.

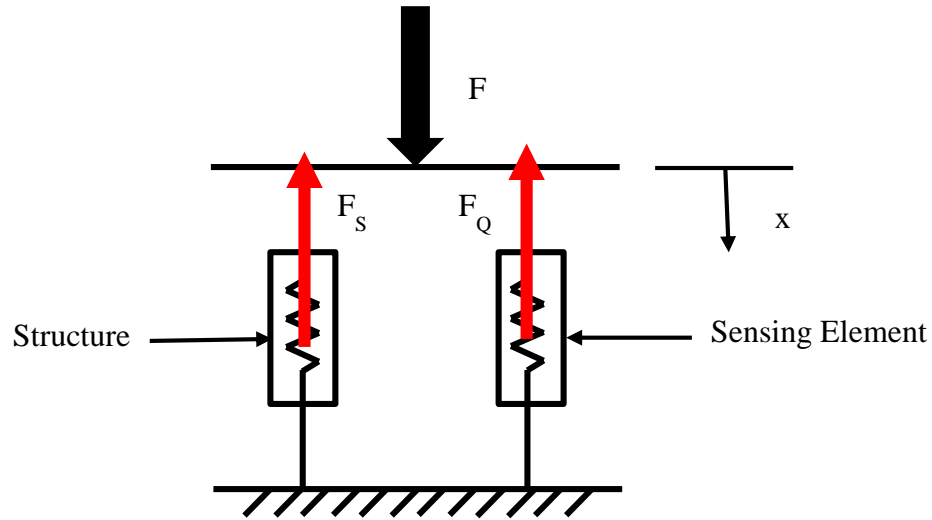


Figure 3.6: Free body diagram of the proposed working principle of the mechanical structure
 In this Figure 3.6, F_S represents the reaction force from the structure and F_Q represents the reaction force from the sensing element under F loading and x is the total deformation of the sensor for that F loading. Using this free body diagram, a mathematical model can be proposed to elaborate the working principle of the proposed 1-DOF tactile sensor.

Considering the static balance of the free body diagram, Equation 3.5 can be expressed as follows,

$$F = F_S + F_Q \quad (3.5)$$

Considering the structural deformation under loading, Equation 3.6 can be used to express F_S as follows,

$$F_S = \frac{E_{Structure} \times A_{Structure}}{t_{Structure}} x \quad (3.6)$$

Hence, stiffness (K_S) of the structure can be express as Equation 3.7,

$$K_S = \frac{E_{Structure} \times A_{Structure}}{t_{Structure}} \quad (3.7)$$

Considering the mechanical deformation of sensing element under loading, Equation 3.8 can be used to express F_Q as follows,

$$F_Q = \frac{E_{QTC} \times A_{QTC}}{t_{QTC}} x \quad (3.8)$$

Hence, stiffness (K_Q) of the sensing element can be express as Equation 3.9,

$$K_Q = \frac{E_{QTC} \times A_{QTC}}{t_{QTC}} \quad (3.9)$$

Hence from Equation 3.5,

$$F = K_S \times x + K_Q \times x$$

Hence the mathematical relationship between the total deformation (x) of sensor and the applied load (F) can be expressed by Equation 3.10,

$$x = \frac{F}{K_S + K_Q} \quad (3.10)$$

3.3.2 Proposed Structural Design 1 for 1-DOF Tactile Sensor

Box shape geometry selected for this conceptual design. To decrease the force acting on the sensing element four springs is used. To guide the movement within the structure four guide pins are used. This ensures structure will not show unusual movements when the force applied. Also force transfer to the sensing element through the structure will be perpendicular to the surface of the sensing element. Due to this maximum sensitivity can be achieved. Figure 3.7, Figure 3.8 and Figure 3.9 shows the conceptual design of this structure. Refer Appendix A for detailed drawings of this design

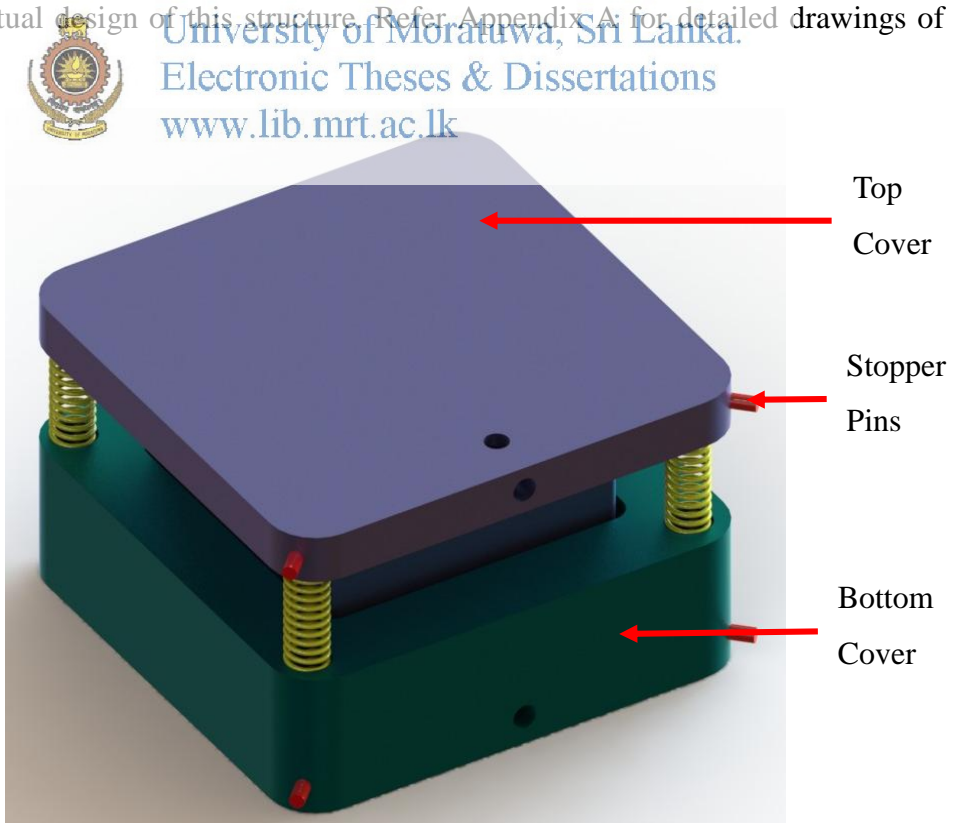


Figure 3.7: Isometric view conceptual design of structural design 1 and component assembly

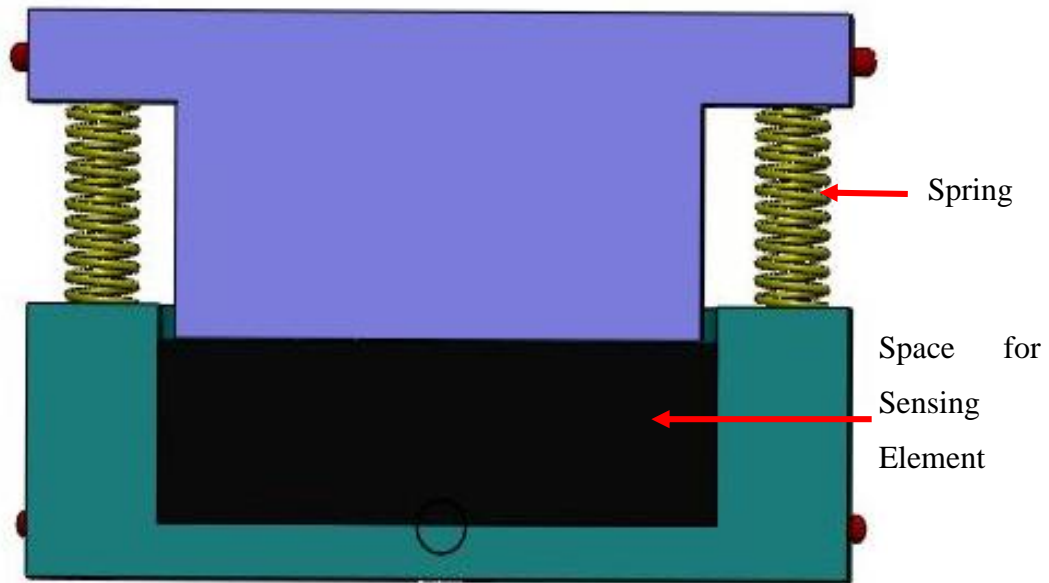


Figure 3.8: Sectional Front elevation conceptual design of structural design 1 and component assembly

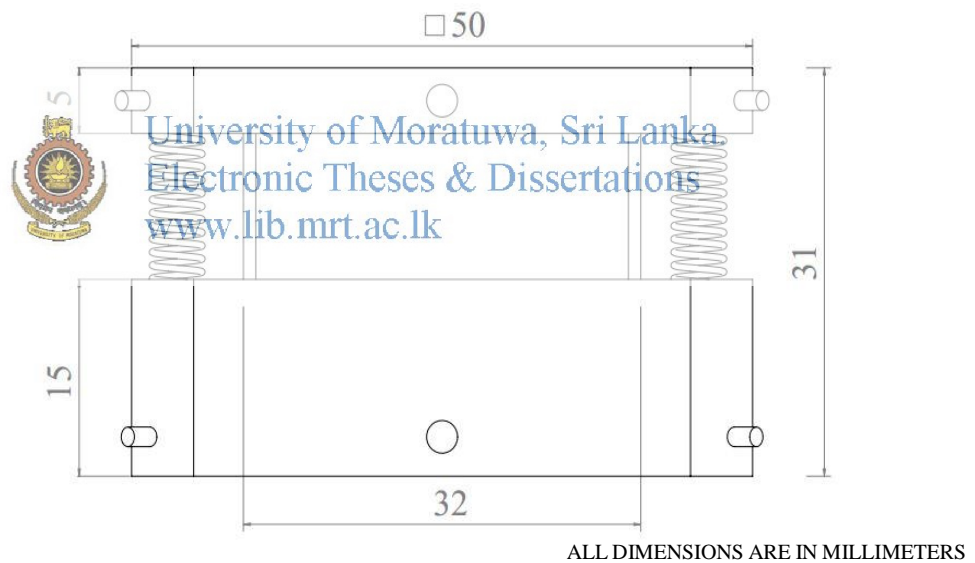


Figure 3.9: Basic dimensions of the proposed sensor structure 1

Following listed limitations and problems occurred when producing the structure according to this design,

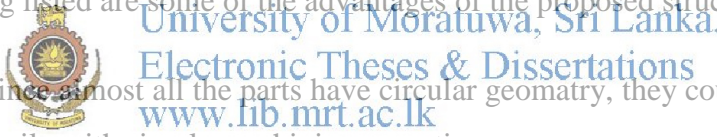
- box shape geometry required lengthy and time consuming machining operations to manufacture.

- Complexity of the structure has increase due to the several different parts in this structure.
- Alighning problems occure when assembling the parts.
- Precision machining operations requiried when machining the guide pins and guide holes because of their dimensional tolarances.
- Even with the guide pins, smooth perpendicular movement can not expect with respect to the force applied surface.

3.3.3 Proposed Structural Design 2 for 1-DOF Tactile Sensor

This design contains piston cylinder system with a single spring. Force will be applied to the top face of the piston. Due to this, piston tend to move along the cylinder axis and transfer that force to the sensing element. Spring applied in this structure will decrease the magnitude of the force applied to the sensing element. Figure 3.10 and Figure 3.11 shows the conceptual design of this structure and the arrangement of sensing element inside the structure and the components of the Sensor Assembly.

Following listed are some of the advantages of the proposed structural design 2.

- 
- Since almost all the parts have circular geomatry, they could be manufactured easily with simple machining operations.
 - Allignment problems won't occure at the assembling stage due to the minimum number of parts and the geomatry of the parts,.
 - Easy manufaturability and simple assembling operations will reduce the overall manufacturing cost and time.
 - It is possible to give a pre compression to the sensing element because of the thread between the base cup and the lid.

Considering the manufacturing and economical advantages, design 2 was selected as the final design for the force scaling down structure. Also flexibility of the design was also taken to acount when finalising the final conceptual design. Figure 3.12 shows the basic dimension of the proposed structure and Figure 3.13 shows the elaborated conceptual design of the design 2 and the arrangement of the components in the Sensor Assembly. Refere Apendix B for detail production drawings of the design.

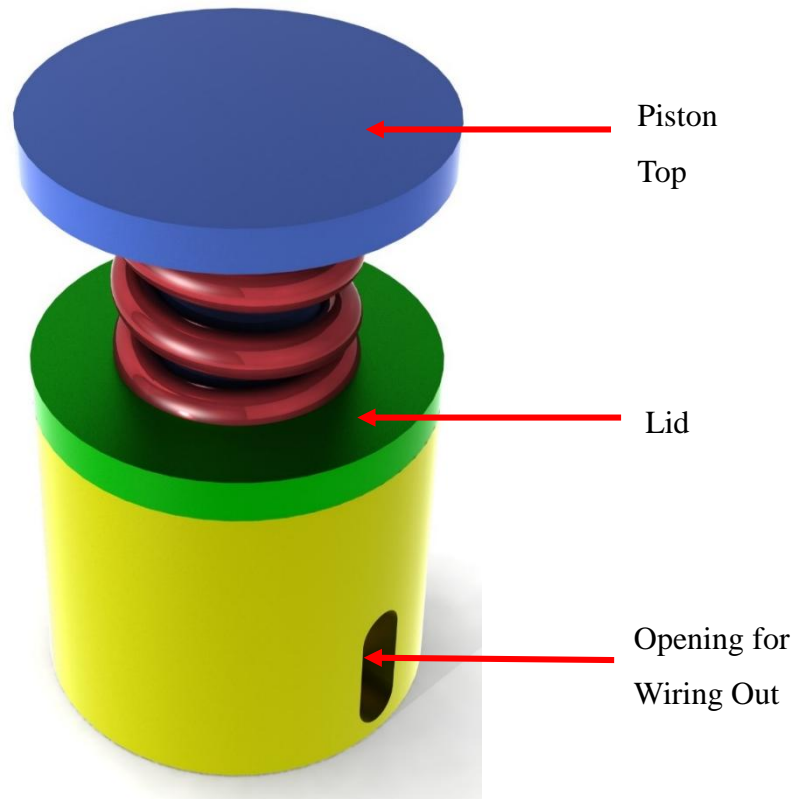


Figure 3.10: Isometric view conceptual design of structural design 2 and component assembly



University of Moratuwa, Sri Lanka.
 Electronic Theses & Dissertations
www.lib.mrt.ac.lk

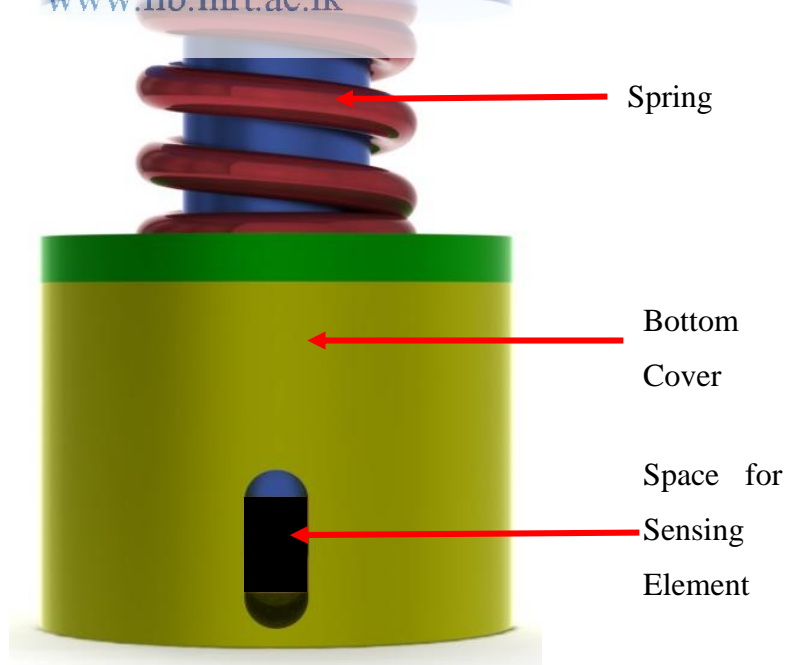
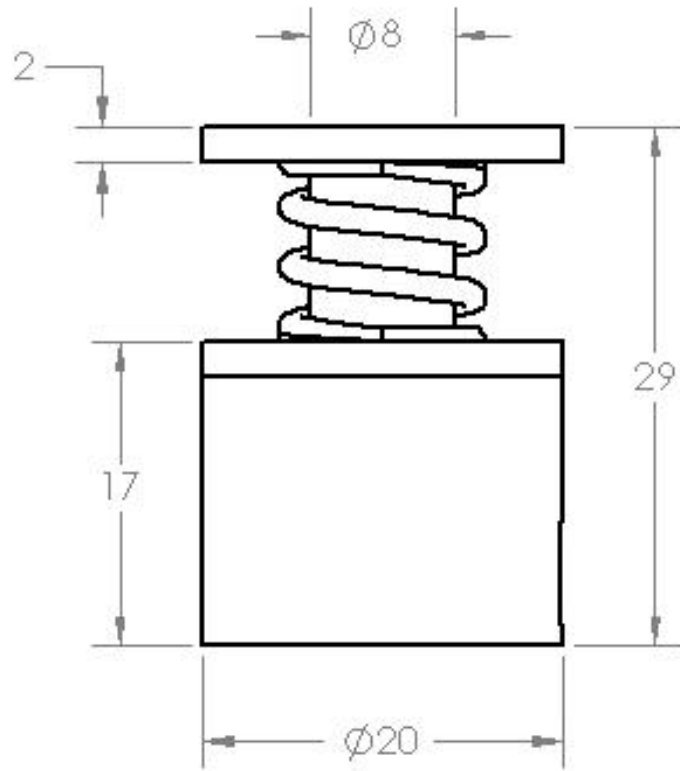


Figure 3.11: Sectional Front elevation conceptual design of structural design 2 and component assembly



ALL DIMENSIONS ARE IN MILLIMETERS

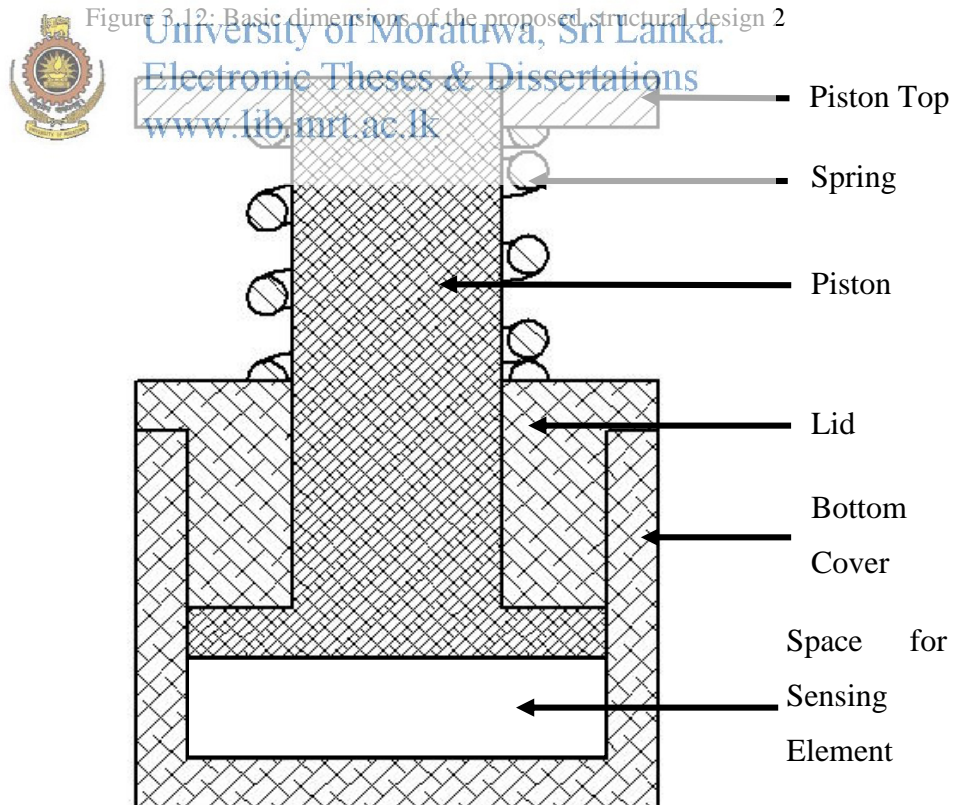


Figure 3.13: Components arrangement in the assembly of proposed structural design 2

3.4 Analysis and Simulation of Proposed 1-DOF Tactile Sensor

In the next stage, using the finite element analysis (FEA) software ANSYS, a structural analysis is performed. One of the major objective of performing a structural analysis is to forecast the behaviour of the sensor for different spring gauges. ANSYS analysis performed here has the capability to indicate amount of deflection of the sensing element for each force value. Table 3.1 shows the inputs for the ANSYS structural analysis.

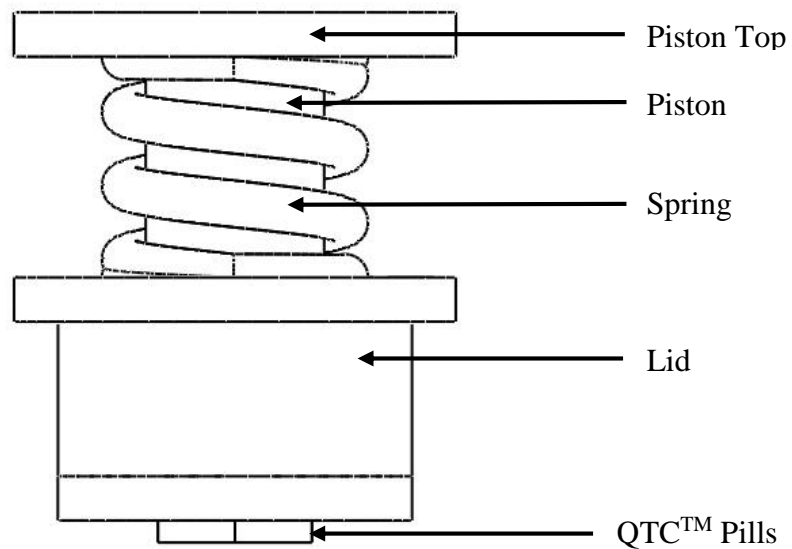
Table 3.1: Input Parameters for the ANSYS finite element analysis

Parameter			Specification		
			Unit	Value	
Material Data	Spring	Material Type	ASTM A228		
		Density	Kg/m ³	7850	
		Modulus of Elasticity	Gpa	210	
		Poisson Ratio	0.313		
	Structure	Density	Kg/m ³	3861	
		Modulus of Elasticity	MPa	28.49	
		Poisson Ratio	0.3		
		Material Type	Aluminum 1060		
		Density	Kg/m ³	2700	
		Modulus of Elasticity	Gpa	70-80	
		Poisson Ratio	0.33		
		Contact Type			Bonded
	Mesh	Element Type	Spring	Hex Dominant	
			Structure		
Sensing Element					
Minimum Element Size		mm	0.5		
Minimum Skewness		1.31E-10			
Average Skewness		0.42366			

For a FEA, there are four different aspects that should be considered.

- Geometry
- Material Data
- Mesh
- Boundary Conditions

For this FEA, corresponding to the structural design 2 of proposed 1-DOF tactile sensor, only the load bearing components were considered. These components were modelled and assembled together using SolidWorks software and imported to the ANSYS software. Figure 3.14 shows the geometry considered for the FEA.



University of Moratuwa, Sri Lanka.
Electronic Theses & Dissertations
www.lib.mrt.ac.lk

Figure 3.14. Geometry Considered for the FEA

The next step of the FEA is to define material properties of each component of imported geometry. In this analysis, Aluminium 1060 material was assigned using the material library available with ANSYS software for structural components such as piston top, piston and lid. Considering QTC™, modulus of elasticity was specified according to the results of previous experiment and density was calculated. Poisons ratio of QTC™ was found by conducting FEA for QTC™ and tallying the results with the experiment results from the previous experiment conducted for QTC™. Data for spring material properties were taken from the data sheet in Appendix C.

A mesh was created according to the parameters specified in Table 3.1. In this mesh hex dominant elements were chosen as the overall mesh elements. In ANSYS, quality of the mesh can be determine by the average skewness and minimum skewness of the mesh. According to the values in Table 3.1 mesh created for this FEA has sufficient quality.

The next important step in conducting an FEA is to define boundary conditions. For this FEA, a boundary load was applied to the top surface of the piston top and fixed constraint was given to the bottom surface of QTC™ elements.

Final step of FEA is to calculate the problems according to the specified parameters. Figure 3.15 and Figure 3.16 shows the displacement plot results of the sensor structure with spring gauges 1.0 mm and 1.5 mm respectively.

Figure 3.17 and Figure 3.18 shows the equivalent stress plot results of the sensor structure with spring gauges 1.0 mm and 1.5 mm respectively.

Figure 3.19 shows the total deformation plot results for the QTC™ pill under loading condition. Figure 3.20 shows the equivalent stress plot results for the QTC™ pill under loading condition.

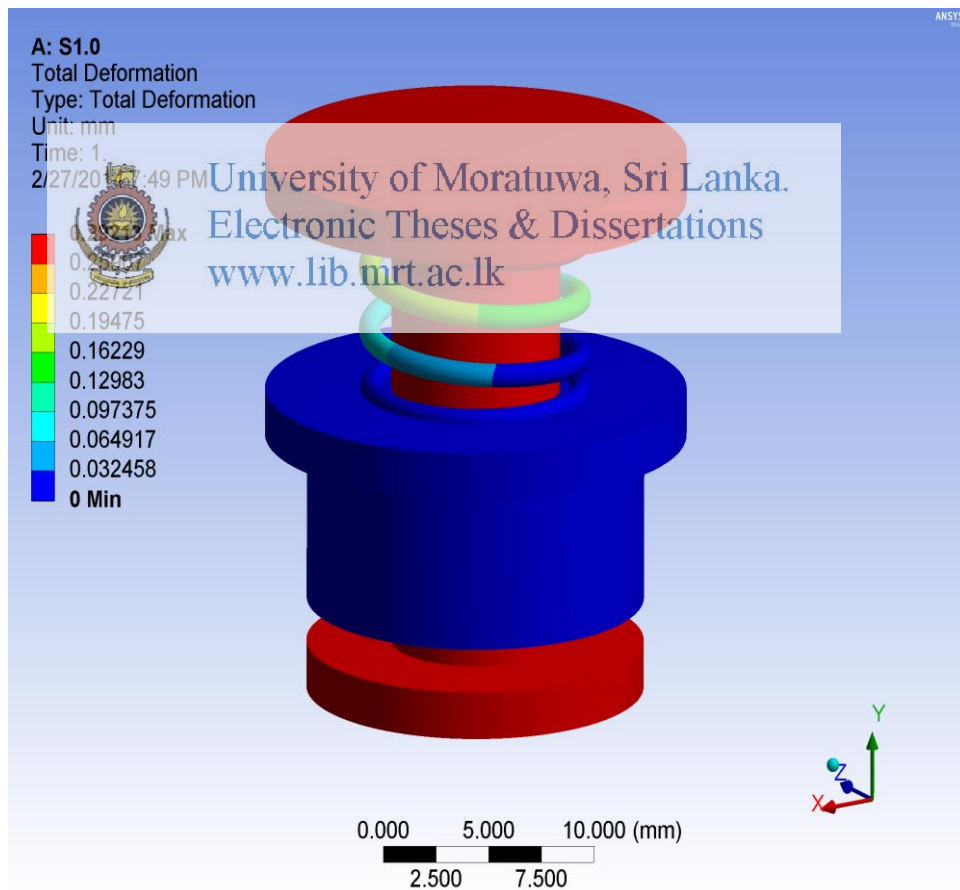


Figure 3.15: Total deformation of the sensor structure under loading for spring gauge 1.0 mm

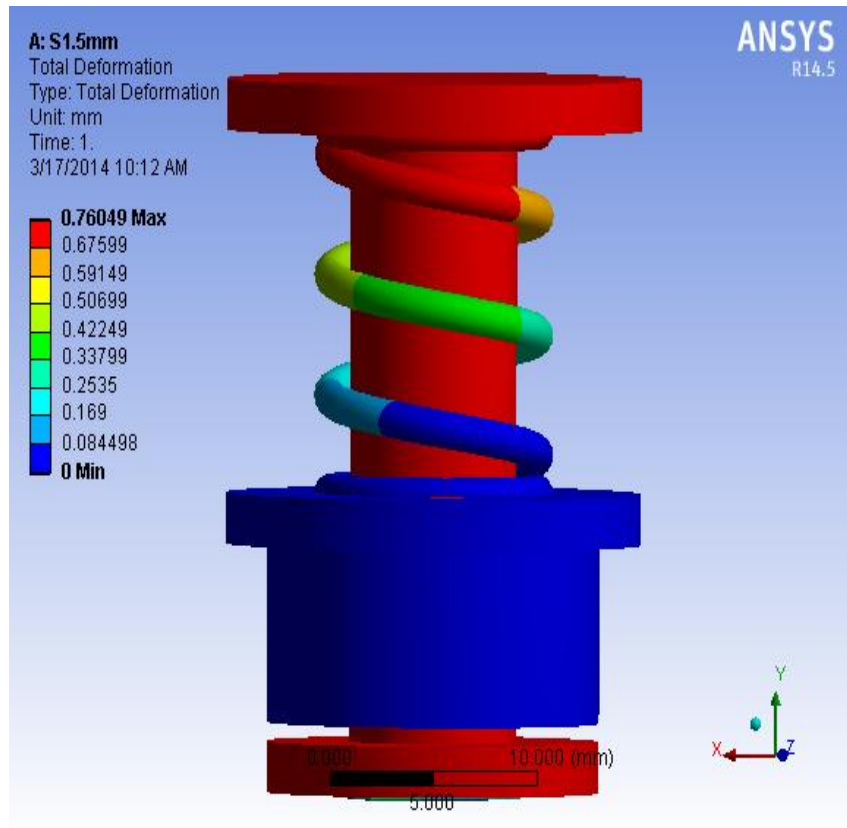


Figure 3.16: Total deformation of the sensor structure under loading for spring gauge 1.5 mm

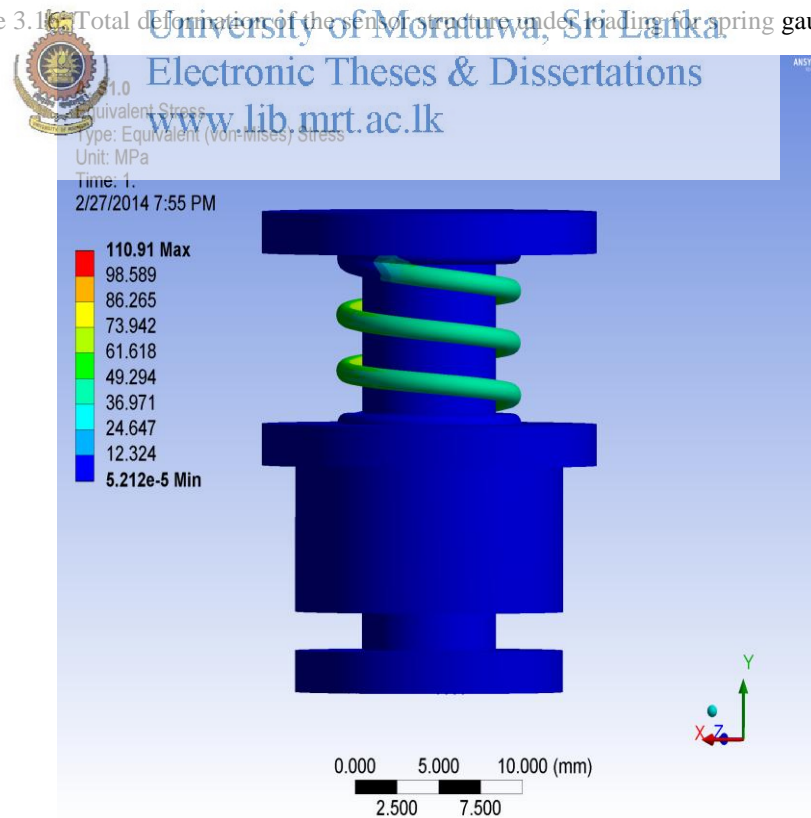


Figure 3.17: Equivalent Stress of sensor structure under loading for spring gauge 1.0 mm.

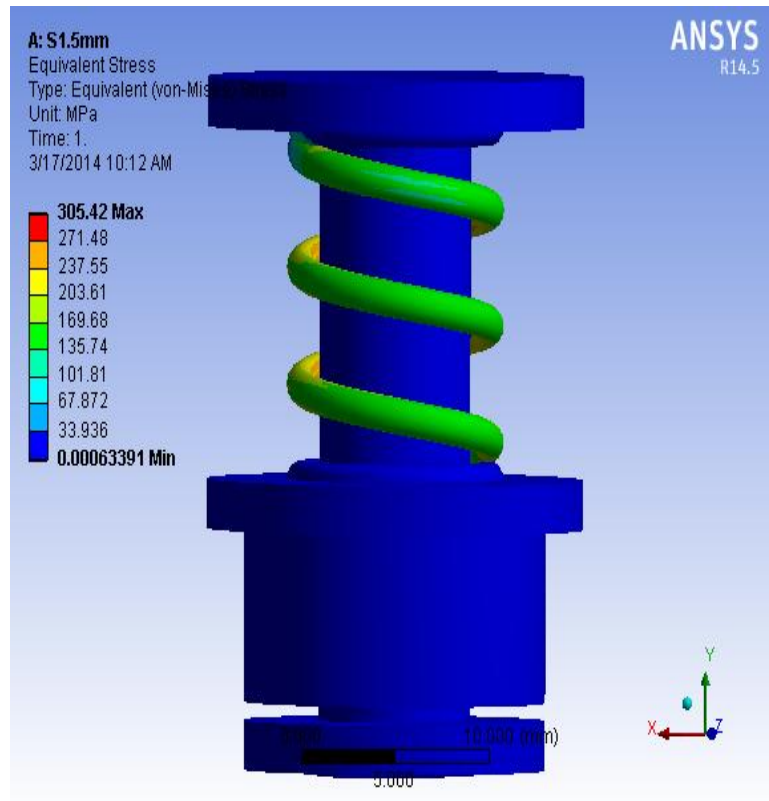


Figure 3.18: Equivalent Stress of sensor structure under loading for spring gauge 1.5 mm.

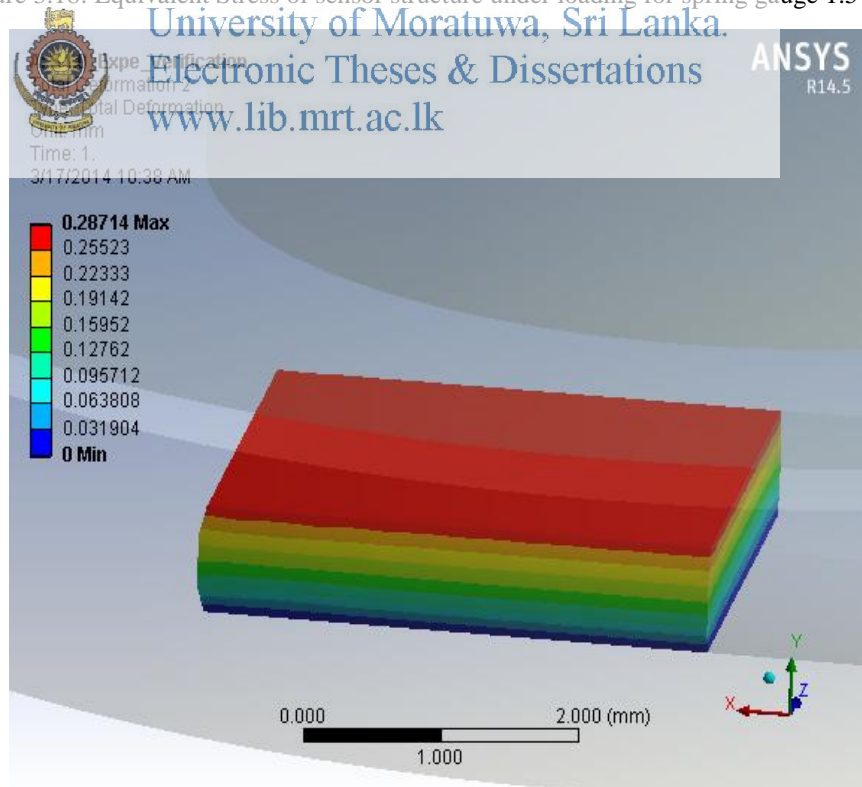


Figure 3.19: Total deformation plot of QTCTM pill.

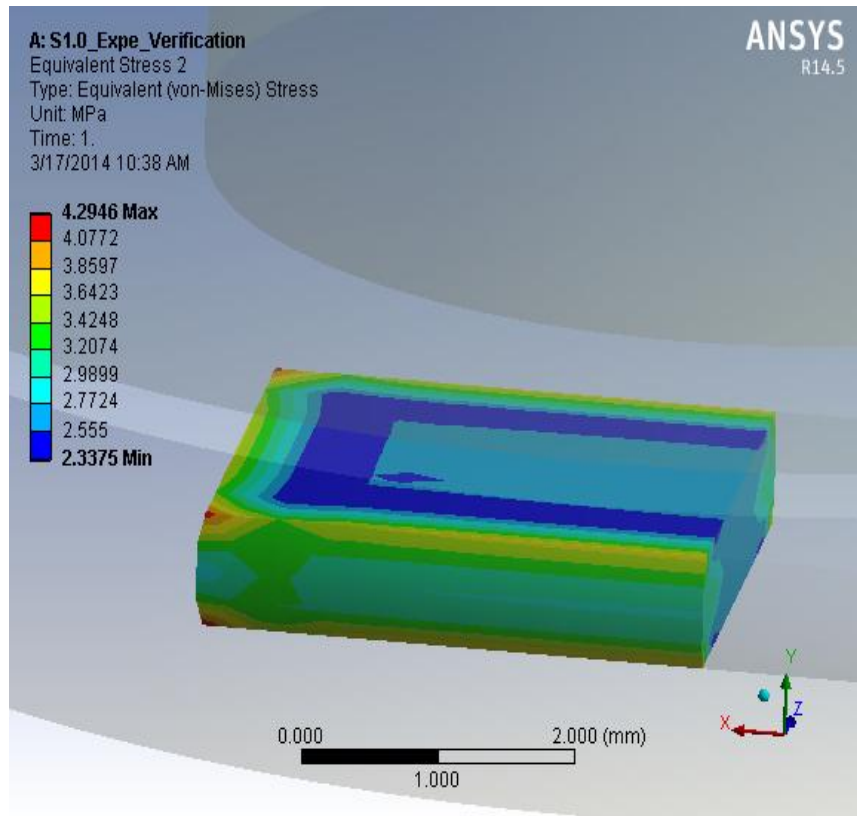


Figure 3.20: Equivalent stress plot of QTCTM pill.

University of Moratuwa, Sri Lanka.

Electronic Theses & Dissertations

www.lib.mrt.ac.lk

This FEA was performed for a range of spring gauges varying from 0.8 mm to 1.8 mm. Purpose of this analysis is to find the behaviour of structure for different spring gauges under loading conditions and the optimum spring gauge for the proposed sensor structure that will be compatible with the application. From this analysis it was identified that the 1.0 mm and 1.5 mm spring gauges are the optimum spring gauges considering the proposed sensor structure.

Table 3.2 shows the results of these two analysis with maximum force range that can be applied for spring gauges 1.0 mm and 1.5 mm. Also it shows the maximum deflection of the sensor for each spring gauges at corresponding maximum force that can be applied. From the results it can be seen that for different spring gauges, force range of the proposed sensor is varying. This characteristic can be used to design tactile sensors with force range suitable for the particular application.

Table 3.2: Results of FEA Analysis for different spring gauges

Characteristic	Unit	Spring Gauge 1.0 mm	Spring Gauge 1.5 mm
Force Range	N	0-250	0-270
Total Deformation (Overall)	mm	0.72733	0.76049
Equivalent Stress (Overall)	MPa	315.74	305.42
Total Deformation (QTC™ pill)	mm	0.71784	0.74293
Equivalent Stress (QTC™ pill)	MPa	10.737	11.206

3.5 Fabrication of Designed 1-DOF Tactile Sensor

After verifying the proposed structure and the working principle through the FEA simulation, the next stage of developing the tactile sensor is to fabricate the sensor using available manufacturing methods. When fabricating the sensor, two major fabrications can be identified regarding the proposed tactile sensor,

- Fabrication of Sensing Element Configuration
- Structural Fabrication

Following sections discuss these two major fabrications in detail.

3.5.1 Fabrication of Sensing Element Configuration

Fabrication of sensing element configuration is one of the major fabrications regarding a sensor development. Electrodes are fabricated in the sensor to take the output of the sensing element for particular loading condition.

In this sensor development stage, an electrode design was proposed as shown in Figure 3.21 (a) to get the sensor output for further decision making. In this electrode design, sensing element (QTC™) is sandwiched between two electrodes and output of the sensor is taken from these two electrodes.

When fabricating the electrode, two copper cladded board was used shaped as geometry shown in Figure 3.21 (b). This geometry is preserved so that the electrical shortages won't occur between the two electrodes.

Another important step of electrode fabrication is to ensure the physical contact between the electrode and the sensing element. For this fabrication, graphite based conductive glue was used to create the physical contact. Since it work as an adhesive, it will not only create a current conducting path between the electrode and the sensing element but also it will bind the sensing element to the electrode.

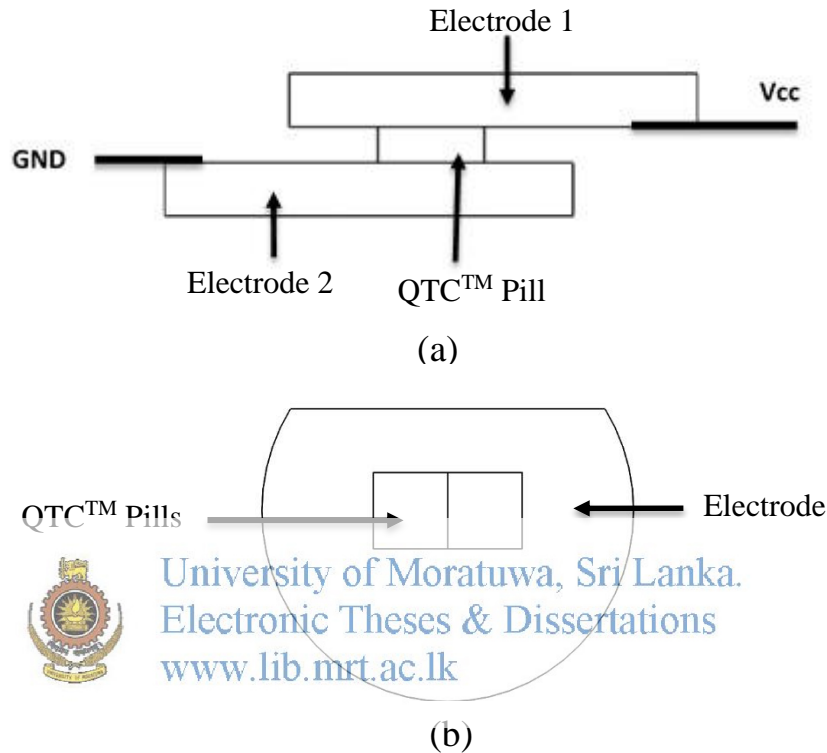


Figure 3.21: Electrode Fabrication; (a) Electrode arrangement with sensing element. (b) Electrode Design

3.5.2 Structural Fabrication and Assembling

Next stage of sensor fabrication is to fabricate structural components. Production drawing of each structural components were generated (refer Appendix B) to fabricate them using machining operations. Since all the structural components have cylindrical geometry, it was decided to fabricate these components using conventional manufacturing processes such as turning, milling and drilling machining operations, preserving the geometrical and dimensional tolerances specified in the production drawings. To perform these machining operations, conventional machining centres were used such as conventional lathe machines, conventional milling machines and

conventional drilling machines. Aluminium has chosen as the material to be used to fabricate these structural components as Aluminium is light weight, durable material with sufficient material properties. After fabricating the structural components, they were assembled together and Figure 3.22 shows the fabricated structural components and the assembled sensor structure.



Figure 3.22: Fabricated structural components and assembled sensor structure

After fabricating the structure, it was assembled together along with the sensing element configuration. Since Aluminium is a conductive material, there can be current leakages through the structure. Such current leakages will add noise to the output signal of the sensor and correct behaviour of the sensing element cannot be tracked so as to measure inputs of this sensor accurately and precisely. But due to the use of copper cladded boards to fabricate electrodes, there won't be such issues. Figure 3.23 shows the fully assembled 1-DOF tactile sensor.

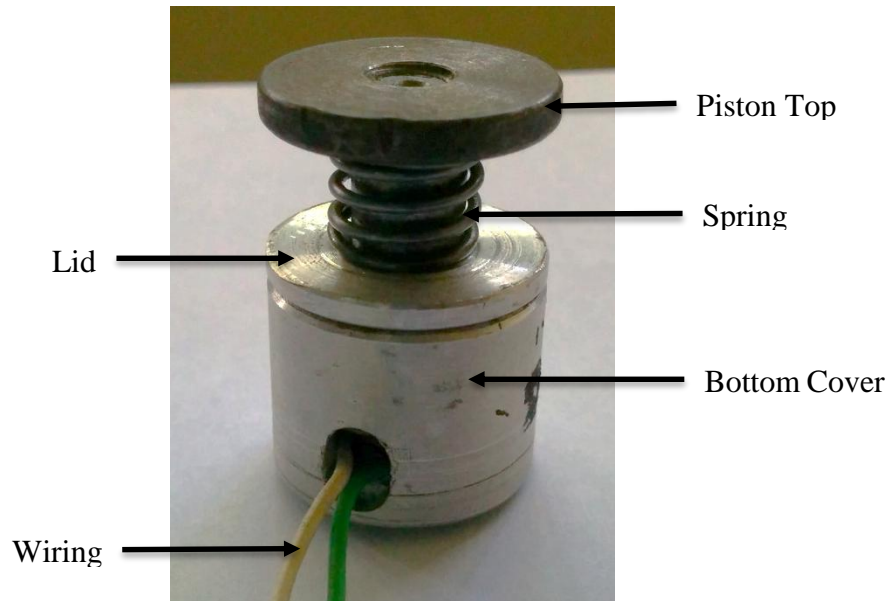


Figure 3.23: Fabricated 1-DOF Tactile Sensor

3.6 Testing of Developed 1-DOF Tactile Sensor and Results

After the fabrication, next stage of developing a sensor is to test and calibrate the sensor for further use in applications. Output variation with regard to the input variation is important when calibrating a sensor. Calibration of sensor is done so that the performance of the sensor will be free of structural errors. Performance errors usually occurs when the sensor output is deviate from expected output for a corresponding sensor input. Usually structural errors are repeatable errors which consistently added to the output at each measurement. These errors can be calculated and compensated at the signal processing stage so that the sensor output is free of structural errors[59].

Hence for the calibration purposes an experiment was designed regarding the developed 1-DOF tactile sensor. In this experiment the main motive was to identify the variation of the sensor output signal with respect to the load applied. Hence, this experiment was designed to measure the sensor output for certain force intervals at both loading and unloading conditions. Universal Tensile testing machine was used in this experiment to apply the load on top to the developed 1-DOF tactile sensor. This developed sensor was connected to a voltage divider circuit, where the fix resistor (R_f) value to be $10\text{ M}\Omega$. Using a digital Multimeter, voltage output across the sensor was

measured. Figure 3.24 shows the system layout of the experimental setup used in this experiment.

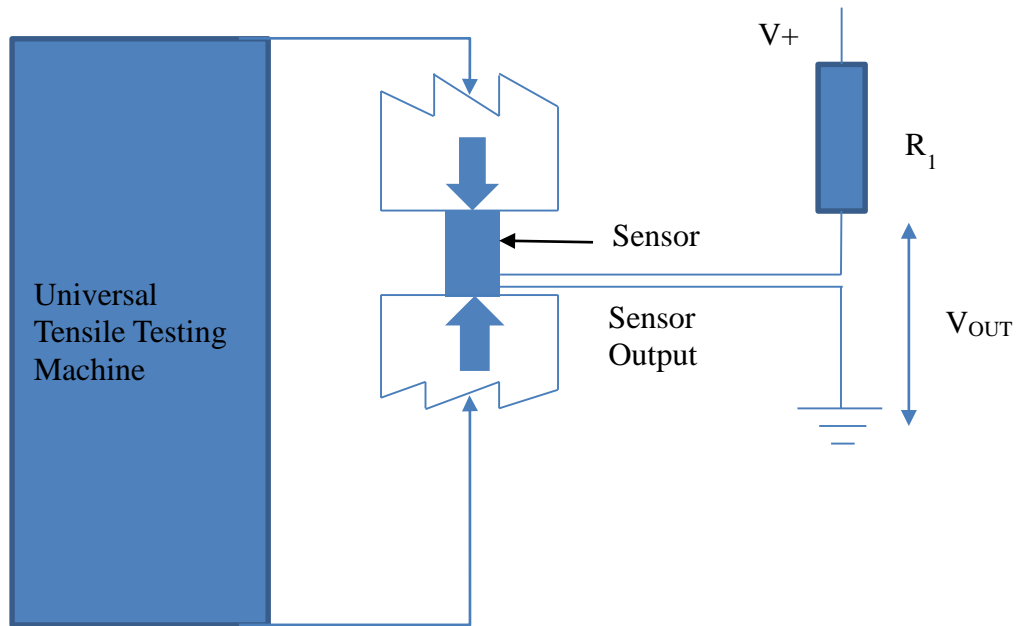


Figure 3.24: System layout of the experimental setup

Figure 3.25 shows the plotted results for this experiment

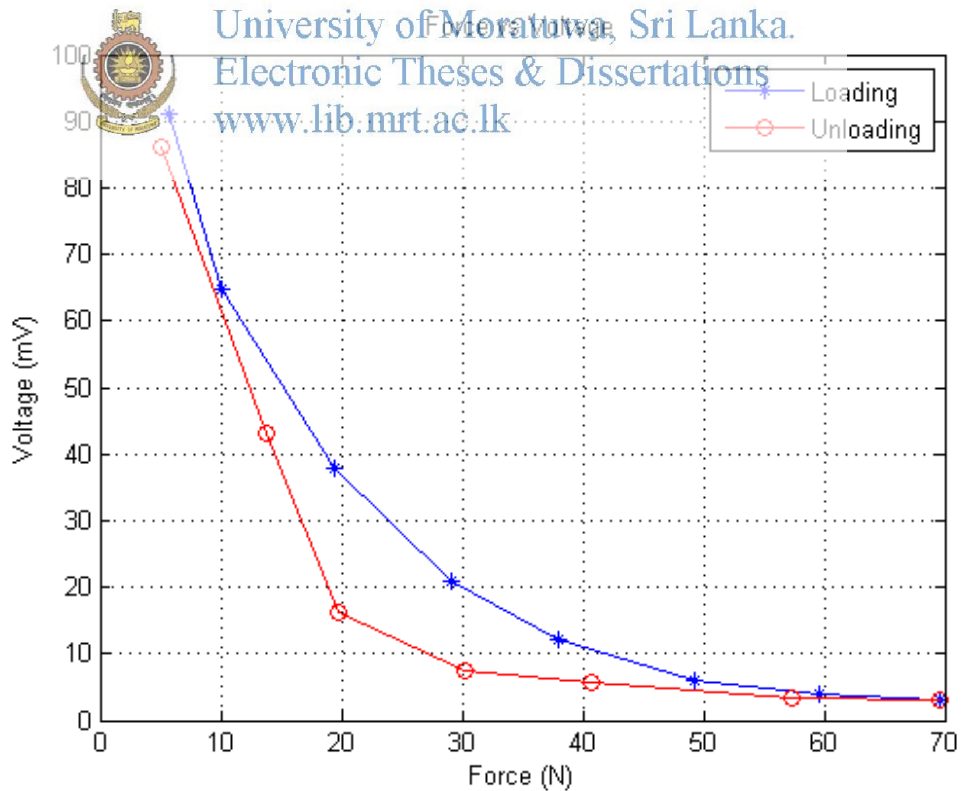


Figure 3.25: Experiment Results; voltage vs. force plot

According to the plot shown in Figure 3.25, the fabricated tactile sensor shows slight hysteresis error. Also from the graph it can be seen that hysteresis error occur during the lower force values. So when measuring forces at high values, hysteresis shown by this sensor will be insignificant. Also by compensating the output with a well versed algorithm, hysteresis of this sensor can be avoided.



University of Moratuwa, Sri Lanka.
Electronic Theses & Dissertations
www.lib.mrt.ac.lk

4 DEVELOPMENT OF ENCLOSED 1-DOF TACTILE SENSOR

4.1 Introduction

While conducting experiments on the developed 1-DOF tactile sensor at stage 1, some issues were identified associated with the sensor.

Since conventional manufacturing techniques were used to fabricate the sensor structure there were some manufacturing errors associated with the fabricated structural components. Some of these errors are poor maintenance of geometrical and dimensional tolerances, low dimensional accuracy and precision associated with the manufacturing technique. Due to these manufacturing errors, alignment Problems Occurred during assembling stage and offsetting errors occurred while transferring force to sensing element. Also due to the insufficient physical contact between electrode and the sensing element, noise was added to the output signal and it might has been one of a cause for the hysteresis error of the developed sensor.

Some other issues associated with the developed sensor structure is lack of overload protection which was not incorporated in the structure and environmental conditions such as dust, humidity affecting the performance of sensing element as it is open to the environment in the current sensor structure.



University of Moratuwa, Sri Lanka
Electronic Theses & Dissertations
www.lib.mrt.ac.lk

To address these issues to a satisfactory level, a novel sensor structure was designed and developed as the next stage 2 of developing a 1-DOF tactile sensor. Novel structural design for the 1-DOF tactile sensor was proposed while utilizing the same working and sensing principle as the developed 1-DOF tactile sensor. This chapter describes the development of this novel enclosed 1-DOF tactile sensor.

4.2 Proposed Structural Design for 1-DOF Enclosed Tactile Sensor

First step of developing this novel enclosed 1-DOF tactile sensor is to design the sensor structure while improving the structural issues identified with previously developed 1-DOF tactile sensor.

Main issues related with previous sensor structure are lack of overload protection, lack of sensing element encasement and high precision and dimensional accuracy. To

address these issues a novel structure was designed with the same working and sensing principle. This novel structure also consist of components with circular geometry as previous and increased number of components comparing with it. Figure 4.1 and Figure 4.2 shows the conceptual design and the components of the designed novel enclosed sensor structure.

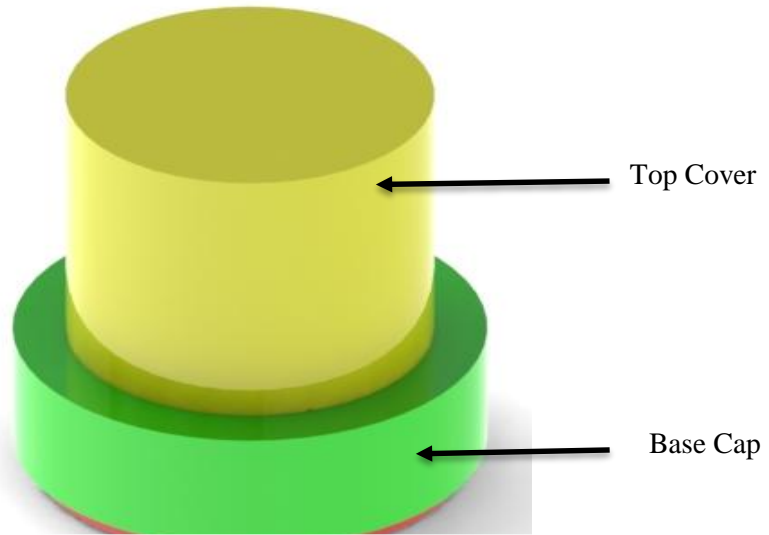


Figure 4.1: Isometric view of proposed design of novel enclosed sensor structure

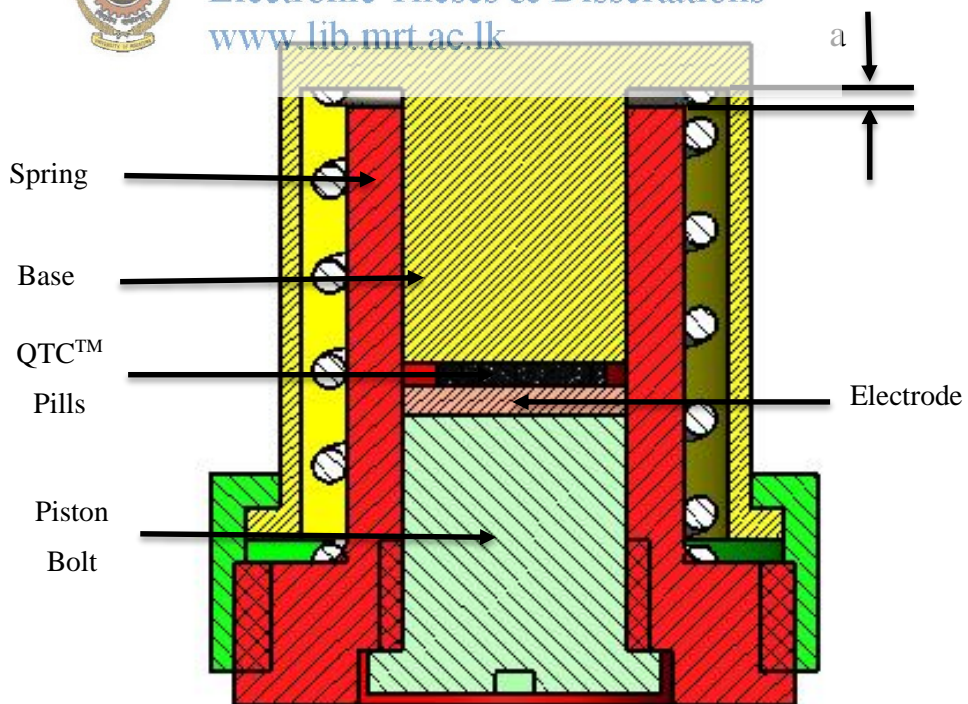


Figure 4.2: Sectional front elevation of proposed design of novel enclosed sensor structure

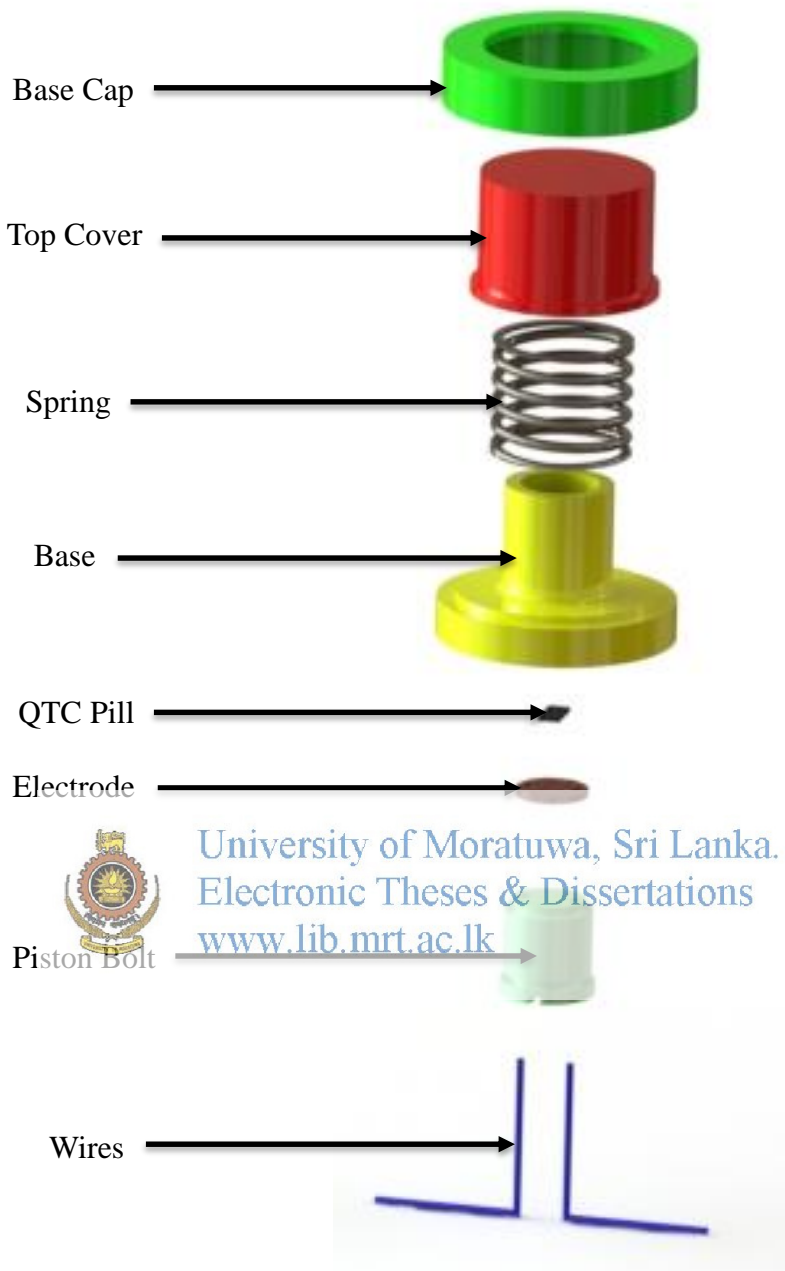


Figure 4.3: Exploded view of the proposed novel enclosed sensor structure

In this sensor structure, force is applied to the top cover and then it is transferred to the sensing element while scaling down the force through the spring. In this design, space between the top cover and the base (dimension a as shown in Figure 4.2) is controlled such that it will provide an overload protection to the sensing element. Overload condition can be set by adjusting the piston bolt and the base cap in the structure. This will affect the force range of the sensor, as this controls the allowable maximum

displacement for the QTC™ pill. Hence, with this newly added feature now force range of the sensor can be adjusted suitable to the application not only by changing the spring used in the structure but also by adjusting the piston bolt and the base cap of the structure.

Another advantage of this structure is that the sensing elements (QTC™ pills) are not open to the environment as they are enclosed in the structure. This will ensure that the environmental conditions such as dust, humidity will not affect the performance of the sensing element.

Arrangement of each and every component with each other in the sensor structure can be described with an exploded view of the sensor structure as shown in Figure 4.3. Refer Appendix D for the production drawings of the proposed structure.

4.3 Analysis and Simulation of Proposed 1-DOF Enclosed Tactile Sensor

Next step of developing this novel enclosed 1-DOF tactile sensor is to validate the proposed sensor structure by analysing the proposed structure in the previous step. Since validation of working principle and impact of spring gauge for sensor range is analysed at the development of 1-DOF Tactile Sensor, in this step FEA was performed solely for validating the proposed sensor structure and to verify whether it follows the proposed working principle at development of 1-DOF Tactile Sensor.

Analysis was performed using COMSOL Multiphysics software, which is a FEA software. Comparing with ANSYS software package, COMSOL Multiphysics software package has several advantages, such as easy to use GUI, inbuilt modules for solve specific problems, added features to specify a problem and so on. Same as in ANSYS, in COMSOL also, following major aspects have to be considered when specifying a problem to conduct a FEA.

- Geometry
- Material Data
- Mesh
- Boundary Conditions

For this analysis, geometry was modelled considering only the load bearing structural components such as top cover, piston bolt, QTC™ pill and spring. These components were modelled in the virtual space using SolidWorks software. Then this 3D model was imported to the COMSOL software using a feature available with COMSOL called Live Link Interface for SolidWorks. In ANSYS software, importing of a model have to follow several tasks such as converting the model into compatible file types, such as IGES, STL, etc. But due to the availability of the Live Link feature in COMSOL, CAD (Computer Aided Drawing) model can be imported to the software easily and there is a possibility to modify to the geometry while performing the FEA. Figure 4.4 shows the CAD model considered for this analysis.



Figure 4.4: Geometry Considered for the FEA

The next aspect to be considered for FEA is to specify the material data related to the geometry considered for FEA. Table 4.1 shows the material and the required material properties to conduct the FEA considering the geometry. In here, material data related to Aluminium 1060, which was assigned to the structural components were taken from the inbuilt material library in COMSOL software. Material data related to QTC™ was taken from the experimental data described in the chapter three.

Table 4.1: Input parameters of FEA

Parameter			Specification	
			Unit	Value
Material Data	QTC	Density	Kg/m ³	3861
		Modulus of Elasticity	MPa	28.49
		Poisson Ratio	0.3	
	Structure	Material Type	Aluminum 1060	
		Density	Kg/m ³	2700
		Modulus of Elasticity	Gpa	70-80
		Poisson Ratio	0.33	
Spring Constant			N/m	2.22E+03
Contact Type			Bonded	
Mesh	Element Type	Structure	Tetrahedral	
		Sensing Element		
	Minimum Element Size		mm	0.12
	Number of Elements		67928	
	Minimum Element Quality		1.41E-01	
	Average Element Quality		0.7188	

The next step of performing a FEA using COMSOL is to construct a mesh for the geometry considered for the FEA. Table 4.1 shows the specified parameters when constructing the mesh for the given geometry. In this mesh, tetrahedral elements were chosen as the mesh element to construct the mesh. In COMSOL, parameter to evaluate the quality of the mesh is known as element quality parameter when comparing to skewness parameter in ANSYS. According to the values specified for minimum and average element quality parameters as shown in Table 4.1, constructed mesh for the given geometry has sufficient quality to perform an optimally accurate FEA.

Specifying the boundary conditions is the next step in FEA using COMSOL. For this FEA, contact type between each component is set to be bonded, so that the components in the given geometry will show the desired behaviour under loading considering the real world situation. Same as FEA discussed in chapter three, a boundary load was given to the top surface of top cover and fixed constraint is given to the bottom surface of the piston bolt. Another important aspect to be considered when specifying the boundary conditions for this FEA is to specify the spring effect to the considered

geometry. Unlike in FEA discussed in chapter three, spring wasn't modelled in the considered geometry for this FEA. In this FEA spring force is calculated at each displacement and add it to the analysis using a feature available with the COMSOL Multiphysics software rather than modelling the spring to add the spring effect. Boundaries selected to apply these boundary conditions are shown in Figure 4.5.

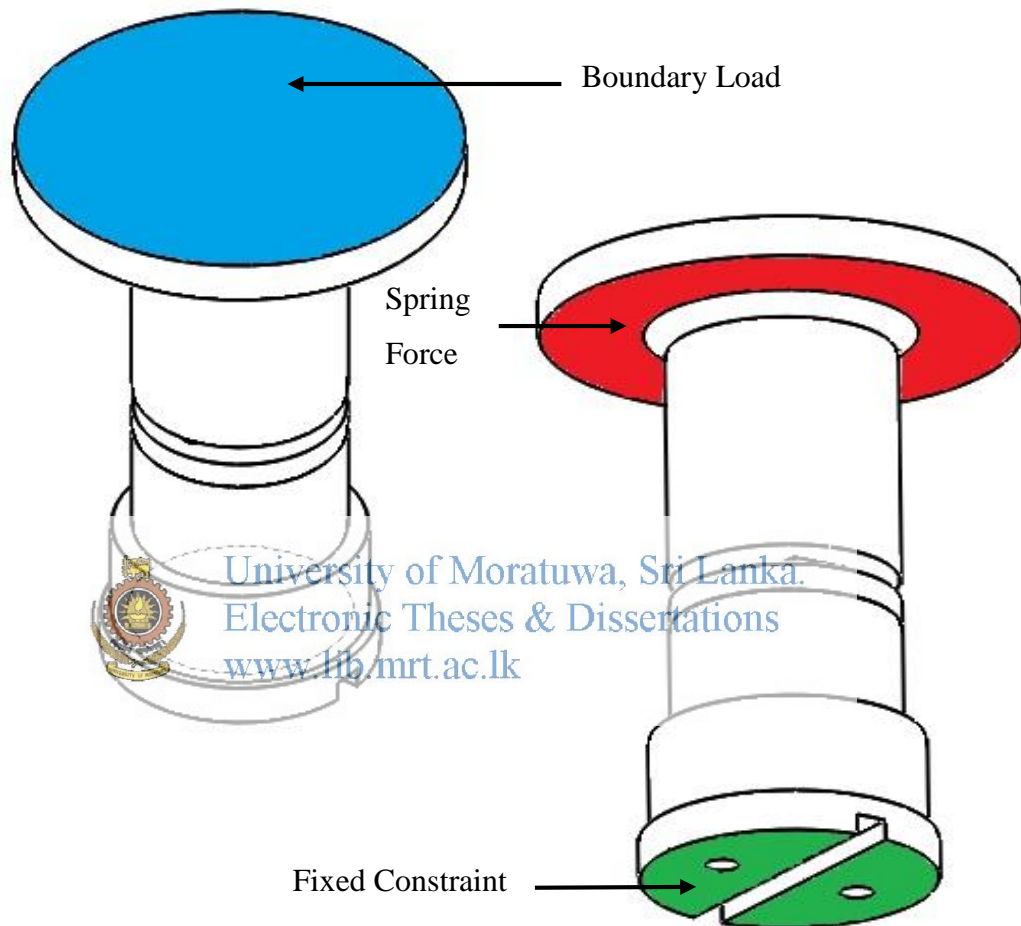
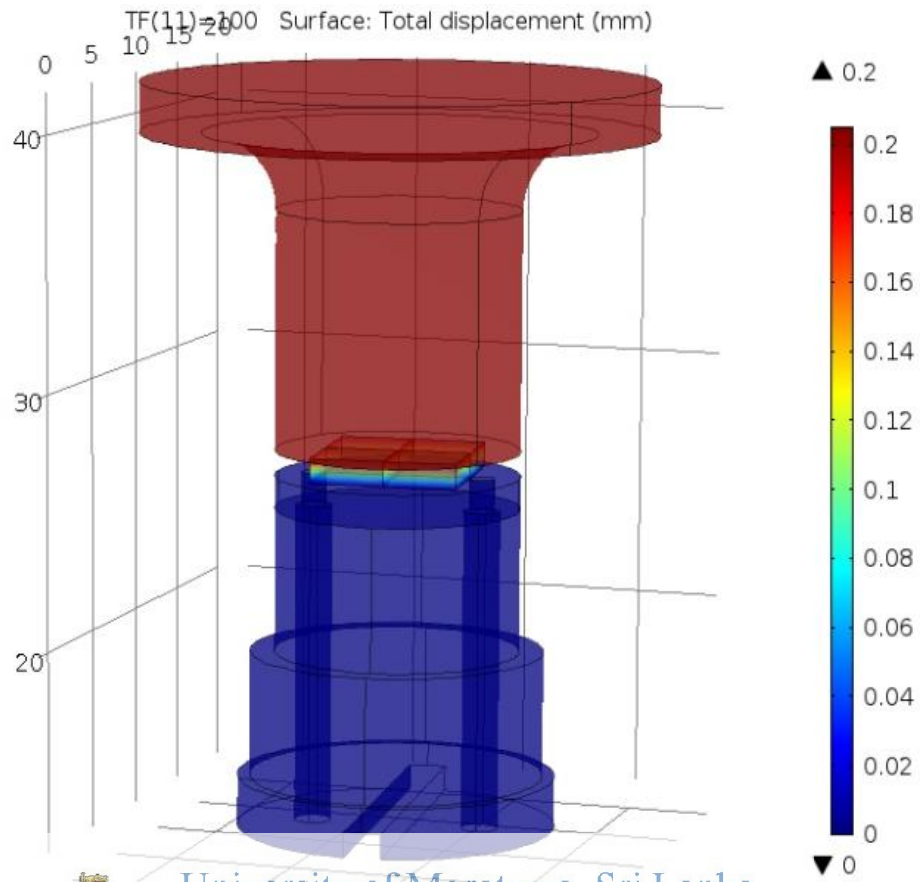


Figure 4.5: Boundaries selected to apply boundary conditions for FEA

Figure 4.6 and Figure 4.8 shows the results of the FEA analysis for sensor structure. According to the results shown in Figure 4.7, proposed structure with sensing element shows a linear relationship between the force applied and the structural displacement. This validate that the proposed structure is working on the working principle described at chapter 3. Also according to Figure 4.9, force applied and the equivalent stress also has a linear relationship Figure 4.10 and Figure 4.11 shows the FEA plot results considering the QTC™ pill.



University of Moratuwa, Sri Lanka.

Electronic Theses & Dissertations

www.lib.mrt.ac.lk

Figure 4.6: Total deformation variation of the sensor structure

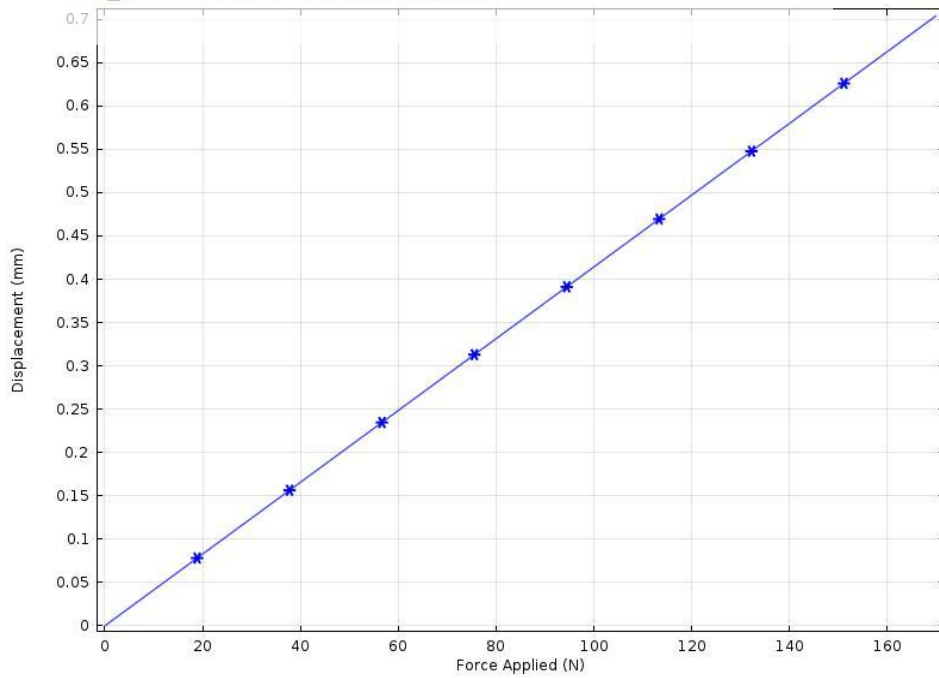
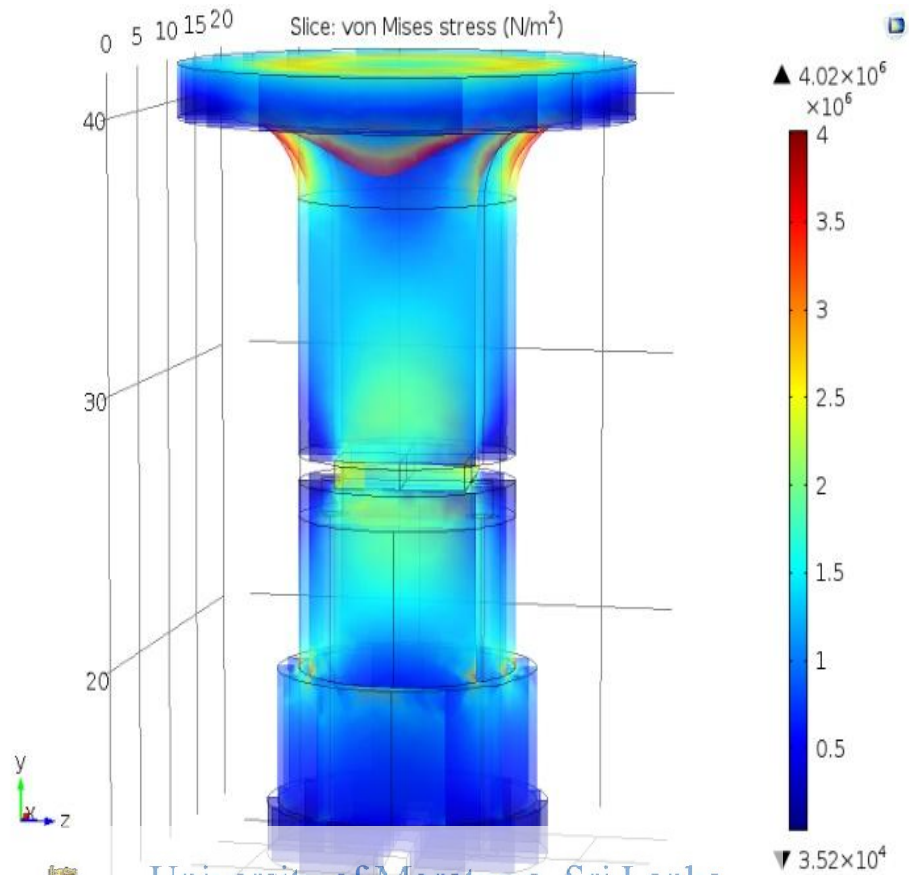


Figure 4.7: Force vs. Deformation plot.



University of Moratuwa, Sri Lanka.

Electronic Theses & Dissertations

www.lib.mrt.ac.lk

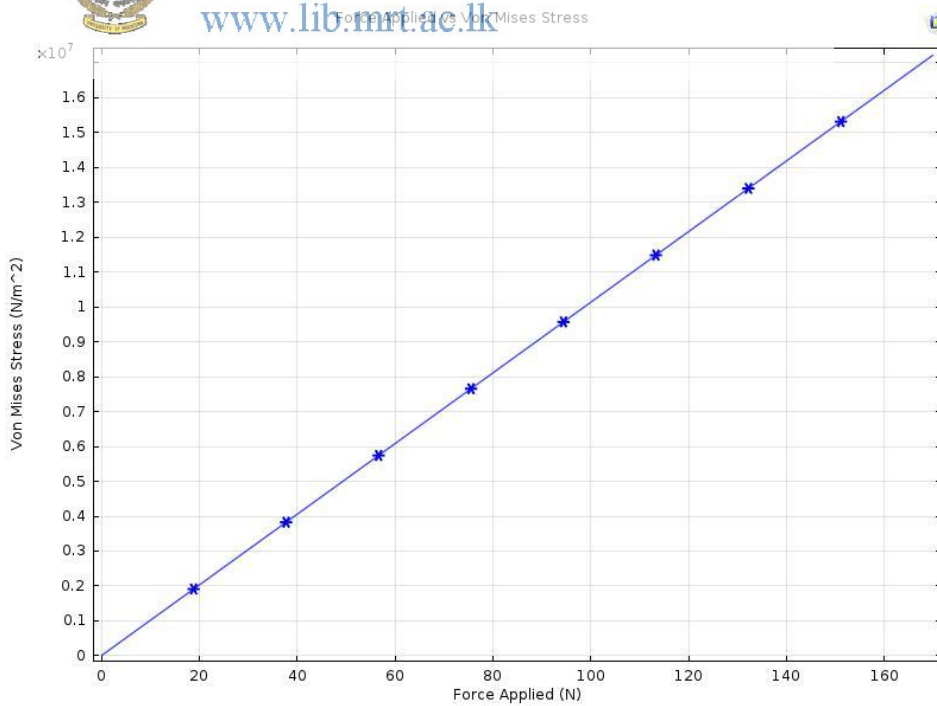


Figure 4.9: Force vs. Equivalent stress plot

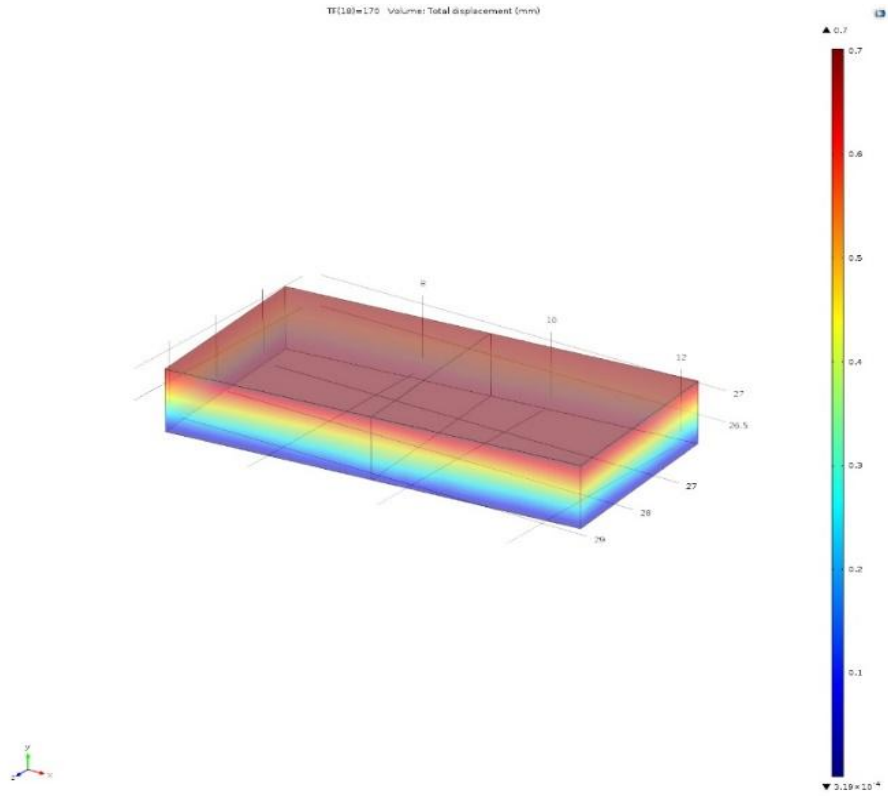


Figure 4.10: Total deformation plot result of QTCTM pill.



University of Moratuwa, Sri Lanka.
Electronic Theses & Dissertations
www.lib.mrt.ac.lk

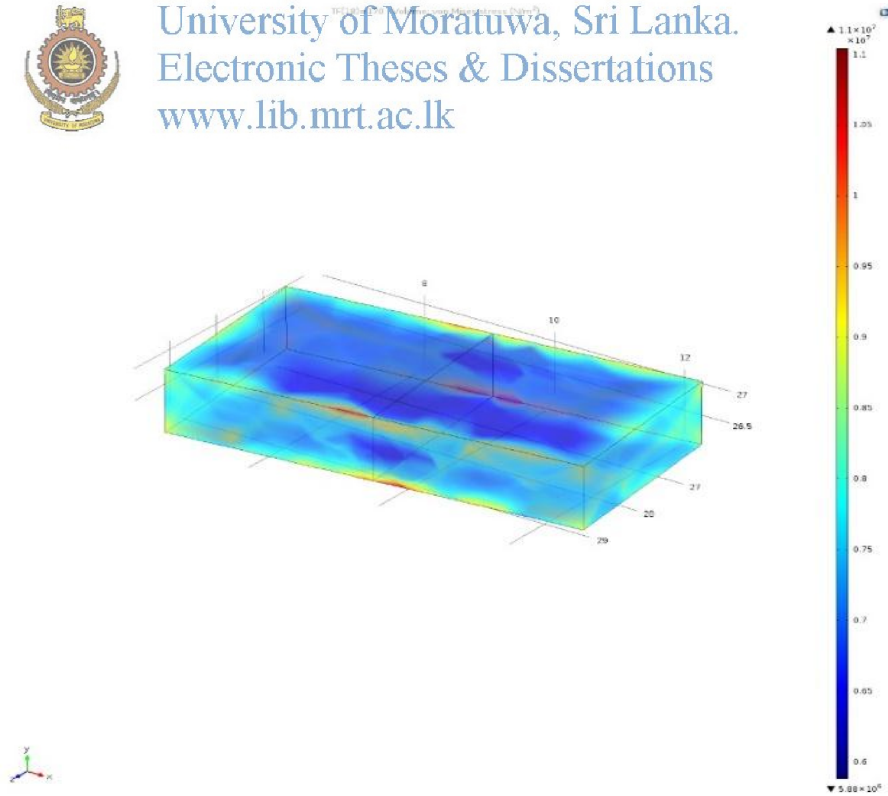


Figure 4.11: Equivalent Stress plot result of QTCTM pill.

4.4 Fabrication of Designed 1-DOF Enclosed Tactile Sensor

After analysing the structure, next step of developing novel enclosed 1-DOF tactile sensor is to fabricate the sensor. Same as in developing 1-DOF Tactile sensor, in this step sensor fabrication can be categorised in to two categories,

- Fabrication of sensing element configuration.
- Structural fabrication

Following subtopics will discuss in detail about these two categories.

4.4.1 Fabrication of Sensing Element Configuration

Electrode designing and fabrication is critical for this sensor, as described in chapter 3 sensor development, there is a possibility of a transmission loss of the output signal through the contact points between QTC™ pills and the electrode. Also noise could be added to the signal through these points. This will be a disadvantage when taking the sensor output for measurements. Also these will may cause for hysteresis error in the sensor. So an electrode was design to minimize the contact points between QTC™ pills and electrode. Figure 4.12 shows the designed electrode. In this design a copper cladded board is used to create electrodes. In this electrode design copper layer is separated to two regions to create two separate electrodes. QTC™ pills are mounted on the copper clad board so that they are touching both these electrodes. Output signal can be taken out from those two electrodes.

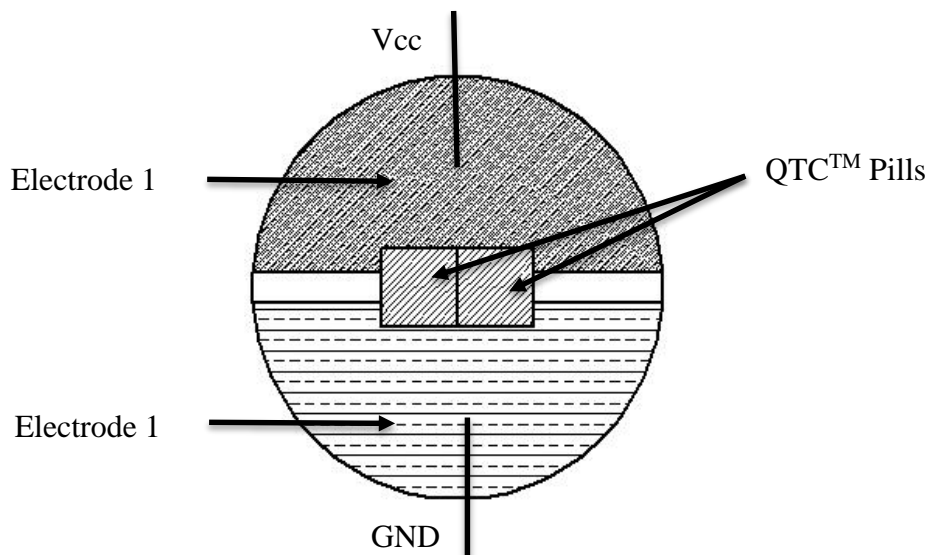


Figure 4.12: Proposed revised electrode design

When fabricating this designed electrode, one of the major issue identified was create the physical contact between the sensing element and the electrode. Since the solution from previous stage of sensor development is not an optimum, it is required to find the best method to create an optimum physical contact. From the literature, it was found that vacuum depositing Aluminium on both surfaces will give the optimum results [60]. Since vacuum depositing facilities are not available in Sri Lanka, next optimum available solution, which is to use silver paste to create the physical contact between electrode and sensing element is used when developing sensing element configuration. Figure 4.13 shows the steps of electrode fabrication and the fabricated electrode arrangement.

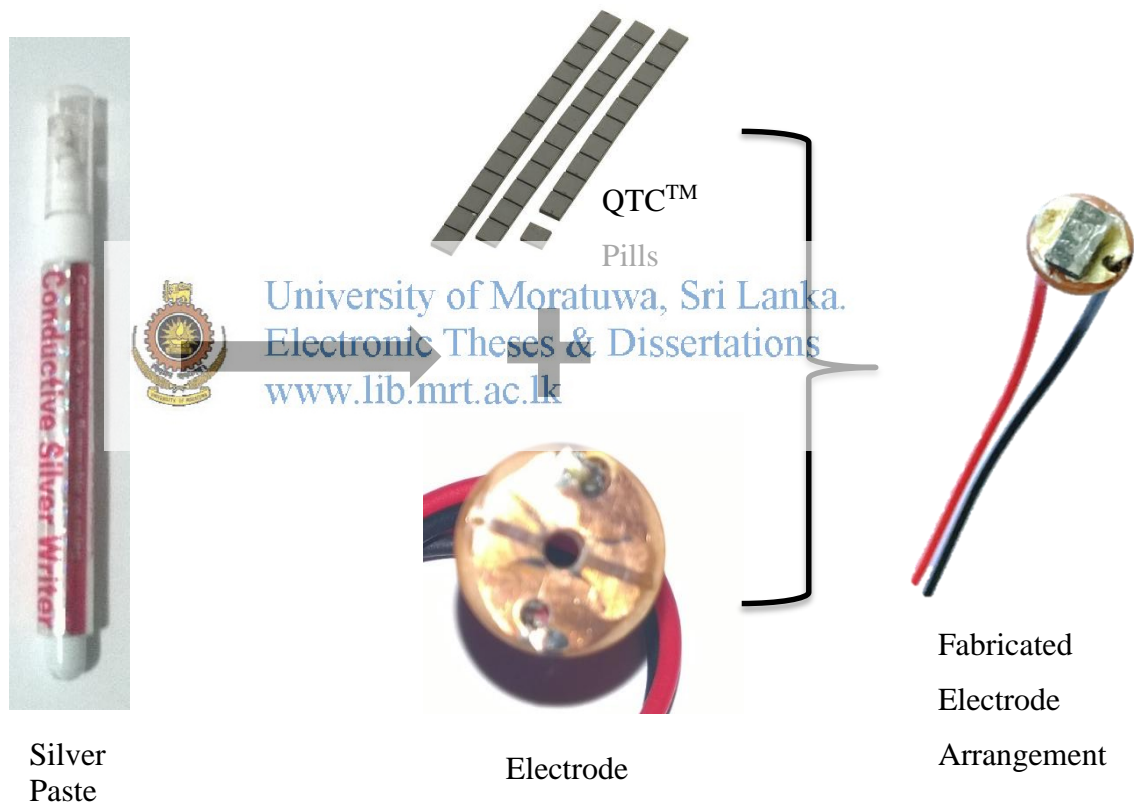


Figure 4.13: Steps of electrode fabrication and fabricated electrode

4.4.2 Structural Fabrication and Assembling

Next step of fabrication of proposed novel enclosed 1-DOF tactile sensor is to fabricate the structural components. Since there were issues related with the structural fabrication at stage 1, such as low dimensional precision and accuracy, much

consideration were done to increase the quality of the fabricated product. With that in mind, production drawings were generated for each structural components with higher dimensional and geometrical tolerances. Refer Appendix D for generated production drawings.

Since the use of high tolerance values in production drawings, conventional machining techniques could not be used to fabricate these structural components. So, it is decided to use CNC machining techniques to fabricate each structural components as with the use of such machining techniques high dimensional precision and accuracy can be maintained.

After fabricating each and every structural components, they were assembled together with electrode configuration. Figure 4.14 shows the fabricated structural components and assembled and finalized novel enclosed 1-DOF tactile sensor.

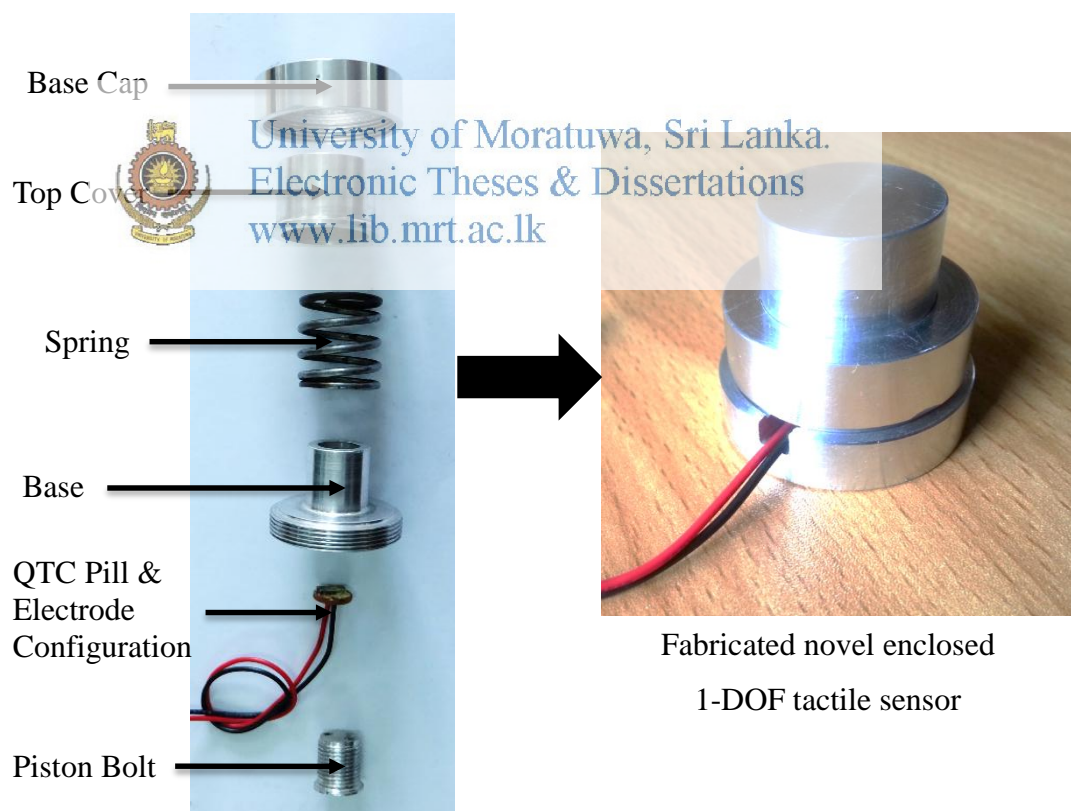


Figure 4.14: Fabricated structural components and Assembled and finalized novel enclosed 1-DOF tactile sensor

4.5 Testing of Developed 1-DOF Enclosed Tactile Sensor and Results

As the next step of developing novel enclosed 1-DOF tactile sensor, experiments were carried out to the fabricated sensor for testing purposes. To conduct these experiments, same electric circuit was used as in stage 1 to get the output signal of the sensor.

Experiments were carried out to find the relationship between the developed sensor output and input, to find the sensitivity of the sensor, to find the sensor range, to find the resolution of the sensor and the repeatability of the sensor. To find all these characteristics, an experiment was designed using Universal Tensile Testing Machine available with the Material Science Engineering Department, University of Moratuwa. Purpose of using this machine to conduct experiment for the sensor is to deliver a gradually increasing and decreasing force to the sensor. Figure 4.15 shows the system layout of the experimental setup and Figure 4.16 shows the experimental setup used to conduct experiments.

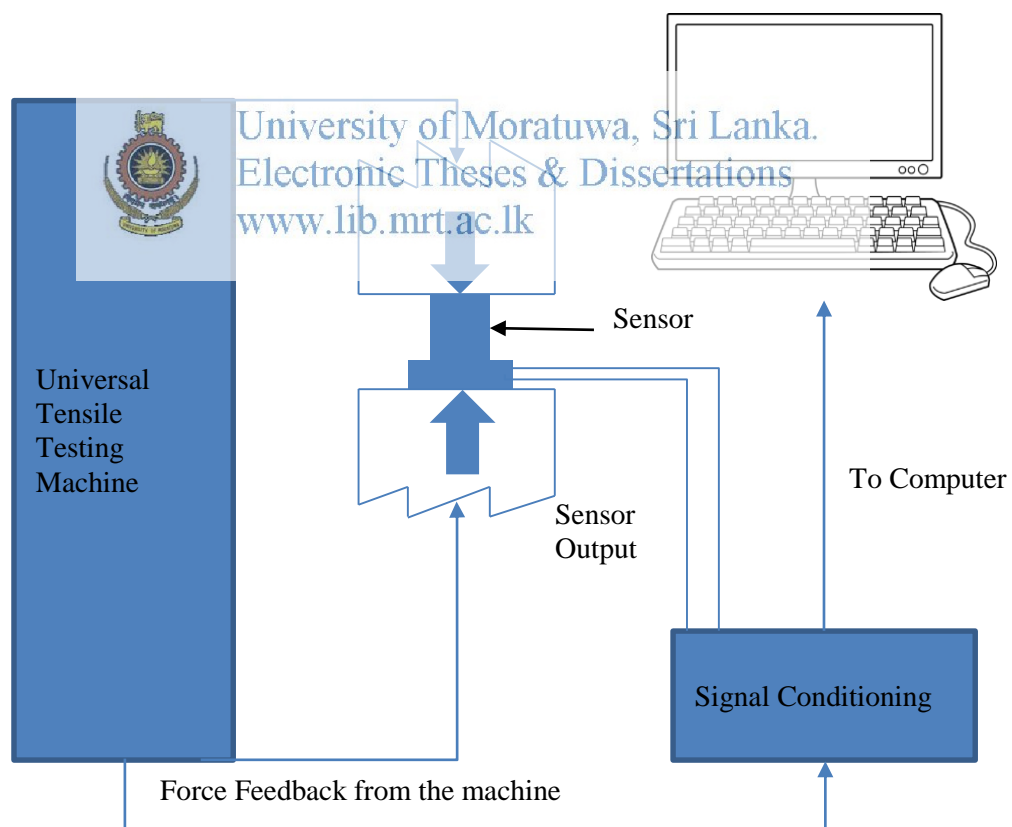


Figure 4.15: System layout of experimental setup

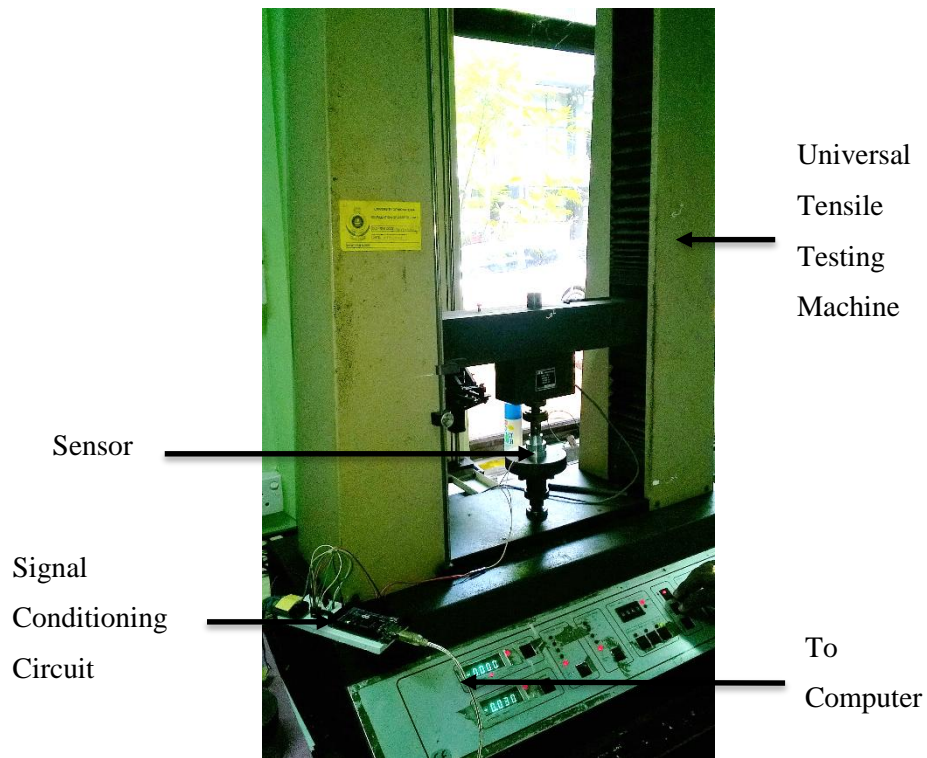


Figure 4.16: Developed experimental setup

Figure 4.17 and Figure 4.18 are the results of these experiments carried out using the above developed experimental setup.



University of Moratuwa, Sri Lanka.
Electronic Theses & Dissertations
www.lib.mrt.ac.lk

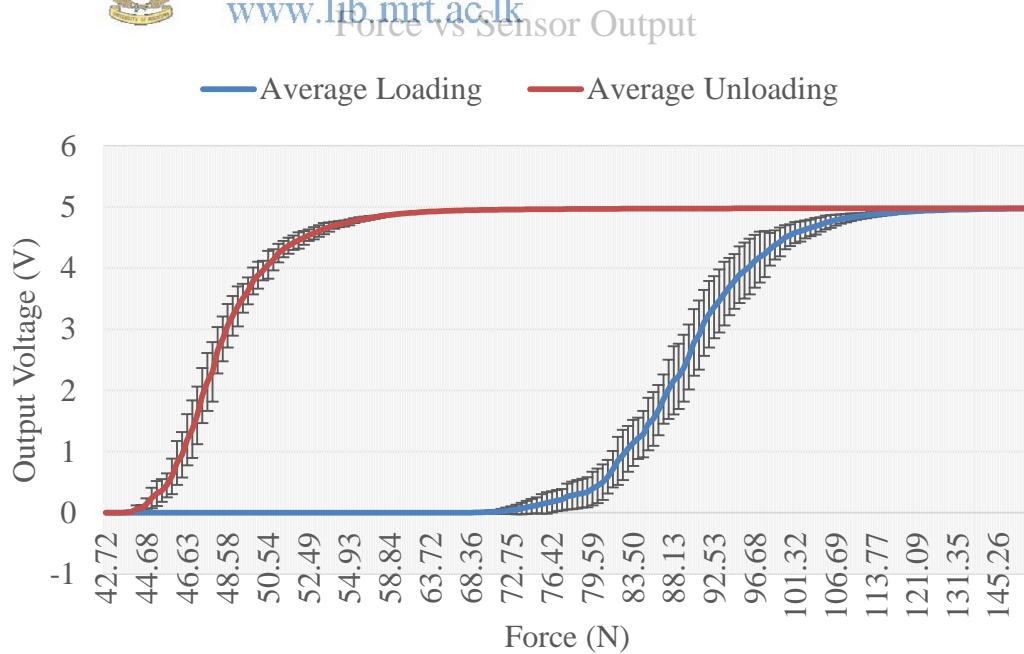


Figure 4.17: Calibration Results for Continuous Loading & Unloading

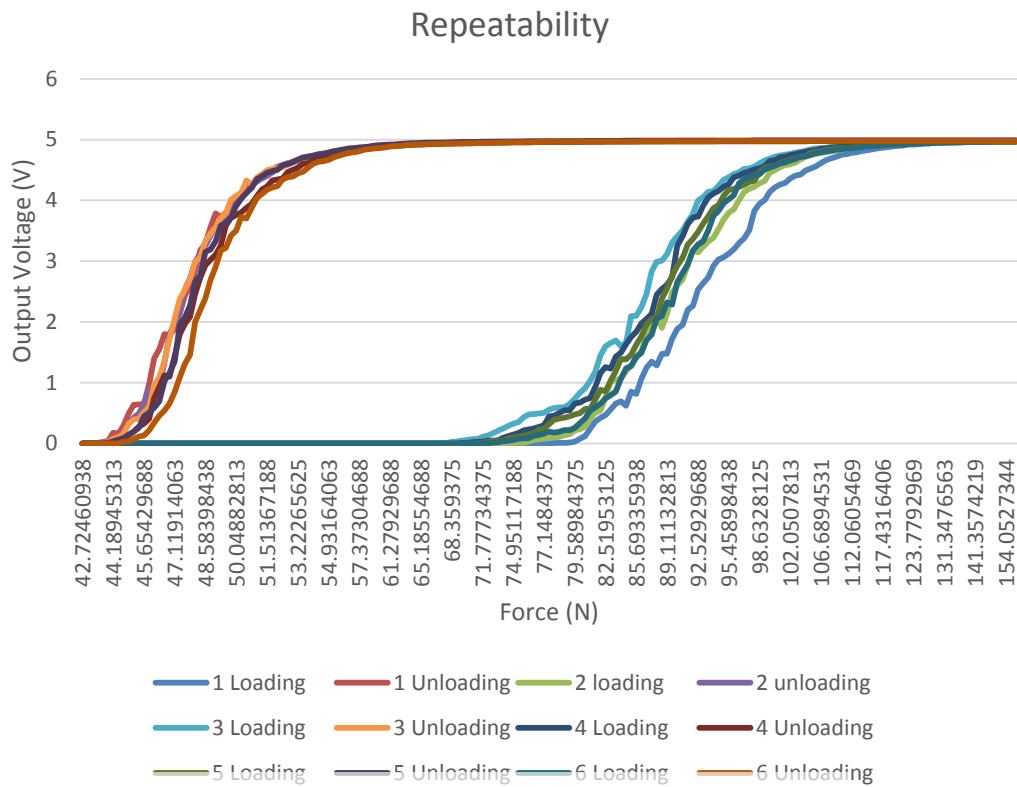


Figure 4.18 Repeatability analysis for various loading & unloading

In these results, figure 4.17 shows the relationship between sensor input and the sensor output with standard deviation at each data point. Also Figure 4.18 shows the repeatability analysis for the developed sensor. Table 4.2 shows the sensor characteristics values calculated from the experimental results.

Table 4.2: Sensor characteristics values calculated for the developed sensor

Sensor Characteristics	Value
Sensor Range	0 – 170 N
Sensitivity	0.2209 V/N
Resolution	0.5 N
Repeatability	± 3 N

According to these results, it can be seen that the hysteresis error of the developed sensor was increased comparing with the experimental results at stage 1. Reasons

behind this phenomena may be due to errors cause by the universal tensile testing machine and errors present in the QTCTM material use for the experiment. Hence, another experiment was conducted using dead weight to compensate the errors cause by the testing machine, and results of this experiment is shown in Figure 4.19.

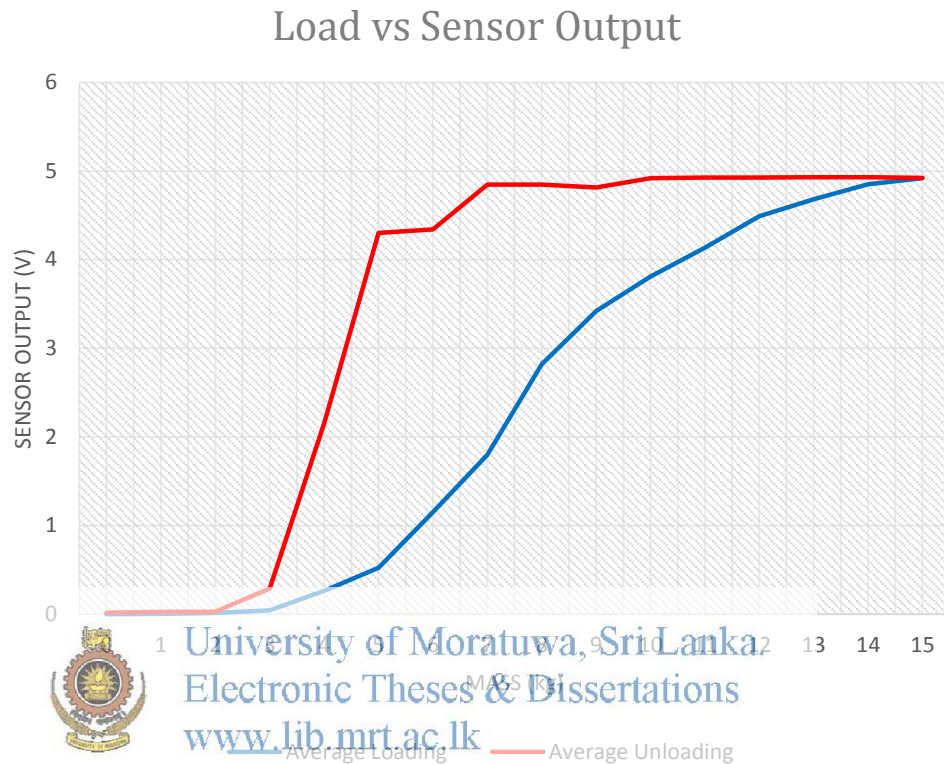


Figure 4.19: Calibration Results for Dead Weight Loading & Unloading

According to the loading and unloading variation shown in Figure 4.19, it can be concluded that the machine errors associated with the universal tensile testing machine was a major factor contributed to the hysteresis error of the developed novel enclosed 1-DOF tactile sensor. Also, it can be concluded that the remaining hysteresis error may be due to the errors present in the QTCTM material used in the experiment.

5 APPLICATION OF TACTILE SENSORS FOR TACTILE IMAGING

5.1 Introduction

Main motive of this research is to develop tactile sensors, so that they can be incorporated with tactile imaging applications. So with that purpose in mind, this chapter describes the work carried out regarding the tactile imaging using the developed tactile sensors.

Content of this chapter can be categorised into two categories,

- Development of a Graphical User Interface for developed tactile sensors.
- Tactile Imaging using developed tactile sensors and graphical user interface.

Main motive behind these work is to assess the feasibility of the use of developed tactile sensor for tactile imaging so as to apply them in tactile imaging applications.

5.2 Development of Graphical User interface

Main motive of developed graphical user interface for developed tactile sensors is to help the users to visualize the output of the developed sensor in a graphical manner. With this motive in mind a graphical user interface was proposed, which was consist with following components,

- Data Acquisition System.
- Signal Conditioning System.
- Data Processing System.

A system layout for the proposed graphical user interface was proposed with above mentioned system components. Figure 5.1 shows the proposed system layout.

In this system layout, a microcontroller based development board was used, which act as a data acquisition system and a signal conditioning system in the proposed graphical user interface. Arduino ATmega 2560 controller, which is a single microcontroller development board based on Atmel microcontrollers, has chosen to use in this proposed system as it has 16 analogue inputs and 54 digital inputs with 10 bit ADC.

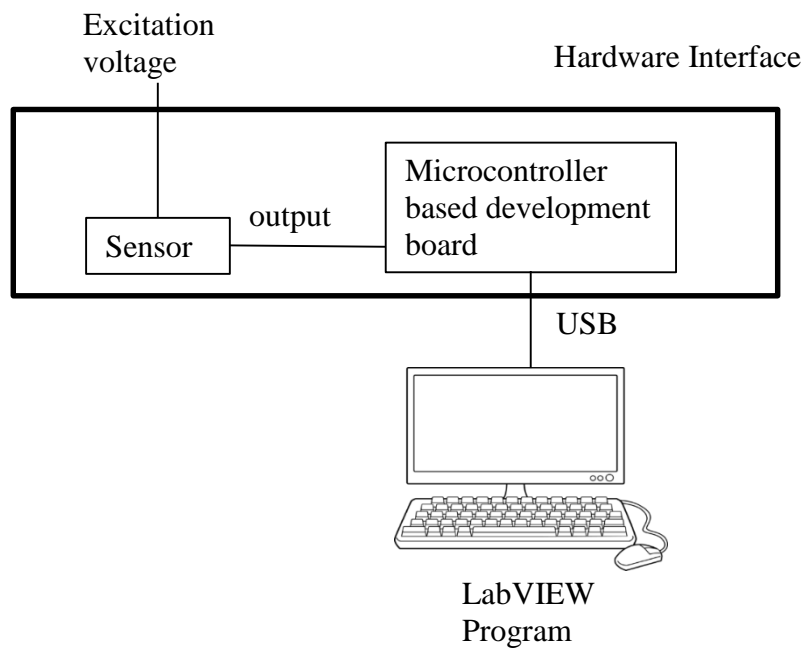


Figure 5.1: Proposed system layout for the graphical user interface

Arduino is basically designed for people with little knowledge about electronics to develop systems based on microcontrollers. Arduino is consist with open source physical computing platform with microcontroller and a development environment to program it. Because of the user friendliness and easy to use characteristic, Arduino has become the most popular development board over the past years. Table 5.1 shows the specification of Arduino Mega 2560.

Table 5.1: Specifications of Arduino Mega 2560

Microcontroller	ATmega2560
Operating Voltage	5V
Input Voltage (recommended)	7-12V
Input Voltage (limits)	6-20V
Digital I/O Pins	54 (of which 15 provide PWM output)
Analog Input Pins	16
DC Current per I/O Pin	40 mA
DC Current for 3.3V Pin	50 mA
Flash Memory	256 KB of which 8 KB used by bootloader
SRAM	8 KB
EEPROM	4 KB
Clock Speed	16 MHz

As per the proposed system layout for the graphical user interface, output of the developed 1-DOF tactile sensor is taken to the Arduino Mega 2560 development board through a voltage divider circuit. As shown in the system layout, hardware interface for the proposed graphical user interface is consist with the sensor and the microcontroller based development board. So with the chosen Arduino Mega 2560 development board a hardware interface was developed as shown in Figure 5.2. In this hardware interface, Arduino Mega 2560 development board will acquire the output signal of the developed sensor and convert that signal from analogue to digital using the built in ADC. Then this converted digital signal will be pass on to computer for further processing.



Figure 5.2: Developed Hardware Interface

This developed hardware interface consists of data acquisition system and signal processing system of the graphical user interface as describe earlier. Considering the other component of the proposed graphical user interface a LabVIEW program was developed which act as a data processing system and a mean to visualize the data graphically. LabVIEW (Laboratory Virtual Instrument Engineering Workbench), is a highly dynamic development to create environment for custom applications that interact with real data and signals in areas such as science and technology.

Figure 5.3 shows the LabVIEW programme and Figure 5.4 shows the GUI developed using LabVIEW software.

When connecting the Arduino to the LabVIEW program, a special interface should be added which is known as LabVIEW Interface for Arduino (LIFA). Refer Appendix E for the Arduino programming codes.

After successfully connecting the Arduino board to the LabVIEW program, block specifying Arduino board can be added to the program as shown in Figure 5.3. Through this programming block, data related to the Arduino board such as board type, communication frequency, etc. can be specified. Since Arduino program need to be run on a loop, a while loop block is used for this LabVIEW program as shown in Figure 5.3. All the commands related to process the sensor output signal and visualization process should be included within this While Loop block to execute the LabVIEW program while communicating with the Arduino development board. As shown in Figure 5.3, input pin block related to Arduino is taken for the LabVIEW program. Sensor output can be taken to the LabVIEW program through this input pin block. After that several data visualization blocks are used as shown in Figure 5.3, to visualize the output of the sensor taken through the input pin block.

Using this developed graphical user interface, users are able to visualize output of the developed tactile sensors. Also this graphical user interface can be used as an aid to construct visual images of a pressure variation of a given surface.

5.3 Tactile Imaging using Developed 1-DOF Tactile Sensors

As mentioned in the literature review, tactile imaging is consist of mapping pressure variation of a surface and present these data in a graphical manner. Based on this concept to create tactile images using the developed tactile sensors and the developed graphical user interface, an experiment was carried out.

5.3.1 Experiment Conducted to Construct Tactile Images Using Developed 1-DOF Tactile Sensors

An experiment was designed to map the pressure variation of a left hand of a person. When mapping the pressure variation of a hand, mapped results will depend on the posture of the human. For this experiment it is decided to use the cow pose which is one of the yoga pose [61] as shown in Figure 5.5.



Figure 5.5: Chosen posture for the experiment
Source: 10 Easy, Essential Yoga Poses [61]

Ultimate goal of performing this experiment is to construct a visual image of the pressure variation of the left hand of a human at chosen posture. To achieve this in an efficient method, it is required to get pressure value of several points of the hand rather than measuring the pressure value of one point. So a data point array was designed so it can be overlap with the hand and measure the pressure variation at each data point. Figure 5.6 shows the data point array construct for the left hand.

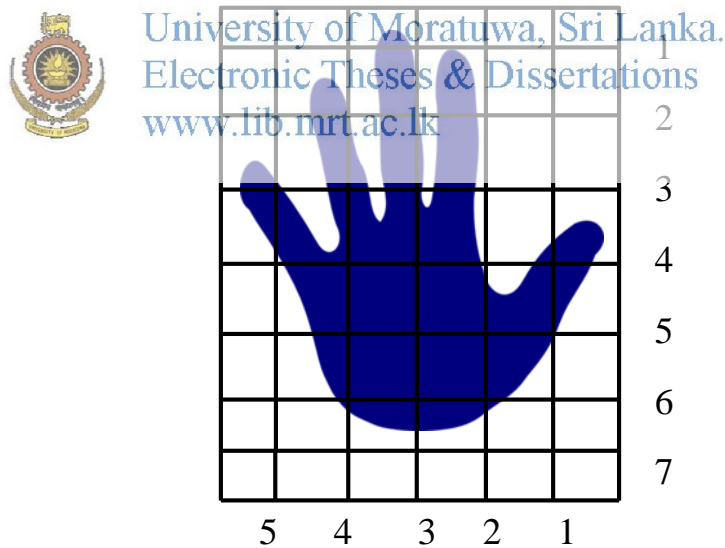


Figure 5.6: Data points considered on the left hand

An experimental setup was developed to acquire pressure data of left hand at each data point as specified in Figure 5.6 . Figure 5.7 shows the developed experimental setup. In this experimental setup for data acquisition and signal conditioning purposed Arduino Mega 2560 development board is used.

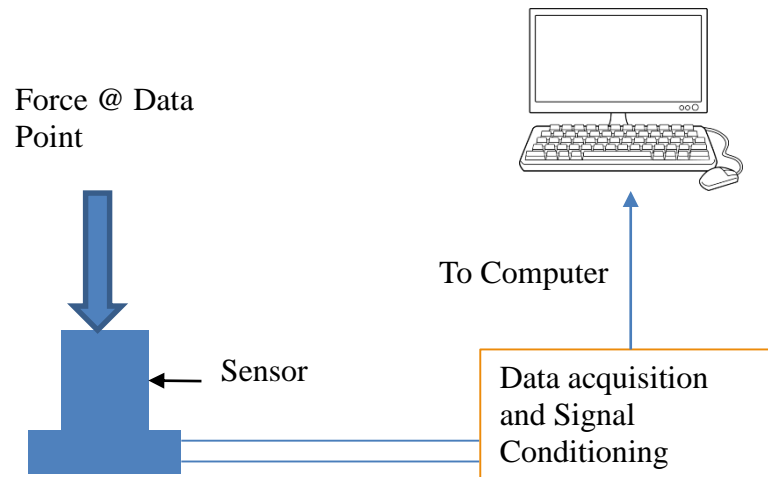


Figure 5.7: System layout of the proposed experimental setup

5.3.2 Results of the Experiment to Construct Tactile Images

Using the developed experimental setup pressure values at each data points were measure and recorded. At each data point, one hundred data values were taken and then take the average of this data set as the final pressure value at each data point. Figure 5.8 shows the graphical representation of pressure values in a graphical manner at each data point.

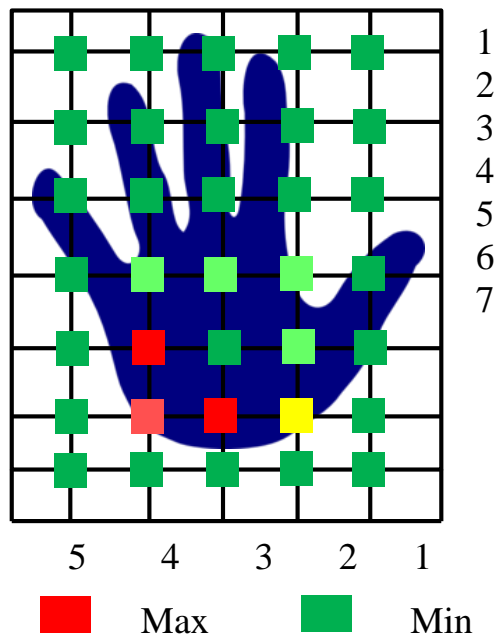


Figure 5.8: Graphical representation of pressure values on data points considered on the left hand

Then using these acquired force values at each data point, a tactile image was constructed using curve fitting toolbox of MATLAB software. This MATLAB toolbox uses different techniques to construct the best fit curve or surface for the given dataset. For this problem, interpolant cubic spline method was used to construct the best fit surface for the specified dataset. In the interpolant cubic spline method, MATLAB tries to fit different cubic polynomial in between sets of three points in a surface [62]. For this fitted surface, Sum of Squared Errors of Prediction (SSE) is taken to be $3.401E-28$ and R-squared is taken to be 1. According to these values, it can be concluded that the fitted surface through this MATLAB toolbox is an optimum fit considering the specified dataset. Figure 5.9 shows the constructed tactile image using surface fitting toolbox according to the pressure variation of the left hand at the given posture. Figure 5.10 shows the constructed colour contour tactile image from the Figure 5.9.

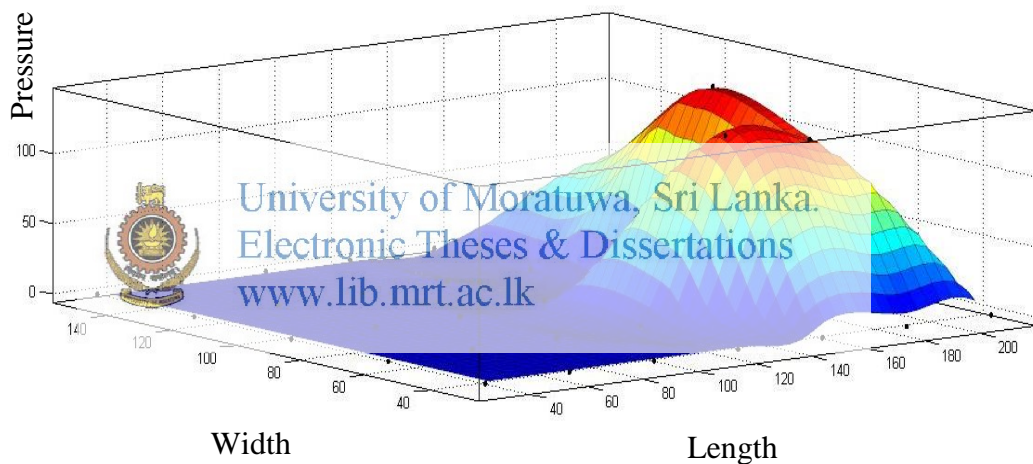


Figure 5.9: Constructed pressure mapping image of the left hand for given posture

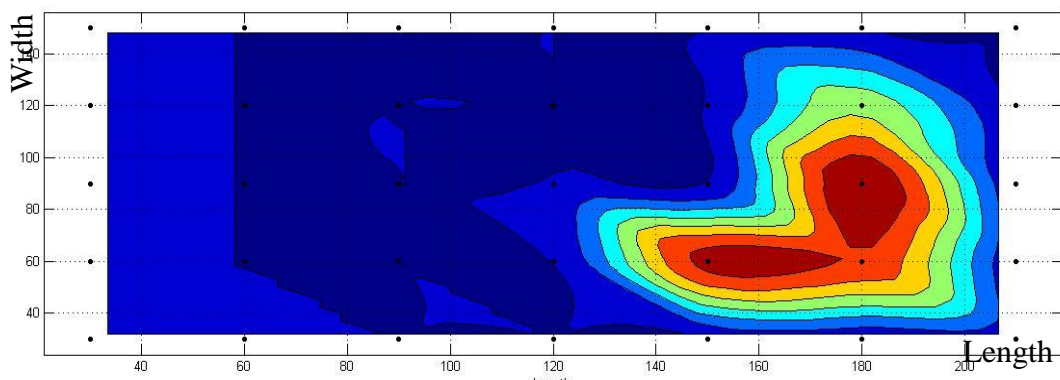


Figure 5.10: Constructed Contour color mapping image of the pressure variation of left hand for given posture.

6 DESIGN AND SIMULATION OF MEMS BASED TACTILE SENSOR

6.1 Introduction

While assessing the feasibility of developed 1-DOF tactile sensors for tactile imaging applications, it came to the attention, that rather than using a single sensor to get data at several data points, it is optimum to have a sensor array covering the whole area at one time [63].

Resolution and the accuracy of tactile sensor array solely depend on the number of tactile sensors present in the array and specifications of tactile sensor [64]. So to increase the performance of such tactile sensor arrays, it is vital to increase the number of sensors (taxels) present in the sensor array [65].

6.1.1 Why MEMS?

Taxel density or the number of sensors present in the array can be increased by miniaturizing the sensors to create a sensor array [66]. But with conventional machining techniques such as conventional lathe and milling operations, and advanced machining techniques such as CNC machining operations, won't allow this miniaturization of sensor beyond a certain limit. Figure 6.1 shows a comparison between a tactile sensor array construct with macro tactile sensors (developed novel enclosed tactile sensor) and a tactile sensor array construct with micro tactile sensors (MEMS tactile sensor).

6.1.1.1 What is MEMS?

Micro Electro Mechanical Systems (MEMS) is a technology, which uses micro-fabrication techniques to miniaturise the mechanical or electro-mechanical devices and structures. Scale of such MEMS elements can vary from few millimetres to all the way up to few micrometres. The main four functional elements of MEMS includes, Micro-Sensors, Micro-Actuators, Micro-Structures and Micro-Electronics. Researchers were able to develop numerous Micro-Sensors over the past decades

varying for almost all the sensing modalities, having much greater performance when comparing with their macro scale versions.

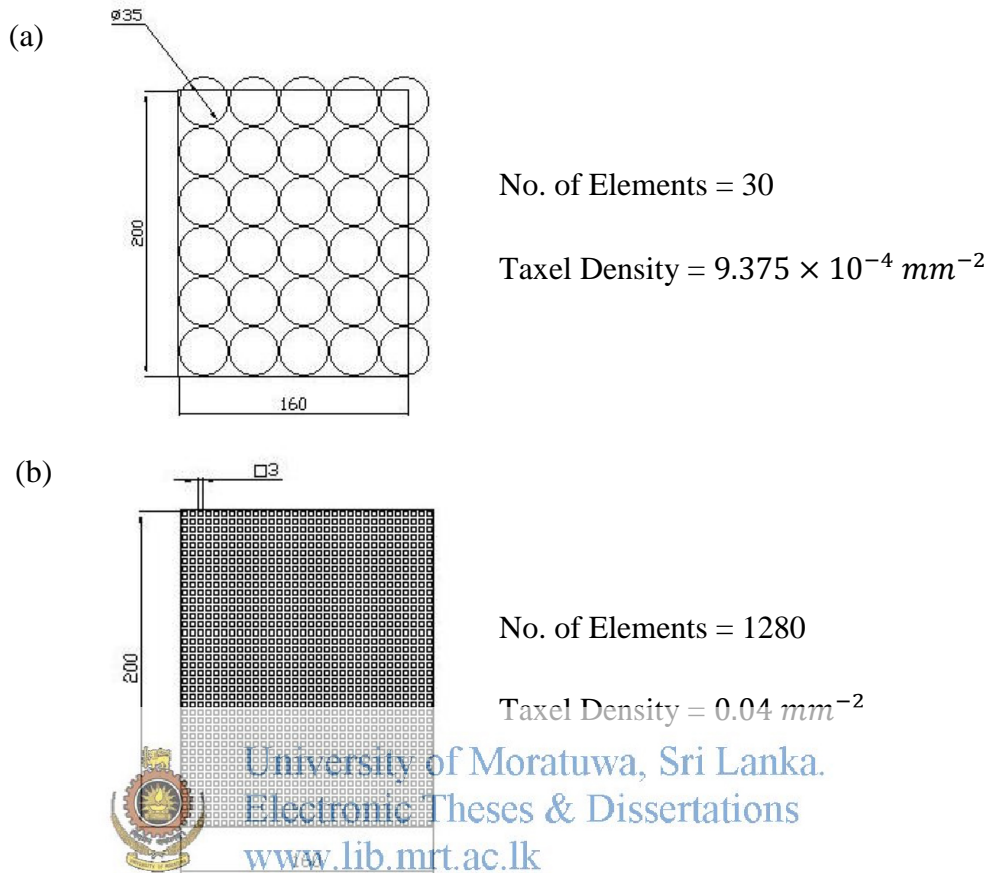


Figure 6.1: Comparison between tactile sensor arrays; (a) Sensor array constructed with novel enclosed tactile sensors. (b) Sensor array constructed with MEMS tactile sensors

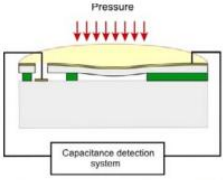
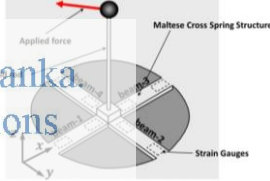
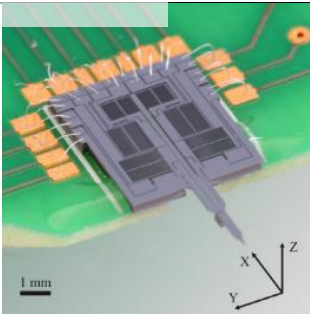
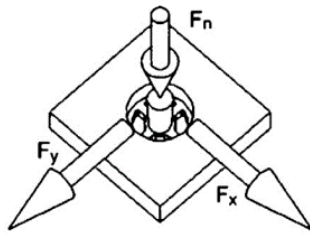
Hence, it is feasible and optimum to design and develop MEMS based or miniaturized tactile sensors to be incorporated with tactile sensor arrays to be used in tactile imaging applications so that their output is more reliable with high accuracy and precision.

6.1.2 Literature Review

MEMS (Micro Electro Mechanical Systems) technology is turning into a favourable solution for miniaturizing of sensing technology [67]. Rather than its small size, there are many promising features associated with MEMS technology such as low weight, high performances, and easy mass-production [68]. What's more, MEMS technology gives the ability to develop tactile sensor arrays with large force range and spatially varying sensitivity[66].

In conjunction with the discussion of sensor performance, it is important to discuss about the degree of freedom (DOF) of a sensor. Most of the available MEMS tactile sensor measurements are limited to fewer number of DOFs [7], [20], [69]. MEMS based tactile sensors with higher number of DOFs are very uncommon, as most of the developed tactile sensors just measure 3 linear DOFs and some more rotational DOFs [6]. Table 6.1 shows some of the work conducted by researchers related to MEMS tactile sensors.

Table 6.1: Literature regarding MEMS tactile sensors

Research	No. of DOF	Sensing Principle	Mechanism
Development of a Biomimetic MEMS based Capacitive Tactile Sensor [66]	1	Capacitive	
A Three-Axis Force Sensor for Dual Fingers Haptic Interfaces [70]	3	Strain Gauges (Resistive)	
Three-axis micro-force sensor with sub-micro-Newton measurement uncertainty and tunable force range [71]	3	Piezoresistive	
A novel haptic platform for real time bilateral biomanipulation with a MEMS sensor for triaxial force feedback [72]	3	Capacitive	

As a response to the miniaturization of tactile sensors and the absence of higher DOF tactile force sensors, a MEMS based 5 DOF tactile force sensor based on Piezoresistive sensing principle is proposed in this research. In miniaturised applications, Piezoresistive sensing principle shows more promising results [20]. This chapter will discuss about the structural design of the 5-DOF MEMS based Tactile Sensor, sensing principle and Finite Element Analysis of structural stability and piezoresistivity.

6.2 Structural Design of 5-DOF MEMS Tactile Sensor

A wagon wheel spring structure was designed for the proposed MEMS tactile sensor as shown in Figure 6.2 and Figure 6.3. Designed wagon wheel spring structure comprises of eight straight flexible beams which converges on a focal stage which will be used as the sensing platform. Despite the fact that some researchers discussed about the utilization of Maltese cross spring structure, which consists of four straight flexible beams and a focal plate, for Multi-DOF MEMS tactile force sensors [70], [73], as per the authors' knowledge, wagon wheel spring structure was never has been come to the consideration of researchers.

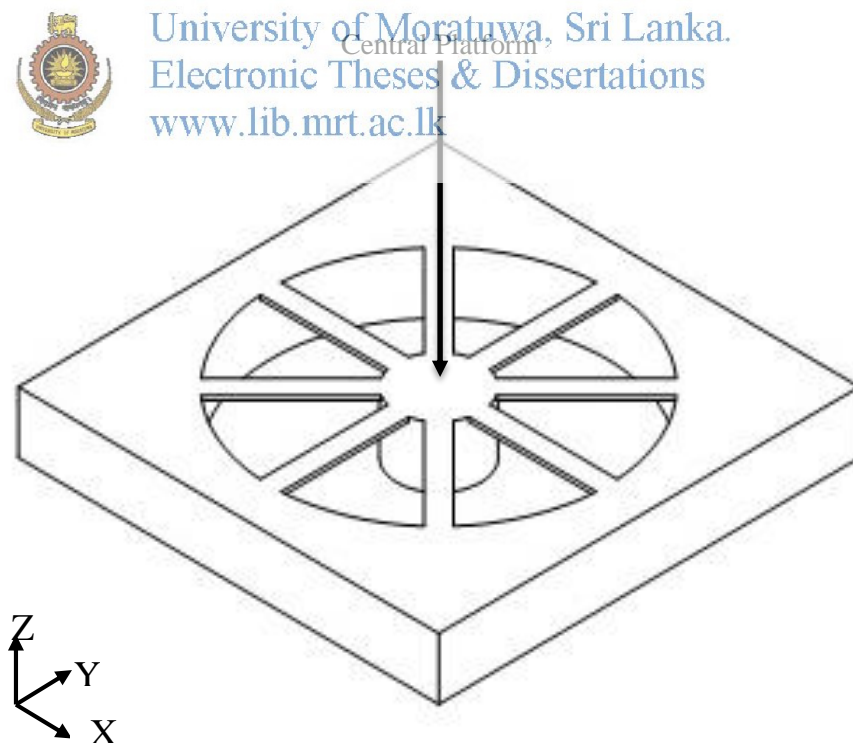


Figure 6.2: Isometric view of the conceptual design of proposed MEMS tactile sensor

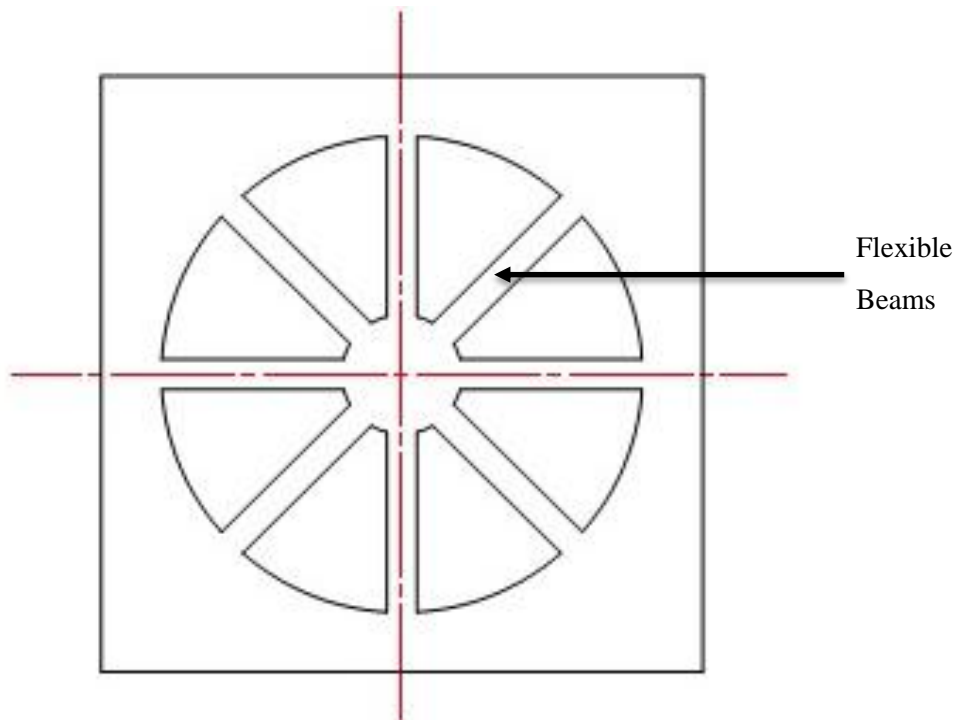


Figure 6.3: Plan view of the conceptual design of proposed MEMS tactile sensor.

Wagon wheel structure would provide the ability to sense force acting on higher number of points due to its support from eight flexible beams. In addition, the improved load bearing capacity of the structure would enhance its range of operation. So in this research, it analyses the use of wagon wheel spring structure for Multi-DOF MEMS tactile force sensor according to the structural specifications given in Table 6.2. For detailed dimensions refer Appendix F.

Table 6.2: Basic dimensions of the sensor structure

Size of the sensor	3 mm x 3 mm x 300 μm
Diameter of central platform	600 μm
Width of a beam	150 μm
Thickness of a beam	30 μm
Length of a beam	900 μm
Angle between two consecutive beams	45 ⁰

6.3 Working Principle of 5-DOF MEMS Tactile Sensor

As indicated by the proposed MEMS sensor structure, it exhibits 5 DOFs, x , y , z and two directions along x - y plane that forms angles 45° and -45° with x -direction. These directions are the force applicable directions to the sensor. For force applied to the sensor through each of the above directions, structural deformation pattern can be anticipated through the sensor structure. Hence, magnitude and the direction of the force applied can be determined by monitoring the structural deformation of the sensor.

The applicable 5DOFs for the proposed sensor structure in detail is as follows, three symmetric planes of x - z (X-direction), x - y (Y-direction), y - z (Z-direction) and two planes through z -axis that form angles 45° (P-direction) and -45° (Q-direction) with x -direction, as shown in Figure 6.4. There are two main structural patterns associated with the proposed sensor structure when forces acting on each defined directions, as shown in in Figure 6.5 and Figure 6.6, which can be used to measure the force applied. When forces acting on X , Y , P and Q directions as mentioned above, structural deformation pattern will be symmetrical (Load Condition A as shown in Figure 6.5) due to the symmetry. Also another structural deformation pattern can be identified when force applied along the z -axis (Load Condition B as shown in Figure 6.6).

Spring effect used in developing 1-DOF tactile sensors, is also incorporated into this proposed 5-DOF MEMS tactile sensor. Rather than using a spate spring to add the spring effect, in this proposed design, spring effect is incited by the deformation of eight flexible beams in the proposed structure. Since this proposed wagon wheel structure contains eight flexible beams spring effect will be much higher when comparing with Maltese cross spring structures having four flexible beams. Hence, sensor range will be higher in this structure.

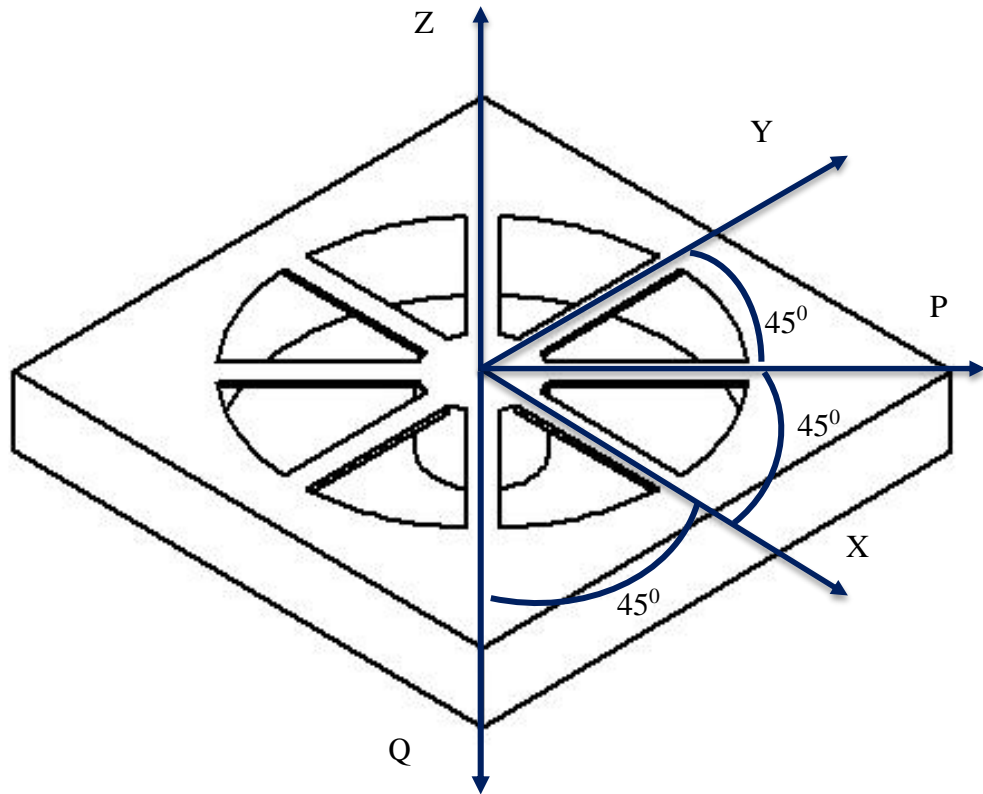


Figure 6.4: Degrees of freedoms of the structure
 University of Moratuwa, Sri Lanka.
 Electronic Theses & Dissertations
www.lib.mrt.ac.lk

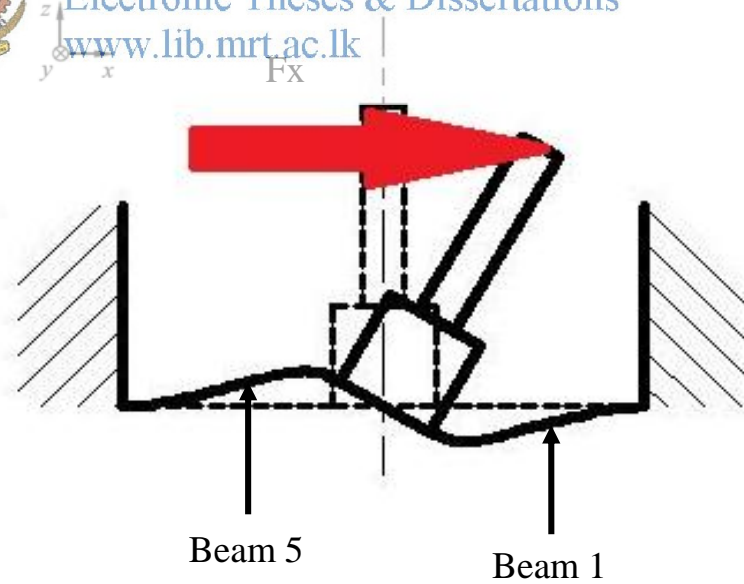


Figure 6.5: Possible structural deformations for loading condition A.

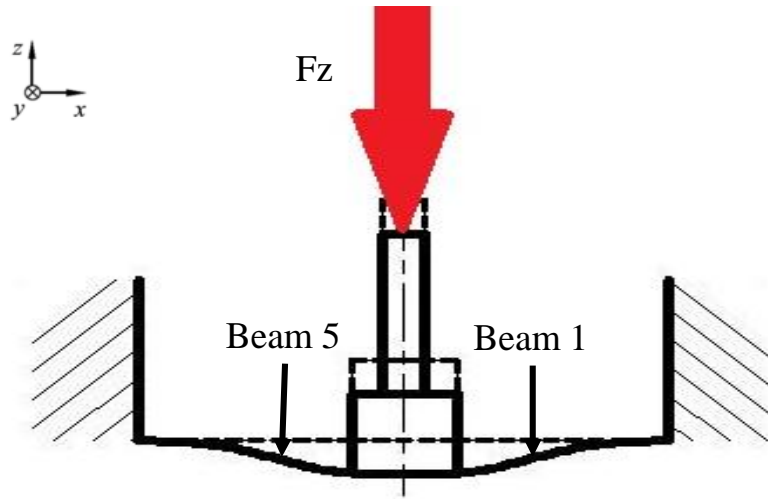


Figure 6.6: Possible structural deformations for loading condition B

6.4 Sensing Principle of 5-DOF MEMS Tactile Sensor

Since the force identification method of the sensor is by observing of the structural deformation, it is essential to incorporate a sensing principal that will give optimum results. From the literature, it was decided to use Piezoresistive sensing principle to convert structural deformation of the sensor into a measurable output. www.lib.mrt.ac.lk

Piezoresistivity is the change of resistance of a material as per the mechanical strain it experiences [74]. This characteristic depend on the material and specially, semiconductor materials has Piezoresistive characteristics. This is an added advantage for MEMS device design and fabrication as materials such as single crystal Silicon and Germanium, which are semiconductor materials, are typical material used in MEMS fabrication.

Single crystal Silicon, which is the selected material for the proposed sensor, permits to integrate Piezoresistive sensing elements on the structure [75]. This is basically due to the Piezoresistive characteristics of Silicon and using these fabricated sensing elements, output of the sensor can be taken with respect to the force applied. Due to the anisotropic nature of Silicon, force direction also can be differentiate easily through the sensor output. Equation 6.1 can be used to calculate the resistance change of a Piezoresistive sensing element.

$$\frac{\Delta R}{R} = \pi_L \sigma_L + \pi_T \sigma_T \quad (6.1)$$

Here π_L and π_T is the Piezoresistive coefficient along longitudinal and transverse direction respectively, σ_L and σ_T is the mechanical stress along longitudinal and transverse direction respectively.

Sensor output can be taken by placing Piezoresistive sensing elements on high stress points under loading conditions along a beam, to identify the magnitude and the direction of the applied force. Table 6.3 shows the specifications of the sensing element, which was proposed to integrate with the sensor structure.

Table 6.3: Piezoresistive element specification

Width		10 μm
Length		50 μm
Thickness		500 nm
Dopant Density	Sensing element	$1.20 \times 10^{19} \text{ cm}^{-3}$
	Connectors	$1.50 \times 10^{20} \text{ cm}^{-3}$



University of Moratuwa, Sri Lanka.
Electronic Theses & Dissertations
www.lib.mrt.ac.lk

It is important to connect the sensing element in a specific order to get the sensor output. In this research sensing elements are orchestrated in a whetstone bridge to get the output. Two whetstone bridge arrangements can be identified, full whetstone bridge and half whetstone bridge arrangement, which can be incorporated with the structure to get the sensor output. Equation 6.2 is related to the output when elements are connected in full whetstone bridge and Equation 6.3 is related to the output when elements are connected in half Whetstone Bridge.

$$V_{out} = \frac{1}{4} \left(\frac{\Delta R_1}{R_1} - \frac{\Delta R_2}{R_2} + \frac{\Delta R_3}{R_3} - \frac{\Delta R_4}{R_4} \right) V_{in} \quad (6.2)$$

$$V_{out} = \frac{1}{4} \left(\frac{\Delta R_1}{R_1} - \frac{\Delta R_2}{R_2} \right) V_{in} \quad (6.3)$$

Here, V_{in} is the input voltage, V_{out} is the output voltage, R_1 , R_2 , R_3 and R_4 are the resistance of sensing element arranged in the sensor structure. Figure 6.7 shows the sensing element arrangement in full Whetstone Bridge and Figure 6.8 shows the sensing element arrangement in half Whetstone Bridge.

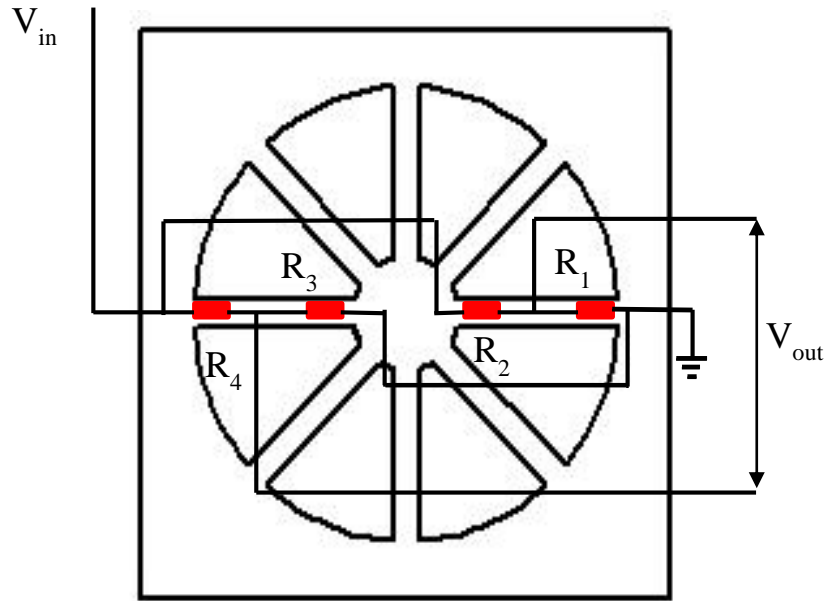


Figure 6.7: Piezoresistive sensing element arrangement in full Wheatstone Bridge.

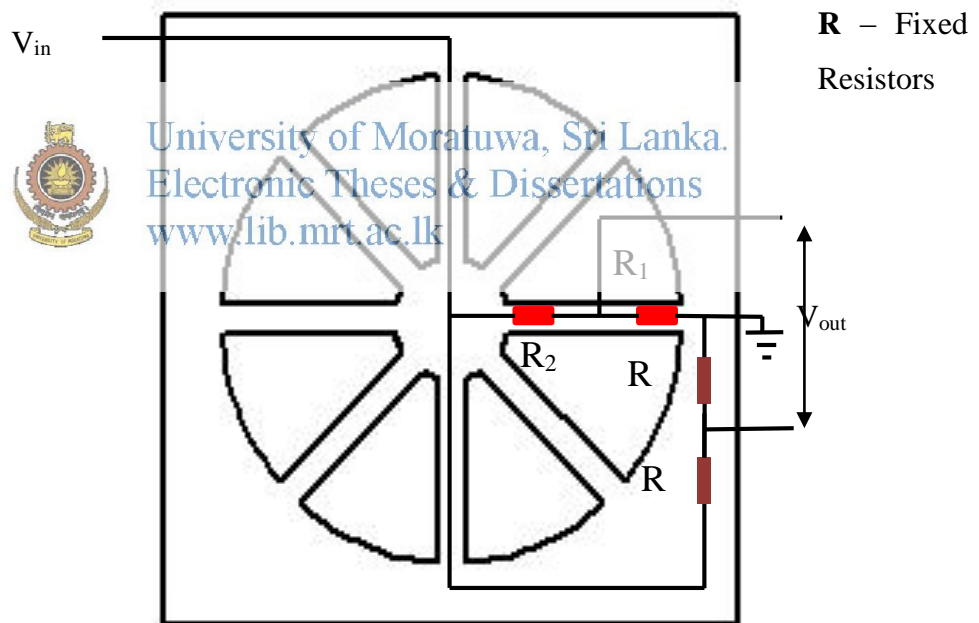


Figure 6.8: Piezoresistive sensing element arrangement in half Wheatstone Bridge.

6.5 Structural Analysis of the Proposed 5-DOF MEMS Sensor Structure

To validate the working principle and optimize the structure, an FEA was performed for the proposed structure. *COMSOL Multiphysics* software was utilized to perform this FEA. Structural deformation pattern for loading condition A and loading condition

B analysed was analysed separately in the conducted analysis. Table 6.4 shows the parameters specified for this structural analysis.

For this analysis also, four basic steps has to be perform, which are structure specification, material specification, specification of boundary conditions and mesh construction. Considering the geometry applicable for this structural analysis, proposed structure shown in Figure 6.2 was modelled with SolidWorks software and imported to COMSOL using the live link interface feature in COMSOL.

The next step of preparing this structural analysis is to specify the materials incorporated with the specified geometry. For this analysis, single crystal Silicon was chosen as the structural material. Since Silicon is the most abundant material in the earth, due to its feasible material properties and semi conductive characteristic, Silicon or Silicon base materials are used in almost all the MEMS based components. For this proposed sensor also, properties of Silicon is optimum and because its anisotropic nature, proposed working principle can be monitored through the proposed sensing principle.



University of Moratuwa, Sri Lanka.

Electronic Theses & Dissertations

www.lib.mrt.ac.lk

The next step is to specify the boundary conditions for the analysis. In this analysis, a boundary load is applied to the structure through the surface as shown in Figure 6.9. Also fixed constraint was applied to the surface as shown in Figure 6.10. As the final step, a mesh was constructed for the specified structure according to the parameters specified in Table 6.4 computed the specified analysis to obtain results.

Table 6.4: Parameters specified for the structural analysis

Parameter		Specification	
		Unit	Value
Material		Silicon (Single Crystal, Anisotropic)	
Mesh	Element Type	Tetrahedral	
	Minimum Element Size	mm	0.03
	Number of Elements	161883	
	Minimum Element Quality	1.22E-01	
	Average Element Quality	0.7389	

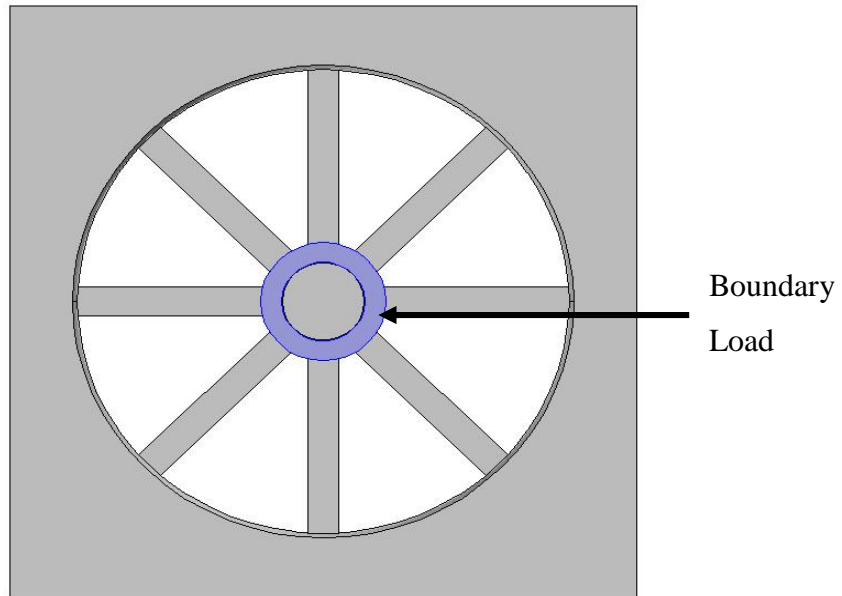


Figure 6.9: Selected boundary to apply boundary load



Figure 6.10: Selected Boundaries to apply fixed constraint boundary condition

After setting up the analysis, it was computed and results were obtained. From the obtained results, it can be seen that the structural deformation pattern for each loading condition is as same as the expected deformation pattern in the working principle. Figure 6.11 and Figure 6.12 shows the displacement plot results of sensor structure for loading condition A and B respectively. Figure 6.13 and Figure 6.14 shows equivalent stress plot results of sensor structure for loading condition A and B respectively.

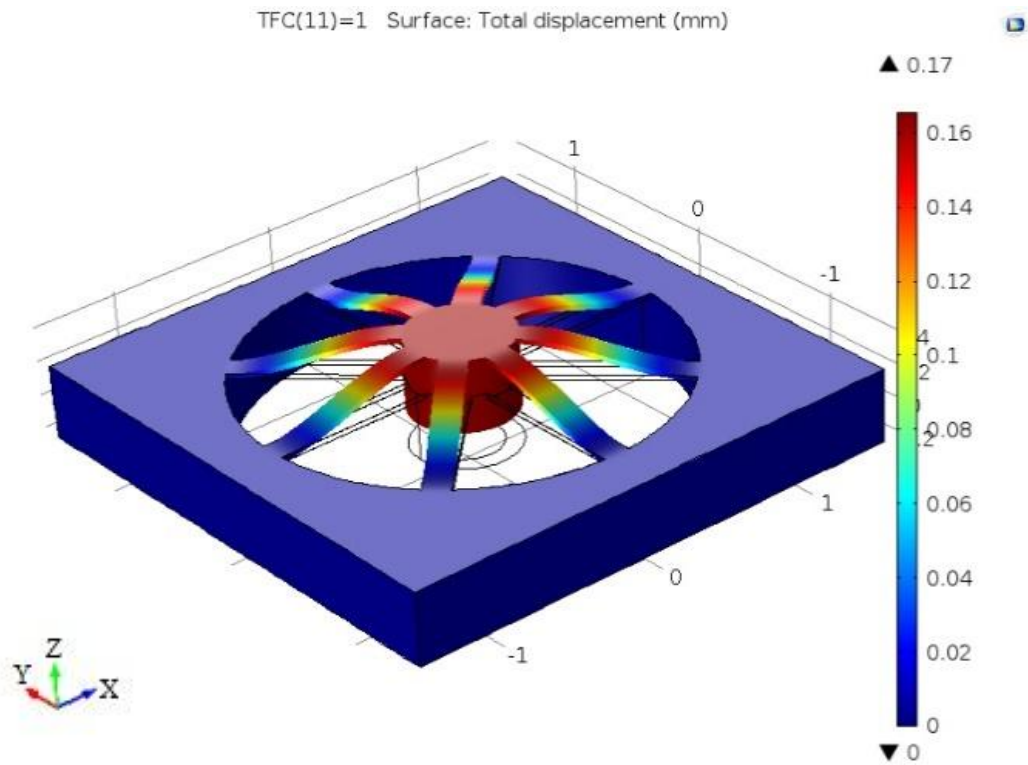


Figure 6.11: Displacement plot of the sensor structure for load condition A

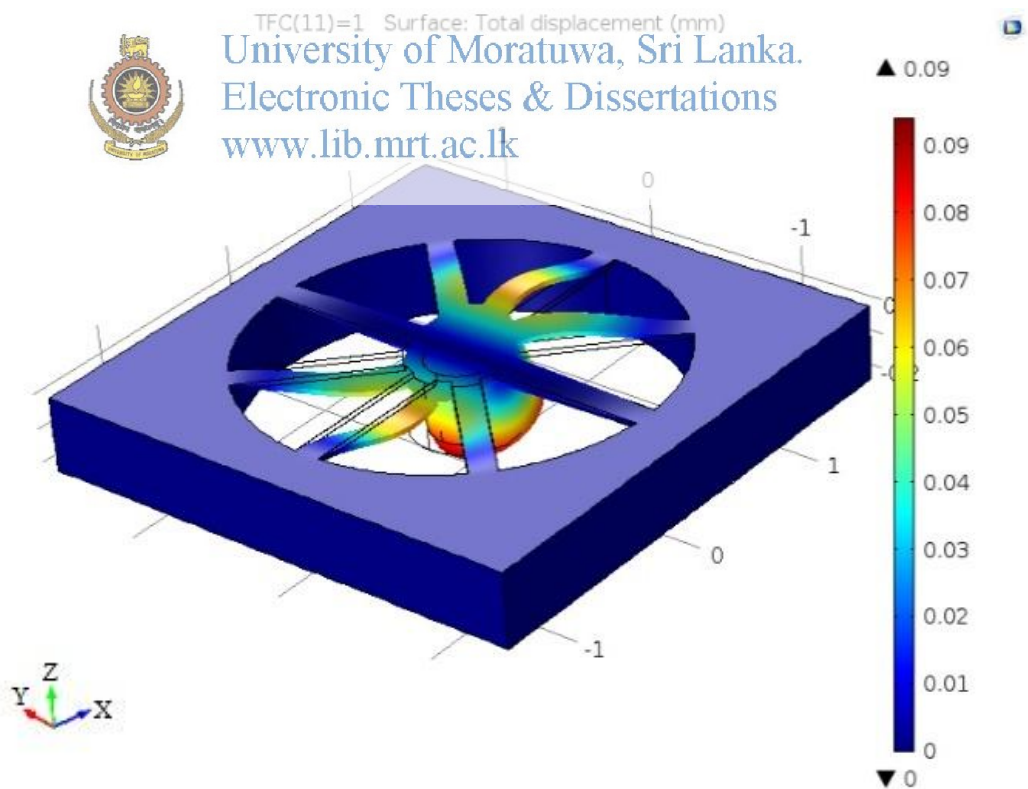


Figure 6.12: Displacement plot of sensor structure for load condition B.

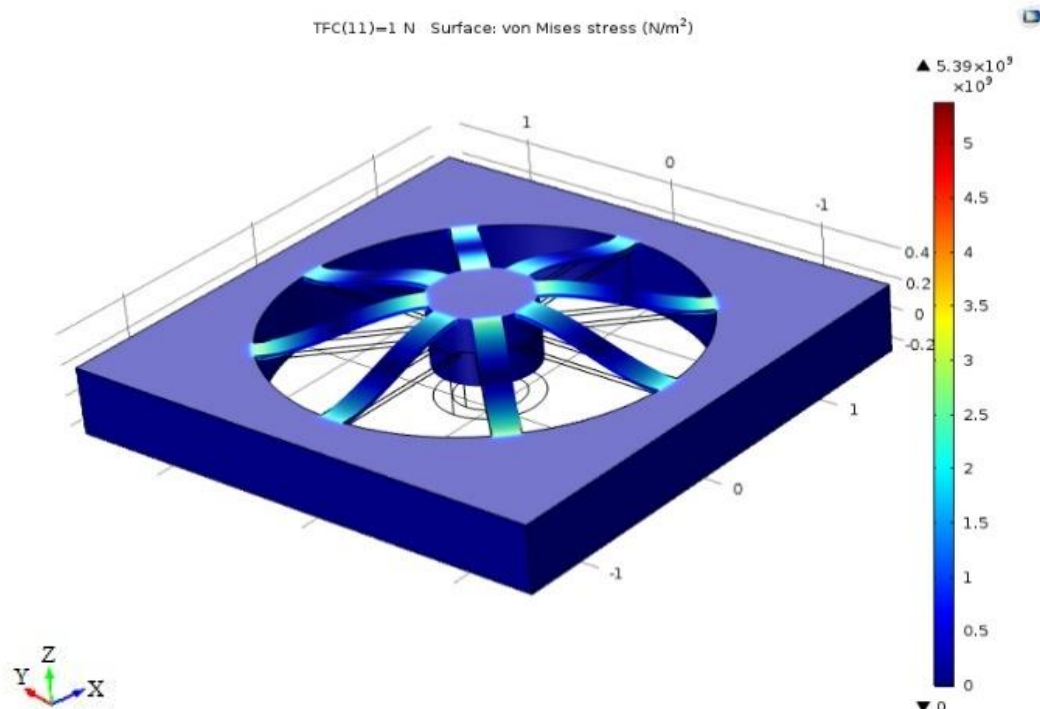


Figure 6.13: Equivalent stress plot of sensor structure for load condition A.

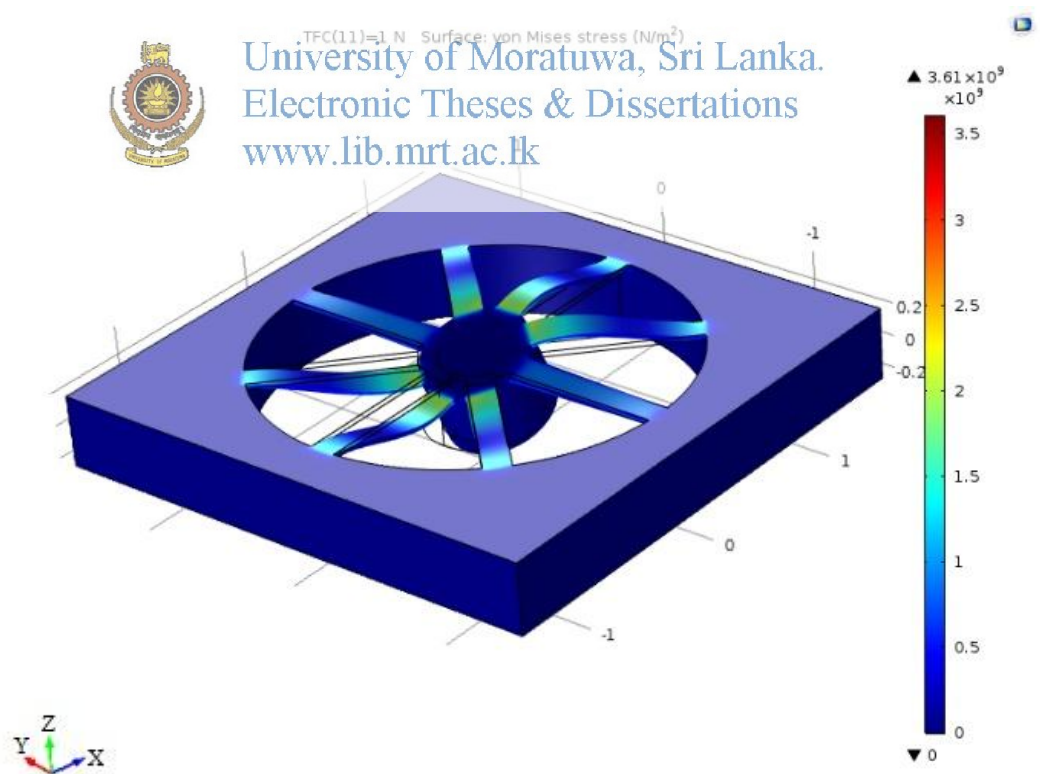


Figure 6.14: Equivalent stress plot of sensor structure for load condition B.

6.6 Sensing Element Placement in Proposed 5-DOF MEMS Sensor Structure

It is crucial to place sensing elements at position where stress is higher under loading conditions for an optimum sensor output [76]. Stress variation along a beam was plotted under loading as shown in Figure 6.15 from the results of the structural analysis. As per this plot two ideal positions can be recognised along a beam to place sensing elements as shown in Figure 6.15. So it was chosen to place the two sensing elements at 320 μm and 1120 μm away from the centre of the sensor structure as appeared in Figure 6.16.

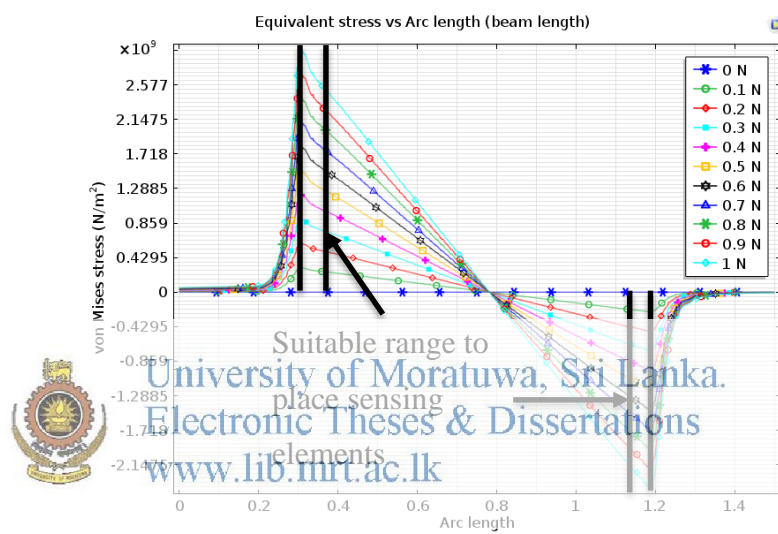


Figure 6.15: Stress variation along a beam under loading and suitable position to place sensing elements

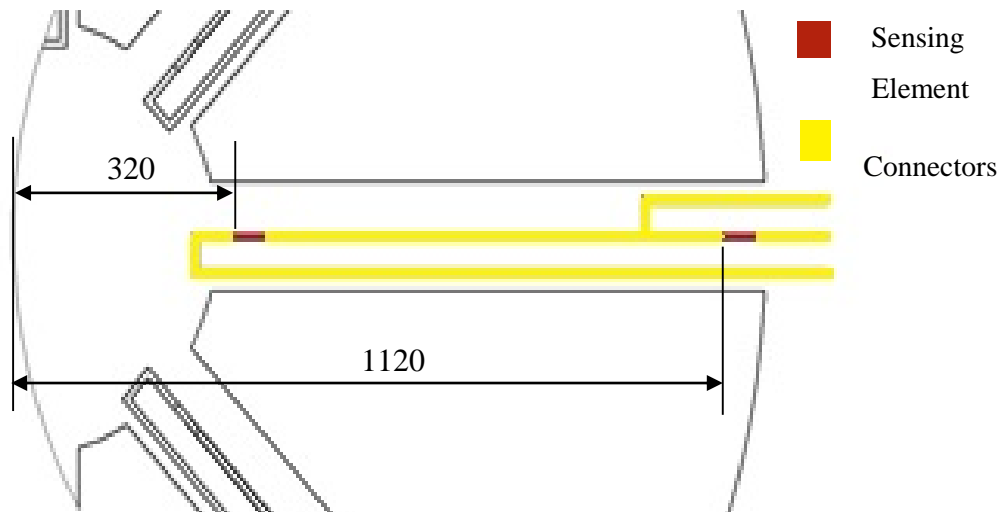


Figure 6.16: integrated sensing elements on the structure and their positions with electrical connections

6.7 Multiphysics Analysis of 5-DOF MEMS Tactile Sensor

A Multiphysics analysis was performed using COMSOL 5.0 Multiphysics software, after integrating Piezoresistive sensing elements in the structure. In this analysis, not only the structural mechanics of structure but also the piezoresistivity variation of sensing elements was analysed concurrently. Main objective of performing this analysis is to simulate the proposed MEMS tactile sensor for given conditions and validate the proposed sensing principle.

For this Multiphysics analysis also, four preliminary steps, which are specification of geometry, specification of material, boundary condition specification and mesh construction, should be completed before computing the problem. Figure 6.17 shows the geometry considered for this Multiphysics analysis using COMSOL. In this geometry, proposed 5-DOF MEMS structure was incorporated with the Piezoresistive elements such as sensing elements and connectors according to the specifications identified through the sensing principle and the structural analysis performed for the proposed structure.

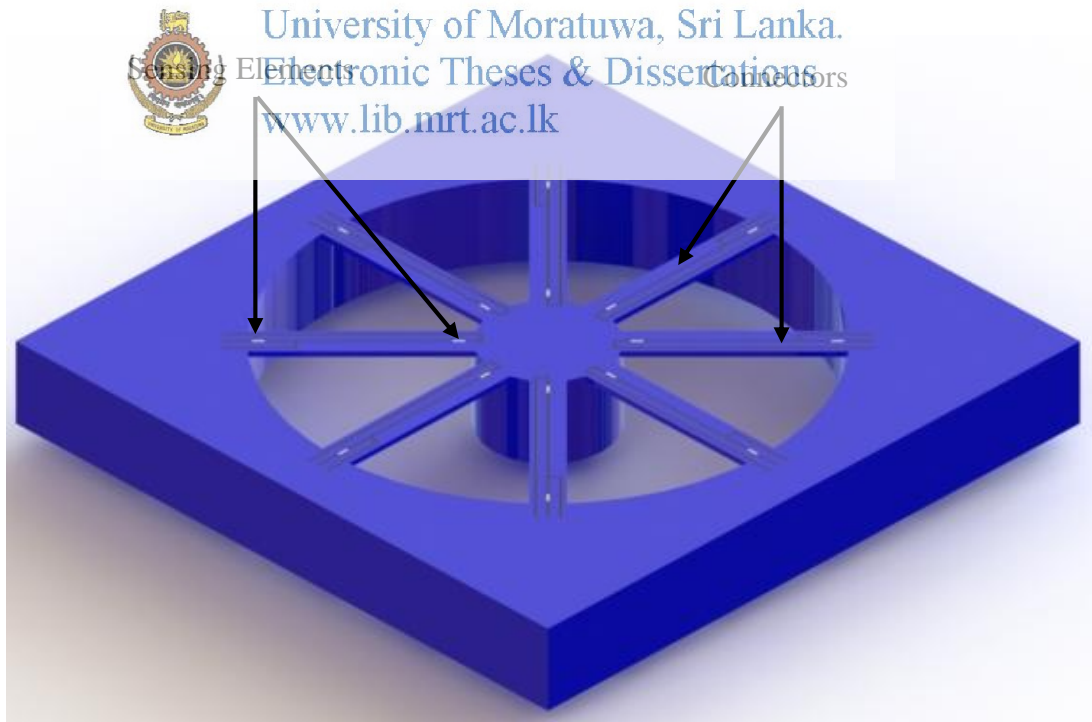


Figure 6.17: Geometry considered for the Multiphysics analysis

The next step of setting up the analysis is to specify the material for each element considered in the specified geometry. For this analysis, as specified in the Table 6.5, lightly doped, single crystal n-Silicon was chosen as the structural material and lightly doped, single crystal p-Silicon was chosen for the Piezoresistive layer. Figure 6.18 shows the specified Piezoresistive layer.

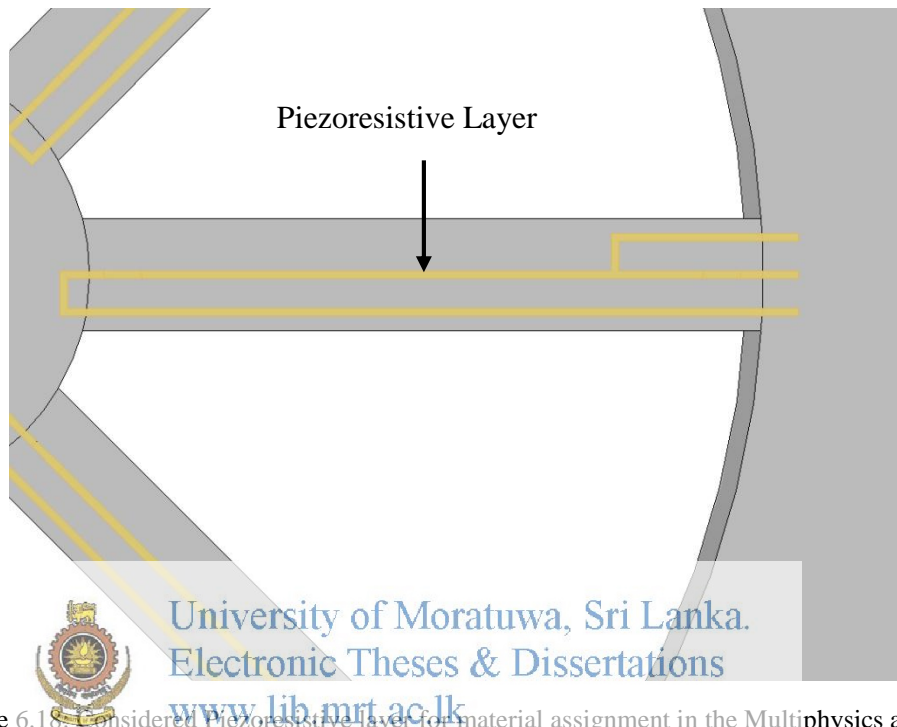


Figure 6.18: Considered Piezoresistive layer for material assignment in the Multiphysics analysis

Table 6.5: Parameters specified for the Multiphysics analysis

Parameter		Specification		
		Unit	Value	
Material	Structure	n-Silicon (Single Crystal, Lightly Doped)		
	Piezoresistors and connectors	p-Silicon(Single Crystal, Lightly Doped)		
Dopant Density	Piezoresistors and connectors	cm ⁻³	1.20E+19	
	Connectors	cm ⁻³	1.50E+20	
Piezoresistive layer thickness		nm	500	
Mesh	Element Type	Structure	Tetrahedral	
		Piezoresistors and connectors		
	Minimum Element Size		mm	0.05
	Number of Elements		194695	
	Minimum Element Quality		1.41E-02	
Average Element Quality		0.6917		

After assigning the materials for the element in the specified geometry, it is required to specify boundary conditions to conduct the Multiphysics analysis. As described in the structural analysis performed for the proposed MEMS 5-DOF tactile sensor, a boundary load and fixed constraint was added to the surfaces as shown in the Figure 6.9 and Figure 6.10 respectively.

Apart from these boundary conditions, another boundary condition was added specifying the Piezoresistive elements in the specified geometry. In this boundary condition layer thickness was set to 500 nm and dopant density was set to be $1.20\text{E}+19\text{ cm}^{-3}$ as specified in the Table 6.5. Figure 6.19 shows the specified sensing elements in the geometry.

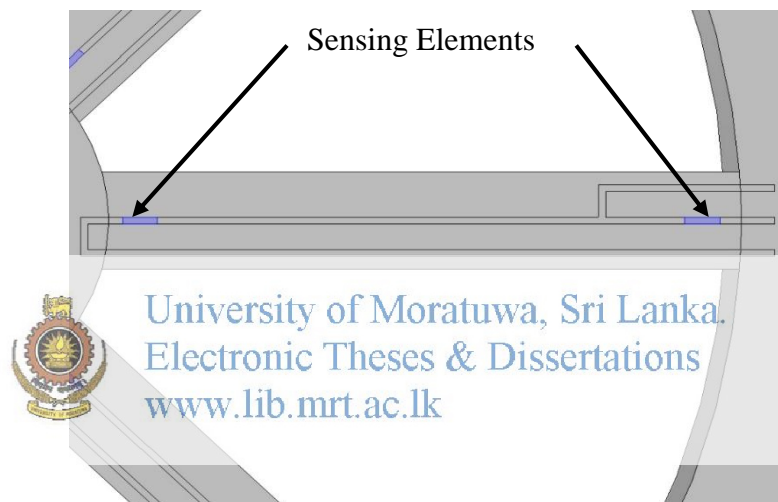


Figure 6.19: Specified thin Piezoresistive sensing elements

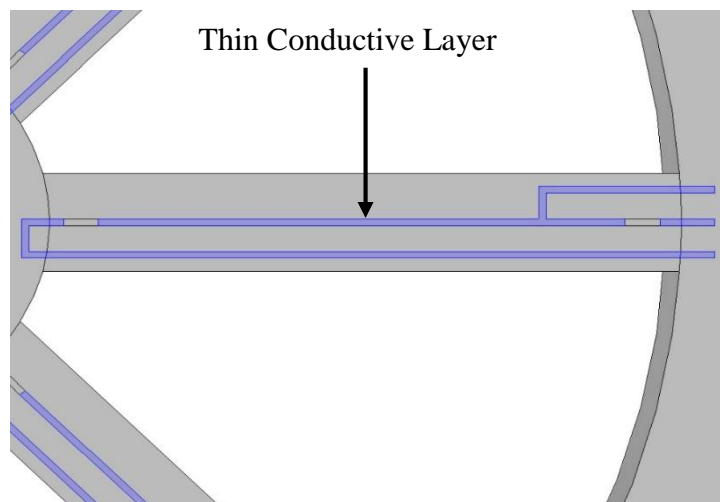


Figure 6.20: Specified thin conductive layer

Also another boundary condition was added specifying a thin conductive layers to specify the connector elements for the Multiphysics analysis. For this boundary condition, parameters were set, so that the layer thickness is 500 nm and dopant density is $1.50E+20 \text{ cm}^{-3}$ as specified in the Table 6.5. Figure 6.20 shows the specified thin conductive layer for the analysis.

The above boundary conditions were added to evaluate the electrical characteristics of the proposed sensor and to supply power to the specified electrical circuitry in the geometry another boundary conditions were added specifying a voltage terminal and ground terminal. For this analysis 3 V was supplied to the voltage terminal. Figure 6.21 shows the specified electrical terminals.

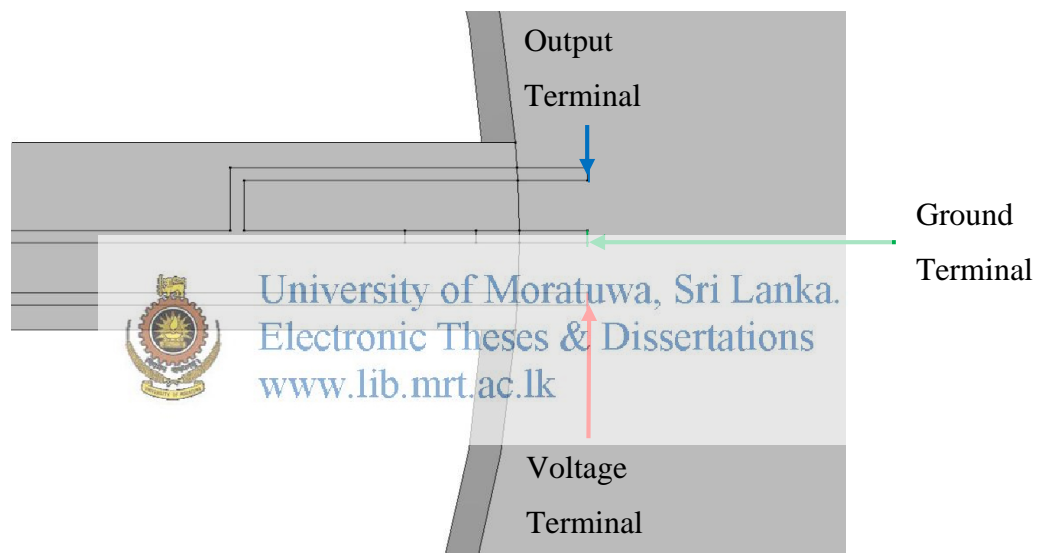


Figure 6.21: Specified electrical terminals for the Multiphysics analysis

After specifying the boundary conditions, a mesh was constructed according to the parameters specified in the Table 6.5. Then, for each and every loading conditions this Multiphysics analysis was performed, and results were obtained for several categories considering the sensor performance such as resistance change of each sensing element, voltage variation in a Whetstone Bridge, voltage outputs of each whetstone bridge and current conducting direction. Figure 6.22 and Figure 6.23 shows change of resistance in sensing element for loading condition A. Figure 6.24 and Figure 6.25 shows change of resistance in sensing element for loading condition B. Figure 6.26 and Figure 6.27 shows potential variation through electrical circuit and current conducting direction.

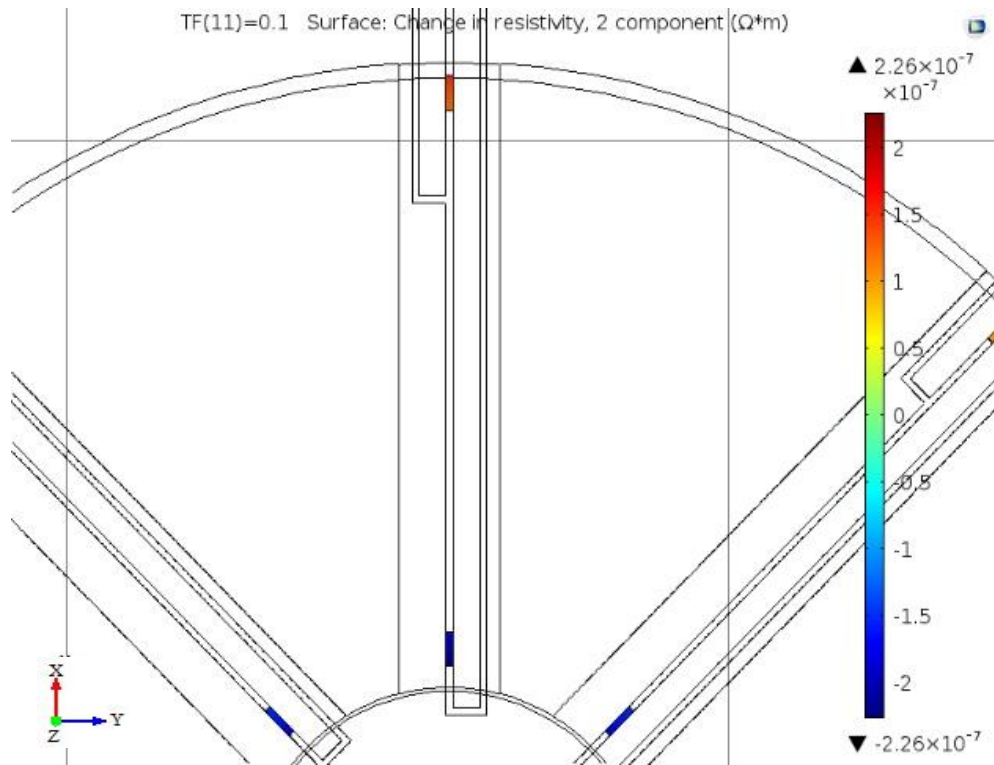


Figure 6.22: Change in resistance of elements in beam 1 for Loading Condition A

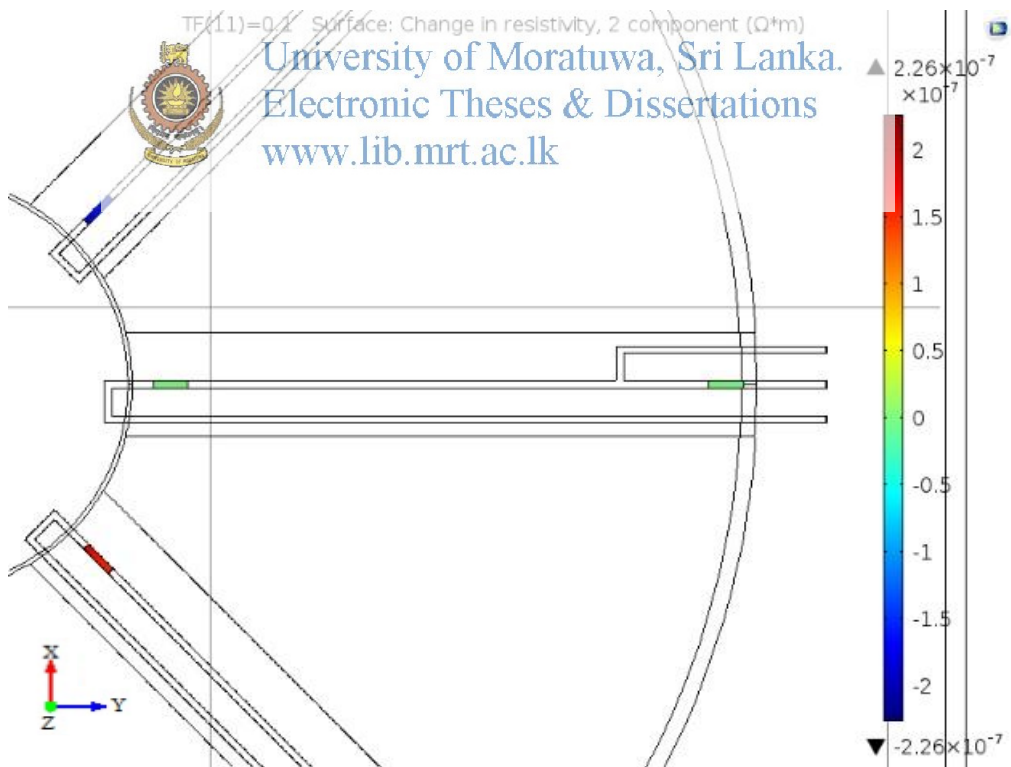


Figure 6.23: Change in Resistance of elements in beam 3 for Loading Condition A

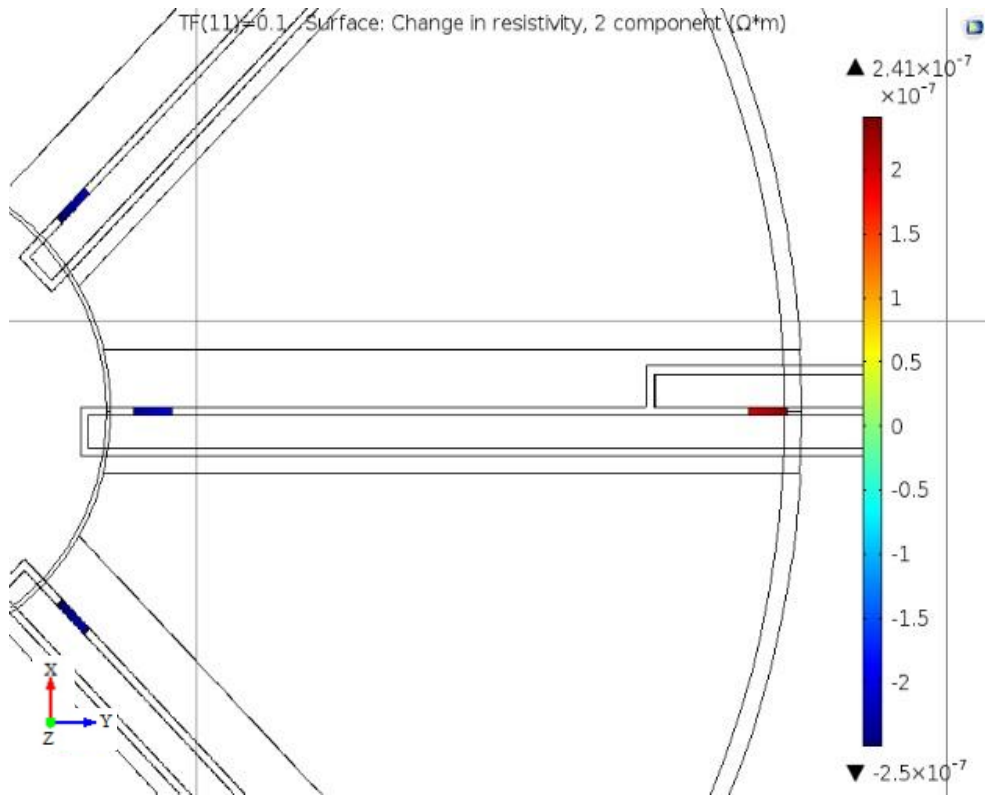


Figure 6.24: Change in Resistance of elements in beam 1 for Loading Condition B

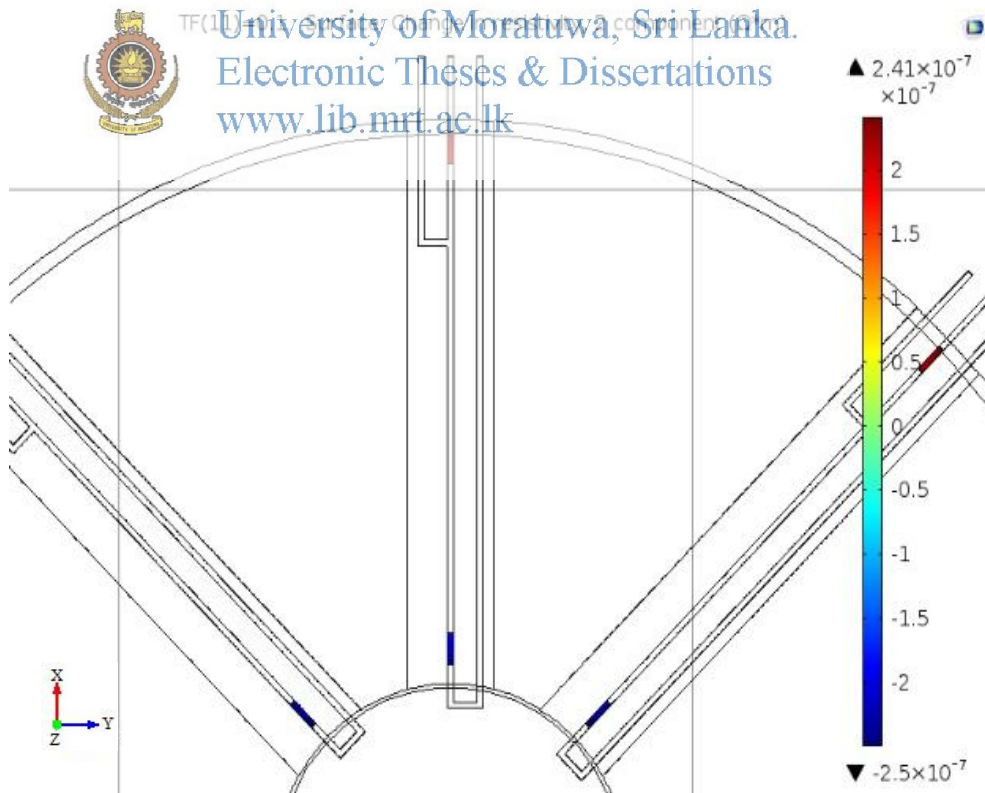


Figure 6.25: Change in resistance of elements in beam 3 for Loading Condition B.

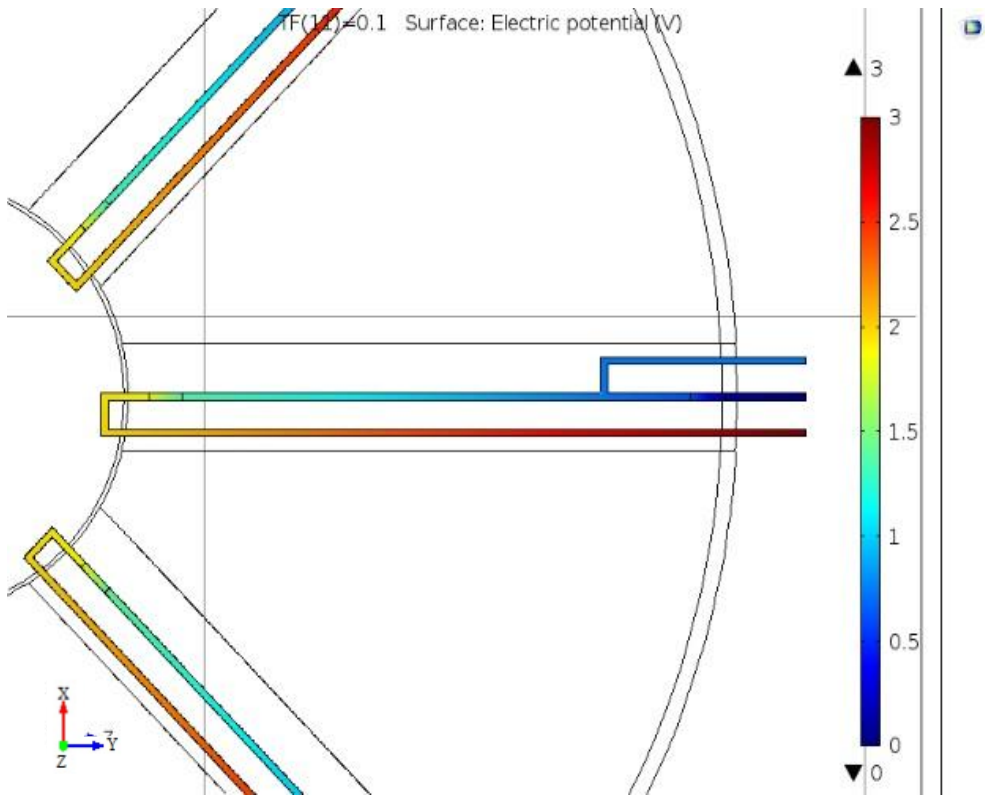


Figure 6.26: Voltage variation of a Whetstone Bridge in a beam

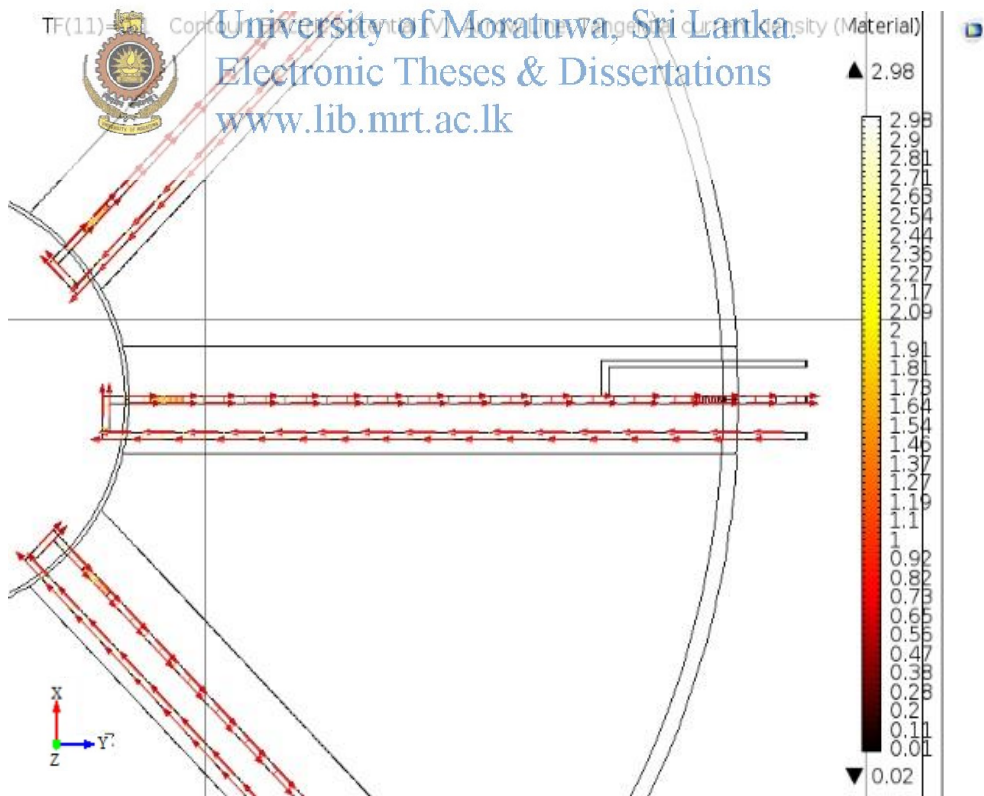


Figure 6.27: Current direction of a Whetstone Bridge

6.8 Results of the Simulation of proposed 5-DOF MEMS Tactile Sensor

Following actions can be identified regarding the proposed MEMS tactile sensor according to the results of the Multiphysics analysis as shown in Figure 6.22, Figure 6.23, Figure 6.24 and Figure 6.25. Considering the loading condition A, it can be identified a pattern for change of resistance in sensing elements of the beams along the force direction and comparing with those sensing elements, resistance change is neutral in sensing elements on the beams perpendicular to the force direction. Considering the loading condition B, change of resistance of sensing elements in all beams has the same pattern with similar change of resistance.

Hence, the output of each whetstone bridge can be calculated from this Multiphysics analysis as it is possible to measure resistance change of each and every sensing elements on the beams. The output voltage variation of each Whetstone Bridge with respect to force variation under loading condition A, is shown in the Table 6.6. When analysing the values of Table 6.6, it can be identified that, for loading condition A where the force is acting on x -direction, first Whetstone Bridge gives the maximum output when comparing with other as shown in the Table 6.6.



Table 6.6: Voltage output for each whetstone bridge for Loading condition A

Total Force (N)	Output (V)				
	Bridge 1	Bridge 2	Bridge 3	Bridge 4	Bridge 5
0.01	-1.47E-02	-7.86E-03	1.26E-03	4.49E-03	7.08E-04
0.02	-2.93E-02	-1.57E-02	2.51E-03	8.97E-03	7.10E-04
0.03	-4.40E-02	-2.36E-02	3.77E-03	1.34E-02	7.12E-04
0.04	-5.86E-02	-3.15E-02	5.02E-03	1.79E-02	7.15E-04
0.05	-7.33E-02	-3.93E-02	6.28E-03	2.24E-02	7.18E-04
0.06	-8.79E-02	-4.72E-02	7.53E-03	2.69E-02	7.21E-04
0.07	-1.03E-01	-5.51E-02	8.79E-03	3.14E-02	7.25E-04
0.08	-1.17E-01	-6.29E-02	1.00E-02	3.58E-02	7.28E-04
0.09	-1.32E-01	-7.08E-02	1.13E-02	4.03E-02	7.33E-04
0.1	-1.47E-01	-7.87E-02	1.26E-02	4.48E-02	7.37E-04

Output voltage variation of each Whetstone Bridge with respect to force variation for loading condition B, is shown in Table 6.7. From the values of Table 6.7, it can be seen that, fifth Whetstone Bridge gives the maximum output for loading condition B when comparing with others as highlighted in Table 6.7.

Table 6.7: Voltage output for each whetstone bridge for Loading condition B

Total Force (N)	Output (V)				
	Bridge 1	Bridge 2	Bridge 3	Bridge 4	Bridge 5
0.01	3.27E-05	5.25E-05	1.18E-05	-4.46E-06	1.26E-03
0.02	7.53E-05	9.78E-05	2.27E-05	-1.82E-05	1.82E-03
0.03	1.19E-04	1.45E-04	3.40E-05	-3.21E-05	2.37E-03
0.04	1.64E-04	1.94E-04	4.56E-05	-4.63E-05	2.93E-03
0.05	2.09E-04	2.45E-04	5.76E-05	-6.07E-05	3.48E-03
0.06	2.55E-04	2.97E-04	6.99E-05	-7.54E-05	4.04E-03
0.07	3.03E-04	3.52E-04	8.26E-05	-9.03E-05	4.59E-03
0.08	3.51E-04	4.08E-04	9.56E-05	-1.05E-04	5.15E-03
0.09	4.00E-04	4.66E-04	1.09E-04	-1.21E-04	5.70E-03
0.1	4.51E-04	5.25E-04	1.23E-04	-1.37E-04	6.26E-03

This phenomenon is helpful in differentiating the force direction of the force applied to the proposed MEMS tactile sensor. Since there are 4 different directions applicable to apply force under loading condition A, according to this phenomena that the proposed sensor exhibit, output values of the Whetstone Bridge along the force direction among first four Whetstone Bridges will be maximum when comparing with others. Whereas, loading condition B can be identified by the maximum values at fifth Whetstone Bridge comparing with others as there are only one force applicable direction for loading condition B.

Subsequent to recognizing the direction of force, magnitude of the applied force can be distinguished using the output values of the Whetstone Bridge which provides the maximum output when comparing with others at each loading condition. Additionally, it can be identified that the relationship between output voltage and force applied is

linear according to the Figure 6.28 considering the loading condition A and Figure 6.29 considering the loading condition B.

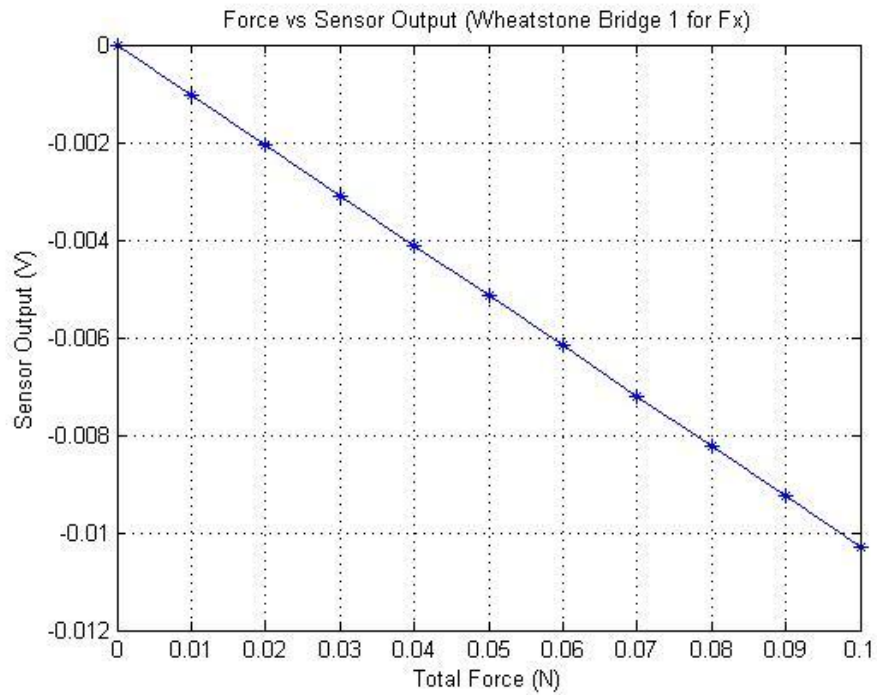


Figure 6.28: Plot result for loading condition A showing the relationship between output voltage of Whetstone Bridge and force applied to the sensor

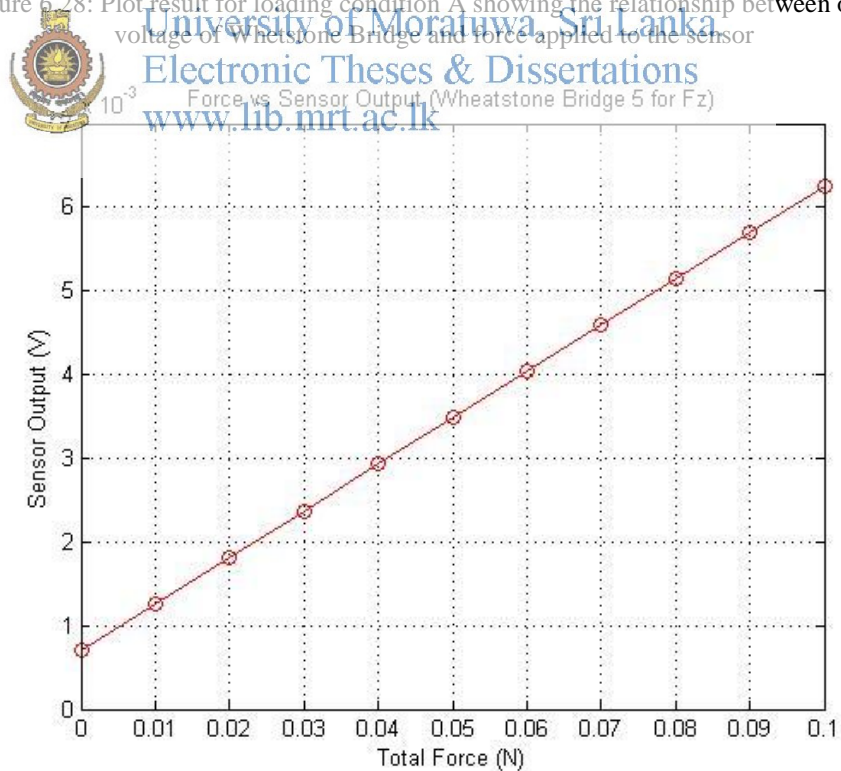


Figure 6.29: Plot result for loading condition B showing the relationship between output voltage of Whetstone Bridge and force applied to the sensor

6.9 Fabrication of Proposed 5-DOF MEMS Tactile Sensor

Next step of developing a sensor is to fabricate the proposed design. But due to unavailability of MEMS production facility, fabricating the proposed MEMS sensor won't be possible regarding this research. But nevertheless, fabrication steps of the proposed MEMS sensor is proposed in this section.

6.9.1 Proposed Wiring Design for 5-DOF MEMS Tactile Sensor

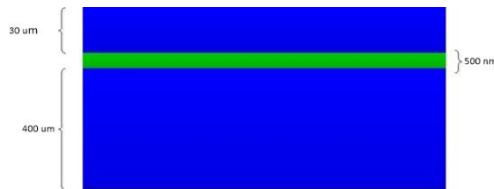
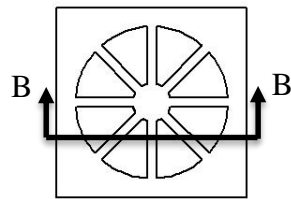
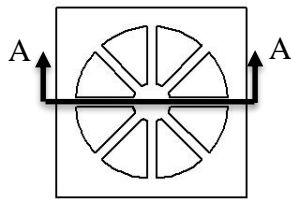
When designing the fabrication process steps for a MEMS sensor, it is crucial to design optimum design for wirings and wire bonding pads of the structure. Figure 6.30 shows the proposed wiring design for designed 5-DOF MEMS tactile sensor.



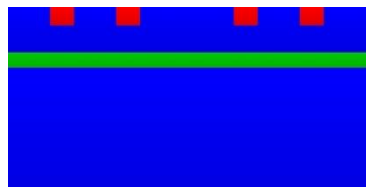
Figure 6.30: Proposed wiring design with wire bonding pads for 5-DOF MEMS tactile sensor

6.9.2 Proposed Fabrication Steps for 5-DOF MEMS Tactile Sensor

Figure 6.31 shows the proposed fabrication steps for designed 5-DOF MEMS tactile sensor. These proposed fabrication steps are unique for this proposed 5-DOF MEMS tactile sensor as all the MEMS related devices follow its own unique fabrication steps.



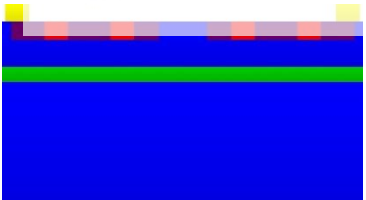
SOI wafer: Si top layer of 30 μ m, SiO₂ middle layer of 500nm and again Si layer of 400 μ m
(Section on A-A)



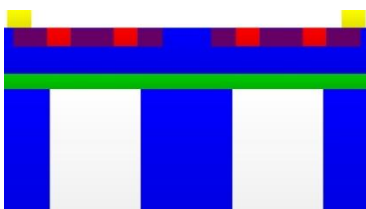
Doping of Piezoresistive elements
(Section on A-A)



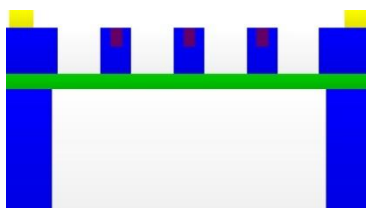
Deposition of Metal for wire bonding
(Section on A-A)



Deep Reactive Ion Etching of Silicon
(Section on A-A)



Fabrication of Beams
(Section on B-B)



Fabrication of Beams
(Section on B-B)

University of Moratuwa, Sri Lanka
Electronic Theses & Dissertations
www.lib.mrt.ac.lk

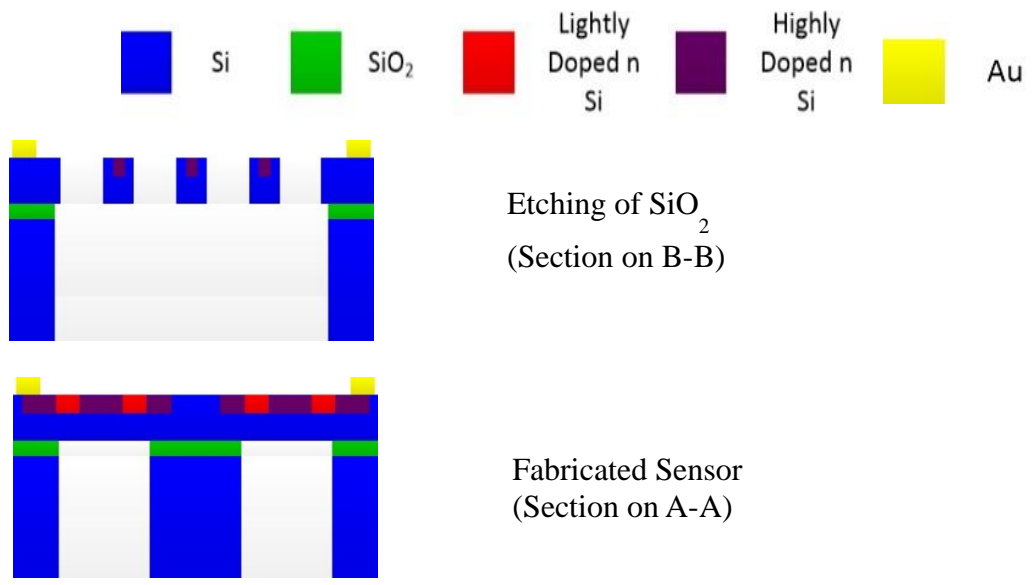


Figure 6.31: Proposed fabrication steps for the designed 5-DOF MEMS tactile sensor.



University of Moratuwa, Sri Lanka.
Electronic Theses & Dissertations
www.lib.mrt.ac.lk

7 CONCLUSION

Tactile sensors use sense of touch to acquire data from the physical environment considering tactile parameters such as force, pressure, temperature, etc. Over the past decades there have been found many sensing principles that can be incorporated with tactile sensors such as Piezoresistive, piezoelectric, capacitive, etc. These each and every sensing principle has their own advantages and disadvantage, hence, it is required to choose optimum sensing principle considering the application to use in a tactile sensor. There can be found many applications of tactile sensors related to robotics, mechatronics, biomedical and industrial field. This is mainly due to the capability of tactile sensors to provide an optimum feedback systems for those applications. Considering biomedical field, tactile sensors are widely used in tactile imaging applications.

Tactile imaging is one of the medical diagnostic technique which generally uses to screen breast or prostate cancer. Other than that there are many applications of tactile imaging such as pelvic organ prolapse screening, minimally invasive surgery, biomedical pressure mapping and so on. It has been proven that, comparing with other cancer screening methods, tactile imaging is a cost effective cancer screening technique. To develop low cost tactile imagers with optimum performance, it is required to develop tactile sensors with better performance for low cost, as tactile sensor is the foremost element in a tactile imager.

In this research, main motive was to develop miniaturized tactile sensors for tactile imaging applications. With that motive in mind, as the first stage of this research, a novel 1-DOF tactile sensor was developed. Working principle and sensing principle of the developed sensor are clearly stated. After the designing, sensor was fabricated and conducted experiments with the purpose of calibrating the sensor and quantify the sensor characteristics accordingly. At this stage, there were some issue found associated with the developed sensor such as, lack of overload protection, manufacturing limitations which cause structural errors, etc.

A novel enclosed 1-DOF tactile sensor was developed as the stage 2 of developing tactile sensors, while trying to overcome the issues identified at previous stage.

Working and sensing principles incorporated with this were same as the one developed at previous stage. Designed sensor was fabricated and tested to calibrate it and also to quantify the sensor characteristics.

With this developed sensor, an experiment was carried out to verify the feasibility to use this sensor for tactile imaging applications. Details of the conducted experiment was stated and tactile image was constructed of a left hand of a person at a certain posture using the acquired data at the experiment. This validate that the developed sensor can be used in tactile imaging applications.

When using sensors in tactile imaging applications, it is better to use sensor array, rather than using a single sensor. To have a sensor array with better performance it is required to have large number of taxels present in the sensor array. Hence, to accomplish this, a design of a MEMS based tactile sensor was presented. Working principle and sensing principle was stated regarding the MEMS based tactile sensor. A Multiphysics analysis was conducted with the purpose of simulating the designed sensor and results of this analysis is presented. Due to the use of wagon wheel structure for this MEMS tactile sensor, number of DOFs of sensor is increased and load bearing capacity of the sensor has improved. Fabrication steps for the proposed sensor was also presented in this research.


Future work of the research lies in fabricating this sensor using MEMS fabrication techniques and calibrate and test the characteristics of the developed sensor.




REFERENCES

- [1] M. I. Tiwana, S. J. Redmond, and N. H. Lovell, "A review of tactile sensing technologies with applications in biomedical engineering," *Sens. Actuators Phys.*, vol. 179, pp. 17–31, Jun. 2012.
- [2] H. I. Jaafar, "Current Trend of Tactile Sensor in Advanced Applications," *Sens. Transducers*, vol. 143, no. 8, pp. 32–43, Aug. 2012.
- [3] R. S. and M. Valle, "Tactile Sensing for Robotic Applications," in *Sensors: Focus on Tactile Force and Stress Sensors*, J. Gerardo and S. Lanceros-Mendez, Eds. InTech, 2008.
- [4] M. H. Lee and H. R. Nicholls, "Review Article Tactile sensing for mechatronics—a state of the art survey," *Mechatronics*, vol. 9, no. 1, pp. 1–31, Feb. 1999.
- [5] M. H. Lee, "Tactile Sensing: New Directions, New Challenges," *Int. J. Robot. Res.*, vol. 19, no. 1, pp. 1–31, Mar. 2000.
- [6] P. Estevez, J. M. Bank, M. Porta, J. Wei, P. M. Sarro, M. Tichem, and U. Staufer, "6 DOF force and torque sensor for micro-manipulation applications," *Sens. Actuators Phys.*, vol. 186, pp. 86–93, Oct. 2012.
- [7] T. Mei, W. J. Li, Y. Ge, Y. Chen, L. Ni, and M. H. Chan, "An integrated MEMS three-dimensional tactile sensor with large force range," *Sens. Actuators Phys.*, vol. 80, no. 2, pp. 155–162, Mar. 2000.
- [8] "FlexiForce e-Book 'Force Sensors for Design' Download," *Tekscan*, 13-Dec-2013. [Online]. Available: <https://www.tekscan.com/flexiforce-e-book-force-sensors-design-download>. [Accessed: 27-Aug-2013].
- [9] "Interlink Electronics." [Online]. Available: <http://www.interlinkelectronics.com/FSR402.php>. [Accessed: 27-Sep-2013].

- [10] M. Shikida, T. Shimizu, K. Sato, and K. Itoigawa, "Active tactile sensor for detecting contact force and hardness of an object," *Sens. Actuators Phys.*, vol. 103, no. 1–2, pp. 213–218, Jan. 2003.
- [11] H.-K. Lee, S.-I. Chang, and E. Yoon, "A Flexible Polymer Tactile Sensor: Fabrication and Modular Expandability for Large Area Deployment," *J. Microelectromechanical Syst.*, vol. 15, no. 6, pp. 1681–1686, Dec. 2006.
- [12] H. B. Muhammad, C. M. Oddo, L. Beccai, C. Recchiuto, C. J. Anthony, M. J. Adams, M. C. Carrozza, D. W. L. Hukins, and M. C. L. Ward, "Development of a bioinspired MEMS based capacitive tactile sensor for a robotic finger," *Sens. Actuators Phys.*, vol. 165, no. 2, pp. 221–229, Feb. 2011.
- [13] "Pressure Mapping System," *Pressure Profile Systems*. [Online]. Available: <http://www.pressureprofile.com/pressure-mapping/>. [Accessed: 20-Aug-2014].
- [14] A. P. Gerratt, N. Sommer, S. P. Lacour, and A. Billard, "Stretchable capacitive tactile skin on humanoid robot fingers-First experiments and results," in *2014 IEEE/RSJ International Conference on Humanoid Robots*, 2014, pp. 238–245.
- [15] J. A. Dobrzynska and M. A. M. Gijs, "Capacitive flexible force sensor," *Procedia Eng.*, vol. 5, pp. 404–407, 2010.
- [16] P. Lang, "Optical tactile sensors for medical palpation," *Can.-Wide Sci. Fair*, 2004.
- [17] M. Ohka, H. Kobayashi, and Y. Mitsuya, "Sensing characteristics of an optical three-axis tactile sensor mounted on a multi-fingered robotic hand," in *2005 IEEE/RSJ International Conference on Intelligent Robots and Systems*, 2005, pp. 493–498.
- [18] H. Kajimoto and S. Tachi, "Optical tactile sensor," EP1321753 A1, 25-Jun-2003.

- [19] Javad Dargahi, Mojtaba Kahrizi, Nakka Purushotham Rao, and Saeed Sokhanvar, "Design and microfabrication of a hybrid piezoelectric-capacitive tactile sensor," *Sens. Rev.*, vol. 26, no. 3, pp. 186–192, Jul. 2006.
- [20] J. Brugger, D. Briand, T. Polster, and M. Hoffmann, "Aluminum nitride based 3D, piezoelectric, tactile sensor," *Procedia Chem.*, vol. 1, no. 1, pp. 144–147, Sep. 2009.
- [21] J. Dargahi, M. Parameswaran, and S. Payandeh, "A micromachined piezoelectric tactile sensor for an endoscopic grasper-theory, fabrication and experiments," *J. Microelectromechanical Syst.*, vol. 9, no. 3, pp. 329–335, Sep. 2000.
- [22] C.-H. Chuang and Y.-R. Liou, "Flexible piezoelectric tactile sensor," US20110266923 A1, 03-Nov-2011.
- [23] J. Dargahi, "A piezoelectric tactile sensor with three sensing elements for robotic, endoscopic and prosthetic applications," *Sens. Actuators Phys.*, vol. 80, no. 1, pp. 23–30, Mar. 2000.
- [24] V. E. G.  *Structure and Properties of Conducting Polymer Composites*. VSP, 1996.
- [25] R. Strümpfer and J. Glatz-Reichenbach, "Conducting Polymer Composites," *J. Electroceramics*, vol. 3, no. 4, pp. 329–346.
- [26] D. S. McLachlan, "Analytical Functions for the dc and ac Conductivity of Conductor-Insulator Composites," *J. Electroceramics*, vol. 5, no. 2, pp. 93–110.
- [27] J. Castellanos-Ramos, R. Navas-González, H. Macicior, T. Sikora, E. Ochoteco, and F. Vidal-Verdú, "Tactile sensors based on conductive polymers," *Microsyst. Technol.*, vol. 16, no. 5, pp. 765–776, Dec. 2009.
- [28] S. Nambiar and J. T. W. Yeow, "Conductive polymer-based sensors for biomedical applications," *Biosens. Bioelectron.*, vol. 26, no. 5, pp. 1825–1832, Jan. 2011.

- [29] Y. W. R. Amarasinghe, A. L. Kulasekera, and T. G. P. Priyadarshana, "Design and simulation of 1-DOF tactile sensor for gripping force measurement," in *2013 IEEE 8th International Conference on Industrial and Information Systems*, 2013, pp. 399–402.
- [30] M. R. Cutkosky, R. D. Howe, and W. R. Provancher, "Force and Tactile Sensors," in *Springer Handbook of Robotics*, B. S. Prof and O. K. Prof, Eds. Springer Berlin Heidelberg, 2008, pp. 455–476.
- [31] N. Wettels, V. J. Santos, R. S. Johansson, and G. E. Loeb, "Biomimetic Tactile Sensor Array," *Adv. Robot.*, vol. 22, no. 8, pp. 829–849, Jan. 2008.
- [32] "iPod," *Apple*. [Online]. Available: <http://www.apple.com/ipod/>. [Accessed: 18-Apr-2016].
- [33] H. Yousef, M. Boukallel, and K. Althoefer, "Tactile sensing for dexterous in-hand manipulation in robotics—A review," *Sens. Actuators Phys.*, vol. 167, no. 2, pp. 171–187, Jun. 2011.
- [34] A. Sarvagyan and V. Egorov, "Mechanical Imaging – a Technology for 3-D Visualization and Characterization of Soft Tissue Abnormalities. A Review," *Curr. Med. Imaging Rev.*, vol. 8, no. 1, pp. 64–73, Feb. 2012.
- [35] A. Hamed, S. C. Tang, H. Ren, A. Squires, C. Payne, K. Masamune, G. Tang, J. Mohammadpour, and Z. T. H. Tse, "Advances in Haptics, Tactile Sensing, and Manipulation for Robot-Assisted Minimally Invasive Surgery, Noninvasive Surgery, and Diagnosis," *J. Robot.*, vol. 2012, p. e412816, Dec. 2012.
- [36] S. Schostek, M. O. Schurr, and G. F. Buess, "Review on aspects of artificial tactile feedback in laparoscopic surgery," *Med. Eng. Phys.*, vol. 31, no. 8, pp. 887–898, Oct. 2009.
- [37] Javad Dargahi and Siamak Najarian, "Advances in tactile sensors design/manufacturing and its impact on robotics applications – a review," *Ind. Robot Int. J.*, vol. 32, no. 3, pp. 268–281, Jun. 2005.

- [38] H. Raalte and V. Egorov, "Characterizing female pelvic floor conditions by tactile imaging," *Int. Urogynecology J.*, vol. 26, no. 4, pp. 607–609, Oct. 2014.
- [39] A. Sarvazyan, T. J. Hall, M. W. Urban, M. Fatemi, S. R. Aglyamov, and B. S. Garra, "An Overview of Elastography – An Emerging Branch of Medical Imaging," *Curr. Med. Imaging Rev.*, vol. 7, no. 4, pp. 255–282, Nov. 2011.
- [40] A. Sarvazyan, "Mechanical imaging:: A new technology for medical diagnostics," *Int. J. Med. Inf.*, vol. 49, no. 2, pp. 195–216, Apr. 1998.
- [41] J. H. Lee and C. H. Won, "High-Resolution Tactile Imaging Sensor Using Total Internal Reflection and Nonrigid Pattern Matching Algorithm," *IEEE Sens. J.*, vol. 11, no. 9, pp. 2084–2093, Sep. 2011.
- [42] J.-H. Lee, C.-H. Won, K. Yan, Y. Yu, and L. Liao, "Tactile Sensation Imaging for Artificial Palpation," in *Haptics: Generating and Perceiving Tangible Sensations*, A. M. L. Kappers, J. B. F. van Erp, W. M. B. Tiest, and F. C. T. van der Helm, Eds., Springer Berlin-Heidelberg, 2010, pp. 373–378.
- [43] C.  and R. Health, "Medical Imaging." [Online]. Available: <http://www.fda.gov/Radiation-EmittingProducts/RadiationEmittingProductsandProcedures/MedicalImaging/default.htm>. [Accessed: 09-May-2016].
- [44] M. Ramezanifard, S. Sokhanvar, J. Dargahi, W. F. Xie, and M. Packirisamy, "Graphical Reproduction of Tactile Information of Embedded Lumps for MIS Applications," in *2008 Symposium on Haptic Interfaces for Virtual Environment and Teleoperator Systems*, 2008, pp. 247–252.
- [45] R. Siegel, J. Ma, Z. Zou, and A. Jemal, "Cancer statistics, 2014," *CA. Cancer J. Clin.*, vol. 64, no. 1, pp. 9–29, Jan. 2014.
- [46] V. Egorov, T. Kearney, S. B. Pollak, C. Rohatgi, N. Sarvazyan, S. Airapetian, S. Browning, and A. Sarvazyan, "Differentiation of benign and malignant breast

lesions by mechanical imaging,” *Breast Cancer Res. Treat.*, vol. 118, no. 1, pp. 67–80, Mar. 2009.

- [47] A. Sarvazyan, V. Egorov, J. S. Son, and C. S. Kaufman, “Cost-Effective Screening for Breast Cancer Worldwide: Current State and Future Directions,” *Breast Cancer Basic Clin. Res.*, vol. 1, p. 91, Jul. 2008.
- [48] V. Egorov, S. Ayrapetyan, and A. P. Sarvazyan, “Prostate mechanical imaging: 3-D image composition and feature calculations,” *IEEE Trans. Med. Imaging*, vol. 25, no. 10, pp. 1329–1340, Oct. 2006.
- [49] A. M. Weber and H. E. Richter, “Pelvic Organ Prolapse:,” *Obstet. Gynecol.*, vol. 106, no. 3, pp. 615–634, Sep. 2005.
- [50] V. Egorov, H. van Raalte, and A. P. Sarvazyan, “Vaginal Tactile Imaging,” *IEEE Trans. Biomed. Eng.*, vol. 57, no. 7, pp. 1736–1744, Jul. 2010.
- [51] V. Egorov and A. P. Sarvazyan, “Mechanical Imaging of the Breast,” *IEEE Trans. Med. Imaging*, vol. 27, no. 9, pp. 1275–1287, Sep. 2008.
- [52] R. E. Weiss, V. Egorov, S. Ayrapetyan, N. Sarvazyan, and A. Sarvazyan, “Prostate Mechanical Imaging: A New Method for Prostate Assessment,” *Urology*, vol. 71, no. 3, pp. 425–429, Mar. 2008.
- [53] V. Egorov, H. van Raalte, and V. Lucente, “Quantifying vaginal tissue elasticity under normal and prolapse conditions by tactile imaging,” *Int. Urogynecology J.*, vol. 23, no. 4, pp. 459–466, Nov. 2011.
- [54] L. Lin, Y. Xie, S. Wang, W. Wu, S. Niu, X. Wen, and Z. L. Wang, “Triboelectric Active Sensor Array for Self-Powered Static and Dynamic Pressure Detection and Tactile Imaging,” *ACS Nano*, vol. 7, no. 9, pp. 8266–8274, Sep. 2013.
- [55] D. Lussey, “Polymer composition,” US6291568 B1, 18-Sep-2001.
- [56] Peratech, “What is QTC?,” 11-Feb-2016. [Online]. Available: <https://www.peratech.com/what-is-qtc.html>. [Accessed: 09-Dec-2013].

- [57] D. Bloor, A. Graham, E. J. Williams, P. J. Laughlin, and D. Lussey, “Metal–polymer composite with nanostructured filler particles and amplified physical properties,” *Appl. Phys. Lett.*, vol. 88, no. 10, p. 102103, Mar. 2006.
- [58] D. Bloor, K. Donnelly, P. J. Hands, P. Laughlin, and D. Lussey, “A metal–polymer composite with unusual properties,” *J. Phys. Appl. Phys.*, vol. 38, no. 16, p. 2851, 2005.
- [59] “Calibration - VectorNav Library.” [Online]. Available: <http://www.vectornav.com/support/library/calibration>. [Accessed: 10-Mar-2014].
- [60] M. Ohmukai, Y. Kami, and R. Matsuura, “Electrode for Force Sensor of Conductive Rubber,” *J. Sens. Technol.*, vol. 2, no. 3, pp. 127–131, 2012.
- [61] admin, “10 Easy, Essential Yoga Poses,” *DennyZen*, 11-Jan-2014. [Online]. Available: <http://www.dennyzen.com/fitnesstips/10-easy-essential-yoga-poses/>. [Accessed: 08-May-2016].
- [62] “Interpolants - MATLAB & Simulink - MathWorks India.” [Online]. Available: <http://in.mathworks.com/help/curvefit/interpolants.html#bsz6baz>. [Accessed: 12-Aug-2016].
- [63] H. Yussof, M. Fahmi Miskon, K. Sugiman, M. A. M. Jusoh, M. Ohka, H. Yussof, and S. C. Abdullah, “Thin Flexible Sheet Handling Using Robotic Hand Equipped with Three-axis Tactile Sensors,” *Procedia Comput. Sci.*, vol. 76, pp. 155–160, Jan. 2015.
- [64] T. Someya, T. Sekitani, S. Iba, Y. Kato, H. Kawaguchi, and T. Sakurai, “A large-area, flexible pressure sensor matrix with organic field-effect transistors for artificial skin applications,” *Proc. Natl. Acad. Sci. U. S. A.*, vol. 101, no. 27, pp. 9966–9970, Jul. 2004.
- [65] P. S. Girão, O. Postolache, J. Miguel, and D. Pereira, “Tactile sensors and their use in industrial, robotic and medical applications,” presented at the IMEKO 20th

TC3, 3rd TC16 and 1st TC22 International Conference Cultivating Metrological Knowledge, Merida, Mexico, 2007.

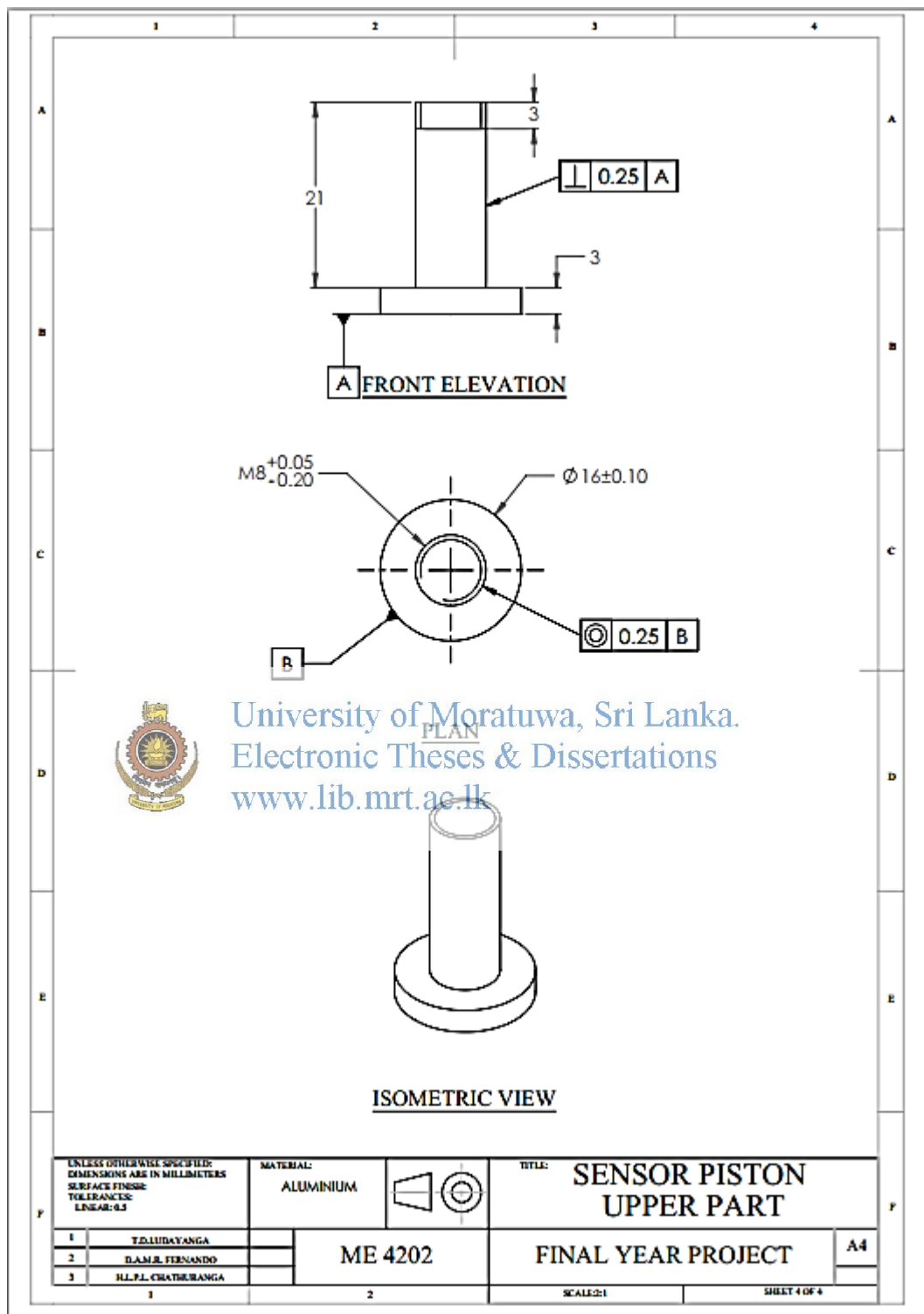
- [66] H. B. Muhammad, C. M. Oddo, L. Beccai, M. J. Adams, M. C. Carrozza, D. W. Hukins, and M. C. Ward, "Development of a Biomimetic MEMS based Capacitive Tactile Sensor," *Procedia Chem.*, vol. 1, no. 1, pp. 124–127, Sep. 2009.
- [67] S. Beeby, *MEMS Mechanical Sensors*. Artech House, 2004.
- [68] F. Khoshnoud and C. W. de Silva, "Recent advances in MEMS sensor technology-biomedical applications," *IEEE Instrum. Meas. Mag.*, vol. 15, no. 1, pp. 8–14, Feb. 2012.
- [69] A. K. Makhtar, H. Yussof, H. Al-Assadi, L. C. Yee, A. H. Esa, B. Ali, and M. A. Ayub, "Normal Force Calibration for Optical Based Silicone Tactile Sensor," *Procedia Eng.*, vol. 41, pp. 210–215, Jan. 2012.
- [70] M. Fontana, S. Marcheschi, P. Salsedo, and M. Bergamasco, "A Three-Axis Force Sensor for Dual Finger Haptic Interfaces," *Sensors*, vol. 12, no. 10, pp. 13598–13616, Oct. 2012.
- [71] S. Muntwyler, F. Beyeler, and B. J. Nelson, "Three-axis micro-force sensor with sub-micro-Newton measurement uncertainty and tunable force range," *J. Micromechanics Microengineering*, vol. 20, no. 2, p. 25011, 2010.
- [72] A. Sieber, P. Valdastri, K. Houston, C. Eder, O. Tonet, A. Menciassi, and P. Dario, "A novel haptic platform for real time bilateral biomanipulation with a MEMS sensor for triaxial force feedback," *Sens. Actuators Phys.*, vol. 142, no. 1, pp. 19–27, Mar. 2008.
- [73] M. Uchiyama, Y. Nakamura, and K. Hakomori, "Evaluation of the robot force sensor structure using singular value decomposition," *Adv. Robot.*, vol. 5, no. 1, pp. 39–52, Jan. 1990.

- [74] M.-H. Bao, “Chapter 5 - Piezoresistive sensing,” in *Handbook of Sensors and Actuators*, vol. 8, M.-H. Bao, Ed. Elsevier Science B.V., 2000, pp. 199–239.
- [75] R. Amarasinghe, D. V. Dao, T. Toriyama, and S. Sugiyama, “Development of miniaturized 6-axis accelerometer utilizing piezoresistive sensing elements,” *Sens. Actuators Phys.*, vol. 134, no. 2, pp. 310–320, Mar. 2007.
- [76] A. Wijesiri and Y. W. R. Amarasinghe, “MEMS Based Microneedle Actuator with Piezoresistive Force Feedback System for Biomedical Applications,” *Int. J. Sci. Eng. Technol.*, vol. 3, no. 12, 2014.



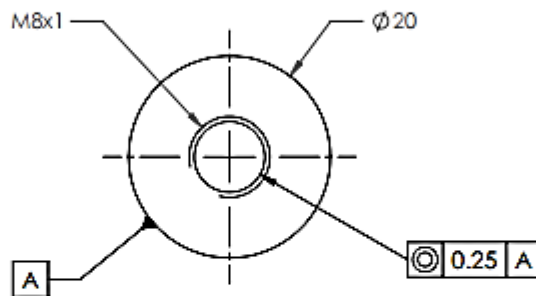
University of Moratuwa, Sri Lanka.
Electronic Theses & Dissertations
www.lib.mrt.ac.lk

Appendix B: Production Drawings of Sensor Structure (Design 2)

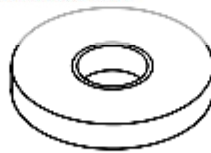




FRONT ELEVATION

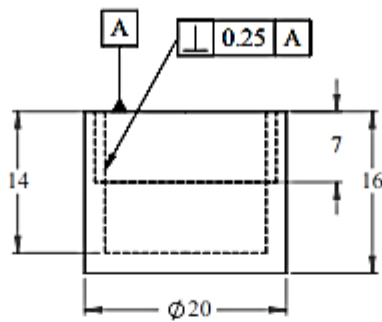


University of Moratuwa, Sri Lanka.
 Electronic Theses & Dissertations
www.lib.mrt.ac.lk

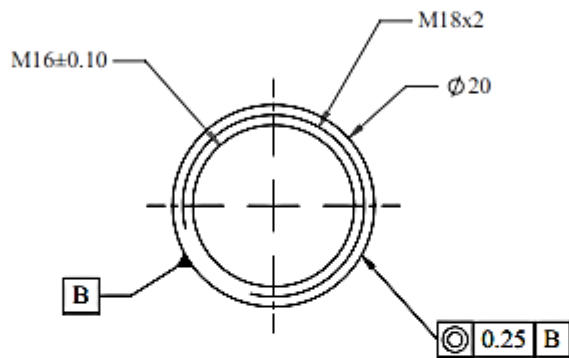


ISOMETRIC VIEW

UNLESS OTHERWISE SPECIFIED: DIMENSIONS ARE IN MILLIMETERS SURFACE FINISH: TOLERANCES: LINEAR: 0.5		MATERIAL: ALUMINIUM		TITLE: SENSOR PISTON LOWER PART
1	T.D. LUDAYANGA	ME 4202		FINAL YEAR PROJECT
2	D.A.M.R. FERNANDO			
3	H.L.P.L. CHATHURANGA			
		SCALE: 1:1	SHEET 3 OF 4	



FRONT ELEVATION



PLAN

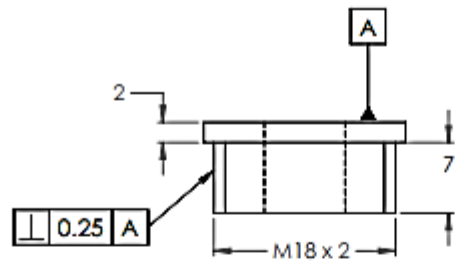


University of Moratuwa, Sri Lanka.
Electronic Theses & Dissertations
www.lib.mrt.ac.lk

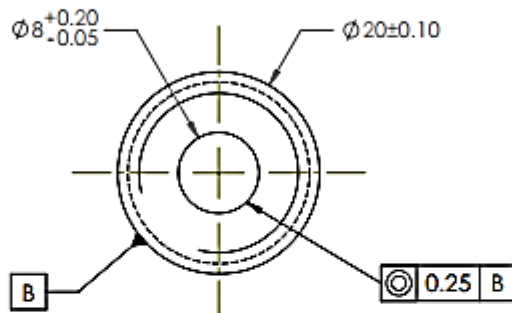


ISOMETRIC VIEW

UNLESS OTHERWISE SPECIFIED: DIMENSIONS ARE IN MILLIMETERS SURFACE FINISH: TOLERANCES: LINEAR: 0.5		MATERIAL: ALUMINIUM		TITLE: SENSOR FEMALE PART
1	T.DIJUDAYANGA	ME 4202		FINAL YEAR PROJECT
2	D.A.M.R. FERNANDEO			A4
3	H.L.P.L. CRATHURANGA			
1	2	SCALE: 1	SHEET 1 OF 4	



FRONT ELEVATION



PLAN



University of Moratuwa, Sri Lanka.
Electronic Theses & Dissertations
www.lib.mrt.ac.lk



ISOMETRIC VIEW

UNLESS OTHERWISE SPECIFIED: DIMENSIONS ARE IN MILLIMETERS SURFACE FINISH: TOLERANCES: LINEAR: 0.1		MATERIAL: ALUMINIUM		TITLE: SENSOR CUP
1	TALLIDAVANGA	ME 4202		FINAL YEAR PROJECT
2	D.A.M.R. FERNANDO			A4
3	H.L.P.L. CHATHURANGA			
1	2	SCALE: 1:1	SHEET 1 OF 4	

Appendix C: Material Properties Chart

ASTM A228


Categories: [Metal](#), [Ferrous Metal](#), [ASTM Steel](#), [Carbon Steel](#), [High Carbon Steel](#)

Material Notes: Cold drawn. High tensile strength and uniform mechanical properties. Music wire springs are not recommended for service temperatures above 121°C (250° F).

Applications: High quality springs and wire forms subject to high stresses or requiring good fatigue properties.

Key Words: spring steel, music wire, AMS 5112, UNS K08500

Vendors: No vendors are listed for this material. Please [click here](#) if you are a supplier and would like information on how to add your listing to this material.

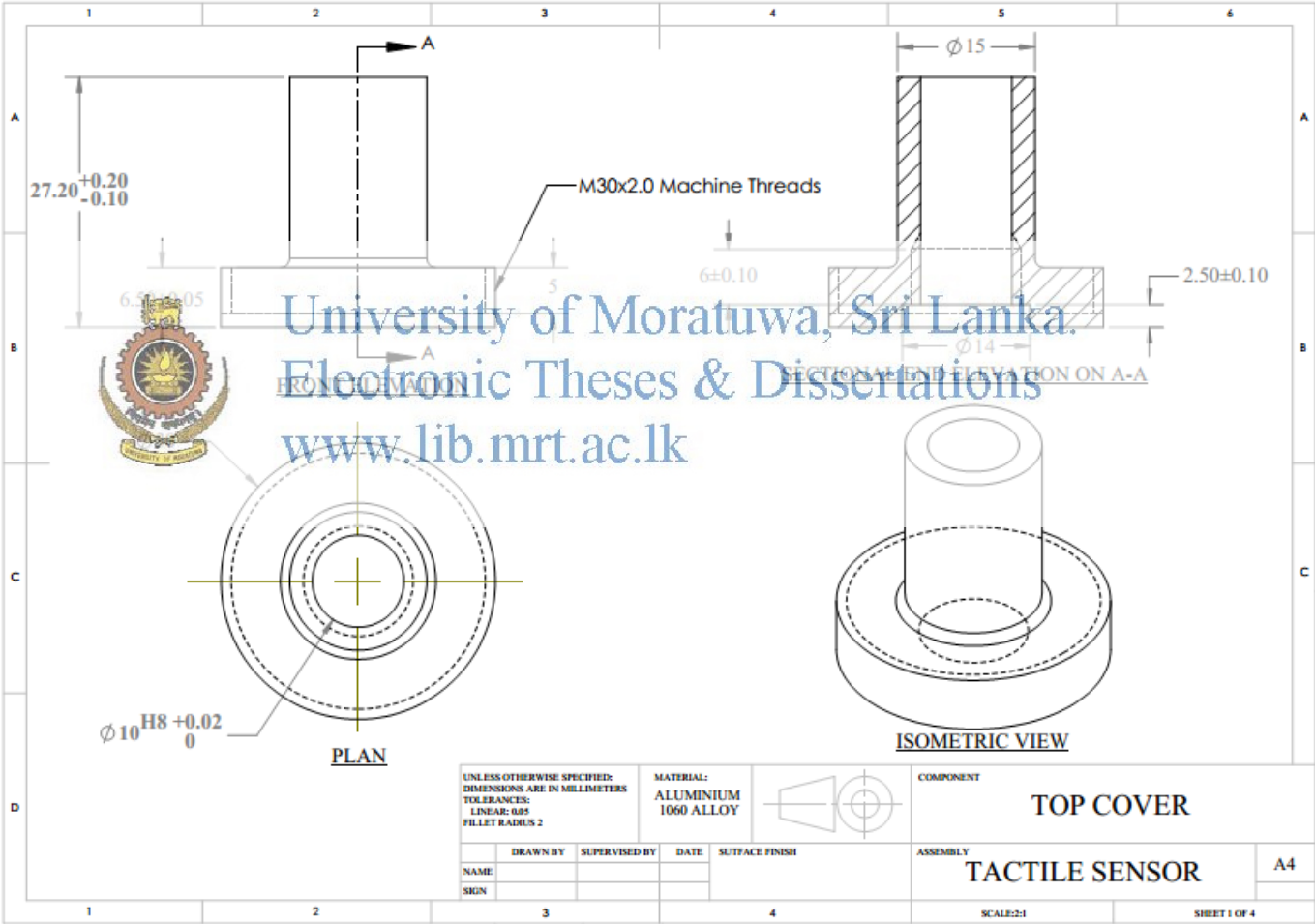
Physical Properties	Metric	English	Comments
Density	7.85 g/cc	0.284 lb/in ³	Typical of ASTM Steel
Mechanical Properties	Metric	English	Comments
Hardness, Rockwell C	41 - 60	41 - 60	
Tensile Strength, Yield 	1590 - 1760 MPa @Diameter 8.25 mm	231000 - 255000 psi @Diameter 0.250 in	
	1640 - 1820 MPa @Diameter 5.26 mm	238000 - 264000 psi @Diameter 0.207 in	
	1690 - 1860 MPa @Diameter 4.59 mm	245000 - 270000 psi @Diameter 0.177 in	
	1740 - 1920 MPa @Diameter 3.81 mm	252000 - 278000 psi @Diameter 0.150 in	
	1770 - 1950 MPa @Diameter 3.56 mm	257000 - 283000 psi @Diameter 0.140 in	
	1800 - 1990 MPa @Diameter 3.15 mm	261000 - 289000 psi @Diameter 0.125 in	
	1870 - 2070 MPa @Diameter 2.54 mm	271000 - 300000 psi @Diameter 0.100 in	
	1940 - 2150 MPa @Diameter 2.05 mm	281000 - 312000 psi @Diameter 0.0787 in	
	2020 - 2230 MPa @Diameter 1.65 mm	293000 - 323000 psi @Diameter 0.0650 in	
	2090 - 2310 MPa @Diameter 1.30 mm	303000 - 335000 psi @Diameter 0.0512 in	
	2170 - 2410 MPa @Diameter 1.05 mm	315000 - 350000 psi @Diameter 0.0394 in	
	2250 - 2510 MPa @Diameter 0.80 mm	327000 - 363000 psi @Diameter 0.0315 in	
	2350 - 2600 MPa @Diameter 0.60 mm	341000 - 377000 psi @Diameter 0.0236 in	
	2500 - 2760 MPa @Diameter 0.45 mm	363000 - 400000 psi @Diameter 0.0177 in	
	2600 - 2880 MPa @Diameter 0.305 mm	377000 - 418000 psi @Diameter 0.0119 in	
	2750 - 3040 MPa @Diameter 0.205 mm	399000 - 441000 psi @Diameter 0.00787 in	
	3030 - 3340 MPa @Diameter 0.105 mm	439000 - 484000 psi @Diameter 0.00394 in	
Modulus of Elasticity	210 GPa	30500 ksi	
Poissons Ratio	0.313	0.313	Calculated
Shear Modulus	80.0 GPa	11600 ksi	
Thermal Properties	Metric	English	Comments
Maximum Service Temperature, Air	120 °C	248 °F	
Component Elements Properties	Metric	English	Comments
Carbon, C	0.70 - 1.0 %	0.70 - 1.0 %	
Iron, Fe	97.8 - 99 %	97.8 - 99 %	
Manganese, Mn	0.20 - 0.60 %	0.20 - 0.60 %	
Phosphorous, P	<= 0.025 %	<= 0.025 %	
Silicon, Si	0.10 - 0.30 %	0.10 - 0.30 %	
Sulfur, S	<= 0.030 %	<= 0.030 %	

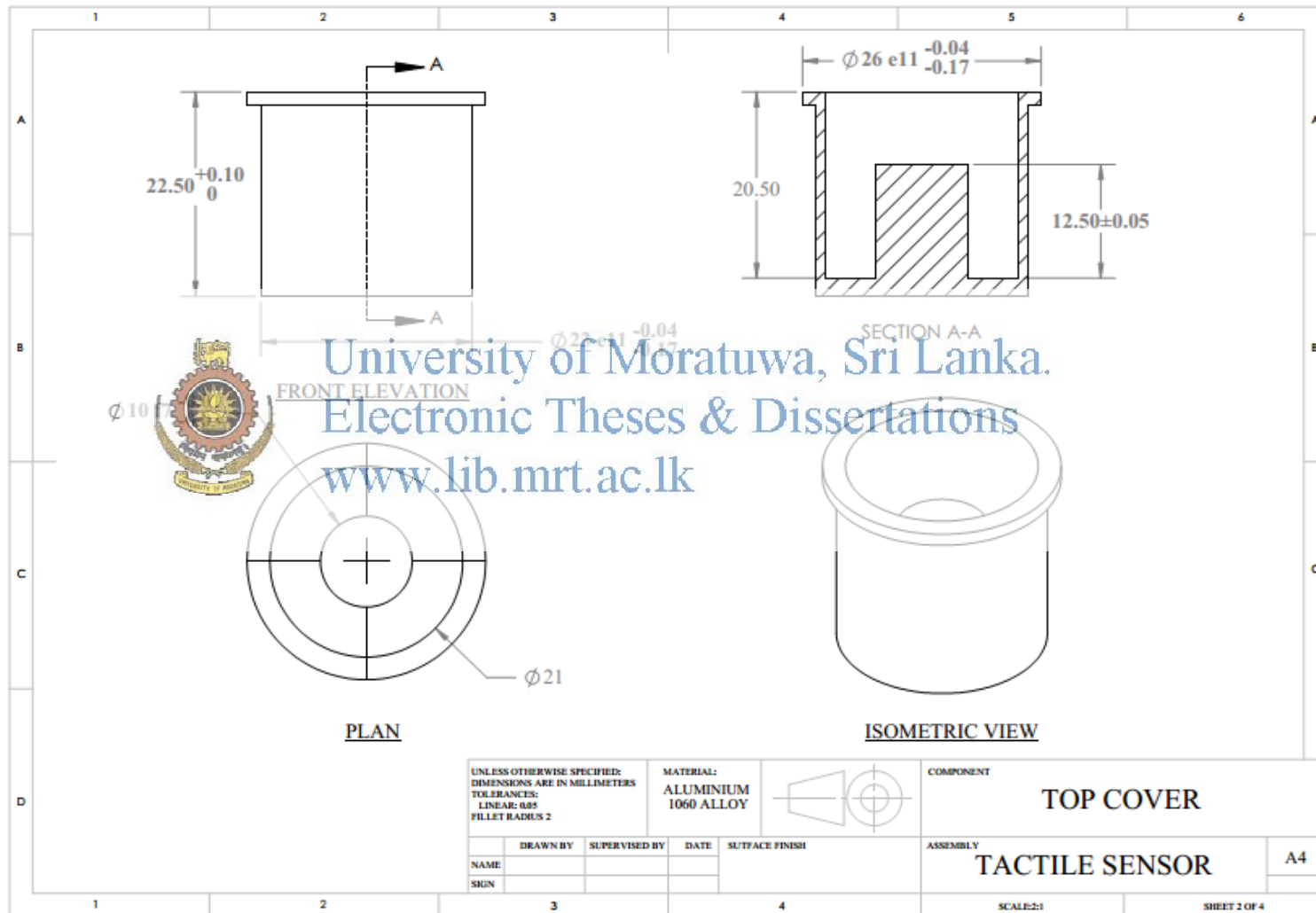


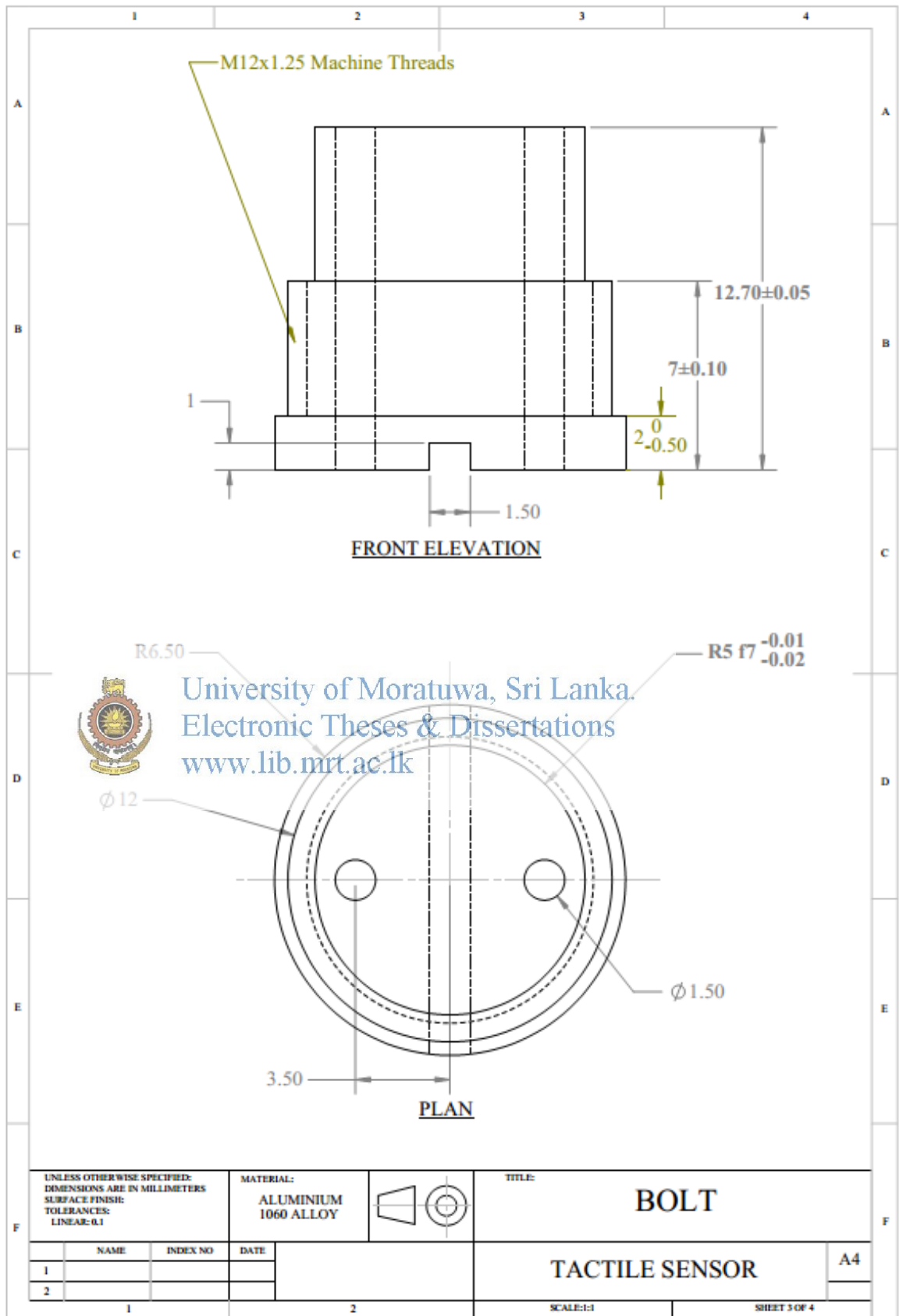
University of Moratuwa, Sri Lanka.
Electronic Theses & Dissertations
www.lib.mrt.ac.lk

Some of the values displayed above may have been converted from their original units and/or rounded in order to display the information in a consistent format. Users requiring more precise data for scientific or engineering calculations can click on the property value to see the original value as well as raw conversions to equivalent units. We advise that you only use the original value or one of its raw conversions in your calculations to minimize rounding error. We also ask that you refer to MatWeb's [terms of use](#) regarding this information. [Click here](#) to view all the property values for this datasheet as they were originally entered into MatWeb.

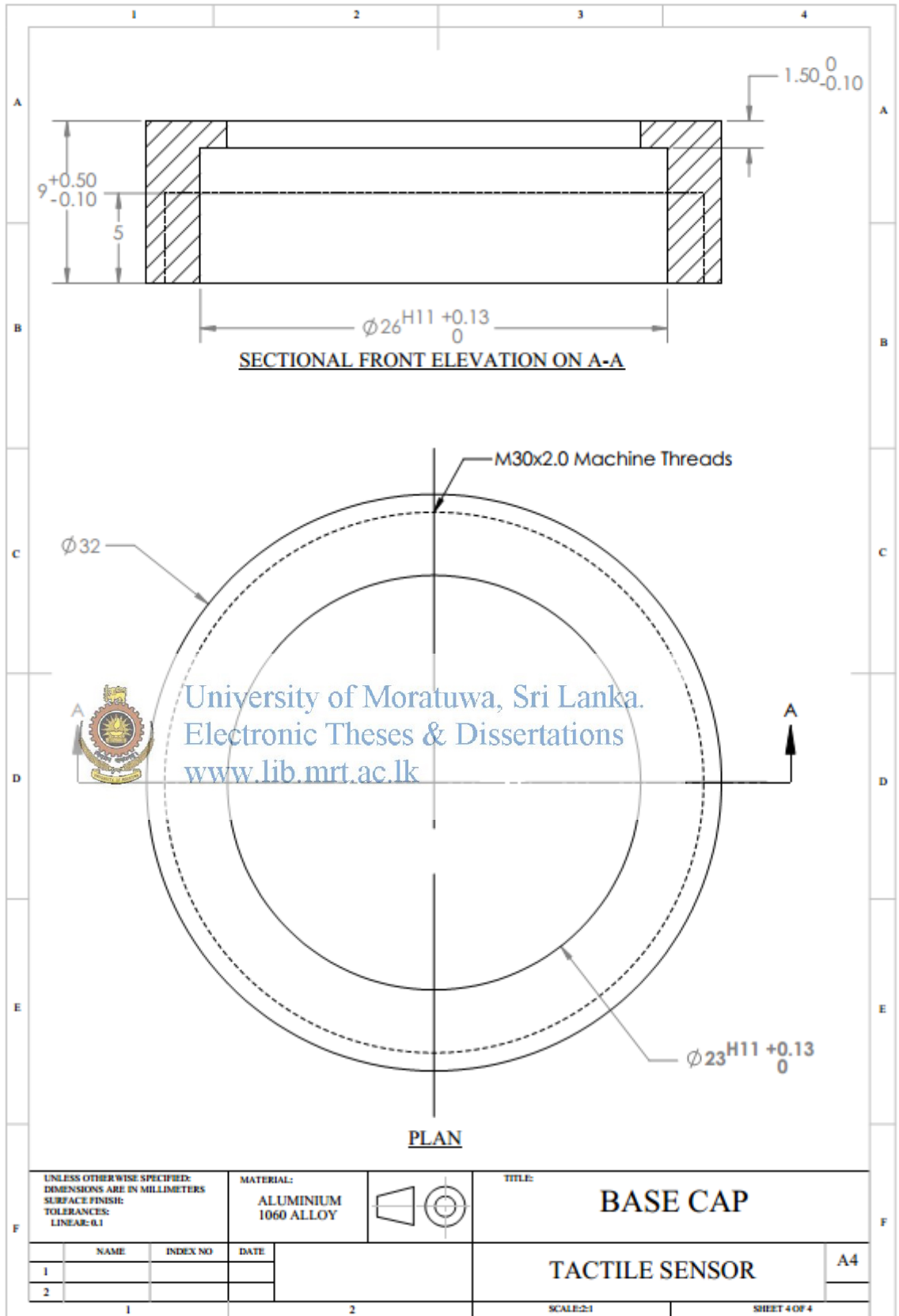
Appendix D: Production Drawings of Sensor structure (Enclosed sensor)







University of Moratuwa, Sri Lanka.
Electronic Theses & Dissertations
www.lib.mrt.ac.lk



Appendix E: Arduino Code of Graphical User Interface

LIFA_BASE

```
// Standard includes. These should always be included.
#include <Wire.h>
#include <SPI.h>
#include <Servo.h>
#include "LabVIEWInterface.h"

void setup()
{
  // Initialize Serial Port With The Default Baud Rate
  syncLV();
}

void loop()
{
  // Check for commands from LabVIEW and process them.

  checkForCommand();
  if(acqMode == 1)
  {
    sampleContinuously();
  }
}
```

LabVIEWInterface.h

```
#define FIRMWARE_MAJOR 02
#define FIRMWARE_MINOR 00
#if defined(__AVR_ATmega1280__) || defined(__AVR_ATmega2560__)
#define DEFAULTBAUDRATE 9600 // Defines The Default Serial Baud Rate (This
must match the baud rate specifid in LabVIEW)
#else
#define DEFAULTBAUDRATE 115200
#endif
#define MODE_DEFAULT 0 // Defines Arduino Modes (Currently Not Used)
#define COMMANDLENGTH 15 // Defines The Number Of Bytes In A Single
LabVIEW Command (This must match the packet size specifid in LabVIEW)
```

```
#define STEPPER_SUPPORT 1 // Defines Whether The Stepper Library Is  
Included - Comment This Line To Exclude Stepper Support
```

```
// Declare Variables
```

```
unsigned char currentCommand[COMMANDELENGTH]; // The Current Command  
For The Arduino To Process
```

```
//Globals for continuous aquisition
```

```
unsigned char acqMode;
```

```
unsigned char contAcqPin;
```

```
float contAcqSpeed;
```

```
float acquisitionPeriod;
```

```
float iterationsFlt;
```

```
int iterations;
```

```
float delayTime;
```

```
/Synchronizes with LabVIEW and sends info about the board and firmware  
(Unimplemented)/
```

```
void syncLV();
```

```
/Sets the mode of the Arduino (Reserved For Future Use)/  
void setMode(int mode);
```



University of Moratuwa, Sri Lanka.
Electronic Theses & Dissertations
www.lib.mrt.ac.lk

```
/Checks for new commands from LabVIEW and processes them if any exists./
```

```
int checkForCommand(void);
```

```
/Processes a given command/
```

```
void processCommand(unsigned char command[]);
```

```
/Write values to DIO pins 0 - 13. Pins must first be configured as outputs./
```

```
void writeDigitalPort(unsigned char command[]);
```

```
/Reads all 6 analog input ports, builds 8 byte packet, send via RS232./
```

```
void analogReadPort();
```

/Configure digital I/O pins to use for seven segment display. Pins are stored in sevenSegmentPins array./

```
void sevenSegment_Config(unsigned char command[]);
```

/Write values to sevenSegment display. Must first use sevenSegment_Configure/

```
void sevenSegment_Write(unsigned char command[]);
```

/Set the SPI Clock Divisor/

```
void spi_setClockDivider(unsigned char divider);
```

/Sens / Receive SPI Data/

```
void spi_sendReceive(unsigned char command[]);
```

/Compute Packet Checksum/

```
unsigned char checksum_Compute(unsigned char command[]);
```

/Compute Packet Checksum And Test Against Included Checksum/

```
int checksum_Test(unsigned char command[]);
```

/Parse command packet and write speed, direction, and number of steps to travel/

```
void AccelStepper_Write(unsigned char command[]);
```

/Returns several analog input points at once./

```
void sampleContinuously(void);
```

/Returns the number of samples specified at the rate specified./

```
void finiteAcquisition(int analogPin, float acquisitionSpeed, int numberOfSamples );
```

/Prints Data to the LCD With The Given Base/

```
void lcd_print(unsigned char command[]);
```

Appendix F: Production Drawings of 5-DOF MEMS Sensor Structure

